PHARMACOMETRICS OF ANTIEPILEPTIC DRUGS: MODELING AND SIMULATION-BASED STUDIES OF LAMOTRIGINE AND CARBAMAZEPINE PHARMACOKINETICS

A DISSERTATION
SUBMITTED TO THE FACULTY OF THE GRADUATE SCHOOL
OF THE UNIVERSITY OF MINNESOTA
BY

BARALEE PRASITTISOPIN

IN PARTIAL FULFILLMENT OF THE REQUIREMENTS
FOR THE DEGREE OF
DOCTOR OF PHILOSOPHY

ANGELA K BIRNBAUM, ADVISOR

NOVEMBER, 2008

ACKNOWLEDGEMENTS

It is difficult as it would be endless to overstate my gratitude to all those who have made success in my PhD study possible. This dissertation is representative of all my hard work in the area of Pharmacometrics, which definitely cannot be accomplished without support from several people. First and foremost, I would like to express my special gratitude to Dr. Angela Birnbaum, my advisor. Without her mentoring; knowledge, not only in Pharmacometrics but every discipline; and perceptiveness, I would never have accomplished this big part of my life. She is a person who is always there listening to me, points out to me the different aspects of my work, and instills me with the highest standard of research skills. Her patience in reading draft after draft of my papers, ideas, including this dissertation is something I am always grateful for.

I also wish to express my sincere gratitude to all my committee members; Dr. Richard Brundage for sharing with me his thoughts, advice, and comments. Moreover, he is a person who introduced me to the field of Pharmacometrics; Dr. James Cloyd who gave me an opportunity to work with his data set; Dr. William Elmquist who may not realize how much he has inspired and made me have a passion in Pharmacokinetics, since I attended the first class of Advance Pharmacokinetics. I would also like to take this opportunity to express my respect and gratitude to all my teachers who have been silent force behind my success.

I would regret if I forget to mention this name, Jae Eun Anh, who always gives me friendship and invaluable advice. I remember running to her office every time I got stuck with my work and she was always there helping me solve those problems. Thank you so much, Jae Eun. One more person who deserves a big thank you is Won Kyung Byon, my good friend ever since the first year of my graduate study. Thank you for sharing all precious moments together. I would like to also thank all my student colleagues in Pharmacometrics group; Manisha Lamba, Varun Goel, and Kyle Baron, for stimulating a fun environment to study and learn. Furthermore, I would like to express my appreciation to NIH and the Royal Thai Government for providing me financial support during my PhD studying.

I owe many thanks to Bodin Tuesuwan, my good and sincere friend since undergraduate study for many of his brilliant ideas both scientific and nonscientific, great soul, and constant friendship. He always made me feel better when I was down by telling me his life was even worse than mine. Let me also say “thank you” to all my friends in Thailand for their moral support, and all my friends in Minneapolis for their generosity and for making my life in MN more colorful.

My deepest gratitude goes to my family for their endless love, support, and encouragement throughout my life. I was extraordinarily fortunate to be part of this family. My father, Banjong Prasittisopin, is a person who always believes and has confidence in me. To me, he is a real giver, without any expectation to get back. My mother, Busakorn Prasittisopin, is the most perfect mother in the world for me. Her

unconditional love, care and support is the greatest thing that strengthens me. No matter how hard it is to follow my dream, I know she will always be there for me. I am also thankful to my brother, Panchapol Prasittisopin, for being supportive and caring. Last but not least, I would like to thank my sister, Busarin Prasittisopin, for being my sister and close friend at the same time and for everything she has done for me.

Words fail me in expressing my appreciation to my husband, Konlayutt Punyawudho. All I can say is he is the most priceless gift to my life. None of this would be possible without his warm love, dedication, patience and encouragement. He is the only person who was, from time to time, able to make me calm down when I was in the heat of the moment. Thank you for having faith in me, understanding me, being my sanctuary, and always being by my side.

Minneapolis, MN

November, 2008

To my mom and dad for their love, support, and encouragement

To my husband for his warm love and understanding

ABSTRACT

The population pharmacokinetic modeling plays a pivotal role in quantitative learning about drugs from sparse data collected in clinical studies. It provides crucial information needed for individualization of dosage regimens especially in special population in which the intensive pharmacokinetic studies are of ethical concern. Lamotrigine and carbamazepine are antiepileptic drugs commonly used in elderly patients; however, dosing these drugs is based largely on studies from adult patients. Pharmacokinetic information of these drugs in elderly patients is limited. The aims of the current dissertation were to determine the population pharmacokinetic parameters of lamotrigine and carbamazepine in the community-dwelling elderly patients, and to quantitatively identify factors that have significant effects on these parameters. The further aim was to characterize the time course of carbamazepine deinduction by an enzyme turnover model. Due to the presence of collinearity between covariates during the covariate model development of lamotrigine, the effect of collinearity on power, bias, and precision of the parameter estimates in the population covariate model was further investigated by means of simulations.

The population pharmacokinetic models of lamotrigine and carbamazepine were successfully developed and the models adequately described the data sets. The important information of drugs' pharmacokinetics was obtained and it can be beneficial in developing dosing strategies for elderly patients receiving these drugs. The time course of carbamazepine deinduction was well described by an enzyme turnover model. This model allowed the estimation of the half-life of the induced enzymes involving

carbamazepine metabolism which is the important parameter for characterizing the time course of carbamazepine deinduction process.

The power of selecting the true covariates depends on sample size of the data set, the magnitude of covariate coefficient, and the degrees of correlation. The investigation of the effect of collinearity between two true covariates revealed that an increasing collinearity between two true covariates not only decreases the power of selecting the true covariate model, but also leads to the biased and imprecise parameter estimates. The results from this study improve the understanding of how and to what extent the collinearity affects the parameter estimates in the covariate model building.

TABLE OF CONTENTS

LIST OF TABLES

Tables **Page**

LIST OF FIGURES

Figures **Page**

ABBREVIATIONS

AED	antiepileptic drug
BUN/CR	blood urea nitrogen/serum creatinine ratio
CBZ	carbamazepine
CBZ-E	carbamazepine-10,11-epoxide
CI	confidence interval
CL	clearance
CL/F	apparent clearance
CRCL	creatinine clearance
CV	coefficient of variation
CYP	cytochrome P450
dOFV	difference in the objective function value
EC_{50}	the concentration producing one-half of the maximum induction effect
Emax	the maximum induction effect
FOCE-I	first order conditional estimation method with interaction
GBP	gabapentin
IIV	interindividual variability
K_a	absorption rate constant
$k_{enz, in}$	zero-order rate of enzyme synthesis
$k_{enz, out}$	first order rate constant of enzyme degradation
LTG	lamotrigine
MAE	mean absolute error
MPAE	mean percent absolute error
MPPE	mean percent prediction error
MSE	mean squared error
OFV	objective function value
OPT	optimism
PB	phenobarbital
PC	predictive check

PD	pharmacodynamics
PHT	phenytoin
PK	pharmacokinetics
PPC	posterior predictive check
p^{pc}	predictive p-value
RUV	residual unexplained variability
SD	standard deviation
SE	standard error
SL-CBZ	stable-labeled carbamazepine
TDD	total daily dose
TDM	therapeutic drug monitoring
T(y^{obs})	statistics from observed data
T(y_i^{rep})	statistics from each replicated data
UGT	uridine 5'-diphosphate-glucuronosyltransferases
V	volume of distribution
V/F	apparent volume of distribution
VPA	valproic acid
VPC	visual predictive check
ε_{ij}	difference between individual predicted concentration and observed concentration
η_j	difference between population and individual parameter estimate
θ	typical value of parameter, fixed effect parameter
σ^2	variance of ε
ω^2	variance of η

CHAPTER 1

Introduction

1.1 Pharmacometrics

The drug development process is more time-consuming, expensive, and complex than it has been in the past (1). At the same time, optimization of pharmacotherapy is needed in order to improve dosing strategies and obtain the maximum efficacy while minimizing adverse events. Tools and technologies are required to improve drug development and pharmacotherapy. Pharmacometrics provides an application of pharmacokinetic /pharmacodynamic (PK/PD) models, statistics, disease progression models, simulations, and computer modeling to enhance an improvement in both drug development and therapeutics. The term pharmacometrics refers to the science of developing and applying statistical and mathematical methods to characterize and predict pharmacokinetics, pharmacodynamics of the drug and biomarker-outcomes behavior (2). In other word, pharmacometrics is the study of pharmacology in a quantitative fashion. In drug development, pharmacometrics involves the study of PK/PD and disease progression models, by means of modeling and simulations. It allows for comparing clinical outcomes from various study designs for determining the optimal dose selection and trial design to be used in the late phase trials. Additionally, it can make use of data already available to answer further questions replacing the need for a costly intensive pharmacokinetic study. Moreover, pharmacometrics can be useful to gain pharmacokinetic information in special populations, such as pediatric, elderly and critically ill patients, in which an intensive pharmacokinetic study may not be applicable.

In the area of pharmacotherapy, pharmacometrics can be applied to individualize drug therapy by prospectively predicting doses to be used in clinical practice to optimize safety and efficacy of the drugs given to patients.

1.1.1 Population pharmacokinetic/pharmacodynamic (PK/PD) modeling

Traditional pharmacokinetic analysis, in which the model is fit to data from each individual separately, involves intensive sampling and a stringent design in a small homogenous group of individuals. These individuals may not be representative of the target population to be treated with the drug. The challenge was to develop a quantitative, yet pragmatic approach to implement the use of data with limited sampling from a clinical study or therapeutic drug monitoring (TDM) setting which is obtained from a target patient population. In the early 1980s, Sheiner, Beal and colleagues published a series of papers presenting a new approach for analyzing PK/PD data (3-6). This was considered an introduction of population pharmacokinetics to the area of clinical pharmacology. Population pharmacokinetics is the study of the sources and correlates of variability in drug concentrations in the population of interest (7). It was first introduced with the intent to estimate population pharmacokinetic parameters from routine clinical care data by means of nonlinear mixed-effect modeling (6). This approach allows data from all individuals to be analyzed simultaneously and facilitates the differentiation between the interindividual and residual variability.

1.1.2 The nonlinear mixed effects model

Nonlinear mixed effects modeling was first introduced to the PK/PD community for analyzing the observational data (data with a limited number of samples and a lack of control over the sampling time) (8). The term "mixed" refers to the combined influence of fixed and random effects on the observed concentrations. The fixed-effect parameters measure the population average value of pharmacokinetic parameters and the average relationship between patient covariates and pharmacokinetic parameters (9). The random effect parameters measure the variability of the pharmacokinetics that is not explained by the fixed effects (i.e., interindividual variability, inter-occasion variability, and residual variability) (10). The nonlinear mixed effects model consists of three sub-models: structural, covariate, and a statistical or variance model. The structural model is the pharmacokinetic/pharmacodynamic model that best describes the measured data. The covariate model describes the relationship between subject specific covariates and pharmacokinetic parameters. The statistical model, consisting of the interindividual and the residual variability, characterizes the overall variability in the measured data.

Using a one-compartment model with a single intravenous bolus dose administration as an example, a general model for the mixed effect modeling to describe the j^{th} measurement in the i^{th} subject can be written as:

$$y_{ij} = \frac{D_i}{V_i} e^{-(CLi/Vi)t} + \varepsilon_{ij}$$

$$\varepsilon_{ij} = N(0, \sigma^2)$$

where y_{ij} is the j[th] measurement in the i[th] subject, D_i is the dose given to each individual, V_i and CL_i are the pharmacokinetic parameters for the i[th] subject, and ε_{ij} is the residual unexplained variability (RUV) (e.g., model misspecification, assay errors, and dosing history errors) for the j[th] measurement in the i[th] subject which is assumed to be normally distributed with a mean of zero and variance σ^2.

The interindividual variability (IIV) allows the pharmacokinetic parameters to vary across individuals and, sometimes, parts of the variability in the pharmacokinetic parameters can be explained by a set of subject specific covariates such as creatinine clearance (CRCL). For example, if the clearance is a function of CRCL, the individual clearance (CL_i) can be described by:

$$CL_i = \theta_1 + \theta_2 \times CRCL + \eta_i$$

where CL_i describes the clearance for an i[th] individual, θ_1 *and* θ_2 describe the linear dependence of CL_i on *CRCL* and η_i is the interindividual variability accounting for the difference between the population mean clearance (TVCL) and CL_i which is assumed to be normally distributed with a mean of zero and variance of ω_{CL}^2. The variance-covariance matrix of ηs for parameters in the model (Ω) will be estimated in this step.

1.2 The covariate model building

Covariates are the variables that are specific to an individual and that describe individual demographics or extrinsic factors such as age, height, weight, smoking status, and co-medications. The covariate model building step is one of the important steps in population PK/PD modeling. The goal of this step is to identify and quantify the relationships between pharmacokinetic parameters and patient specific covariates, and to explain part of the variability in the pharmacokinetic parameter. From a survey of the literature of the population PK/PD model building strategies by Dartois (11), covariate testing is one of the main objectives for 70% of the published population pharmacokinetic modeling papers. The covariate model building step can be time consuming and difficult especially if a large number of covariates are considered. Several approaches (e.g., graphical assessment, generalized additive model (GAM) (12), stepwise forward inclusion and backward elimination (13)) have been used for selecting important covariates. Among several approaches, the stepwise procedure is the most frequently used in covariate model building (14). However, the stepwise procedure is affected by general problems. It suffers from the risk of including false covariates into the model especially when the sample size is small and a high correlation among covariates is presented (15). Also, a limited power to select important covariates in small data sets is observed (16). Moreover, the stepwise procedure tends to overestimate the covariate coefficient when that covariate is selected to be included in the model, which is known as a "selection bias" (15-17).

1.2.1 Collinearity

When multiple covariates are considered, a common problem that may arise is the collinearity among covariates. Collinearity refers to the presence of a nearly exact linear relation among the independent variables (18). In other words, collinearity refers to a situation in which independent variables are highly correlated. When two highly correlated covariates are simultaneously entered into a model, several consequences are of concern (19). First, the regression coefficients tend to have a large sampling variability. This leads to a statistical non-significance of the estimated regression coefficients, even though true relationships exist. Second, the estimated coefficients tend to vary from sample to sample. Third, an incorrect magnitude of the coefficients may be obtained. Finally, the estimated coefficients may exhibit signs that are wrong and not physiological possible. A study by Ribbing and Jonsson (15) shows that when the correlation between the true and false covariates increases, the risk of selecting the false covariate (or making type II error) is higher because the false but highly correlated covariate is sometimes substituted for the true covariate. Another situation that frequently occurs in population covariate model building is when two true covariates are highly correlated and, commonly, both of them are considered to be tested for their significance in covariate model building. This situation may impact the power of selecting the true covariates. Unfortunately, until now, no investigation regarding the impact of the correlation between two true covariates on the power of selecting the true covariates during stepwise covariate model building in the population pharmacokinetic modeling has been made.

1.3 Model evaluation

A population pharmacokinetic model can be developed based on either descriptive or predictive purposes. Therefore, model evaluation should be performed depending on the intended use of the developed model (20). For a descriptive model, it is developed to explain the variability of the pharmacokinetics of a drug in the population. Therefore, the model should be assessed for its goodness of fit, reliability and stability. When the model is developed for predictive purposes, an assessment of the predictive performance should be required. Several approaches have been applied for model evaluation in the population PK/PD analysis including internal validation (e.g., data splitting, resampling techniques, and simulations) and external validation (21). However, only the resampling techniques and simulation-based techniques will be emphasized in this dissertation.

1.3.1 Resampling technique: nonparametric bootstrap

1.3.1.1 The bootstrap confidence interval

The confidence intervals of parameters obtained from NONMEM are generally estimated by assuming the asymptotic normality, which is only true when sample size is large (22). As an alternative to the asymptotic confidence intervals, the nonparametric bootstrap can be applied to obtain the confidence intervals of the parameter estimates in a nonsynthetic way (no asymptotic normal distribution is assumed). The bootstrap method was first introduced by Efron in 1979 (23). The idea of the nonparametric bootstrap is to repeatedly generate a pseudosample with the same size as the original (observed) sample by sampling with replacement from the original data. For each pseudosample data set, the bootstrap estimate of the statistic of interest can be computed. These steps will be

repeated many times to empirically obtain the observed statistic's sampling distribution. In population PK/PD modeling, the bootstrap approach is applied to re-estimate the final parameter estimates and their 95% confidence intervals (CI). These CI do not make any assumptions about the underlying distribution of the parameters. The bottom line is if the parameter estimates from the bootstrap approach are in close agreement with the values obtained from NONMEM, those parameter estimates are proved to be reliable. To obtain a bootstrap 95% CI, a large number of the bootstrap data sets (≥ 200) are generated. The final population pharmacokinetic model is fitted to each of the bootstrap data. The parameter estimates obtained from all of the bootstrap data are rank ordered. The values at the 2.5^{th} and 97.5^{th} percentile of the rank ordering values are used as the lower and upper boundaries of the bootstrap 95% CI (20).

1.3.1.2 The bootstrap predictive performance assessment

Another application of the bootstrap approach is for the predictive performance assessment. This approach is attractive because it does not require an external data set, therefore, the entire data set can be used for model development. Moreover, the bootstrap provides a nearly unbiased estimate of prediction error with considerably less variance than the cross-validation approach (24). In general, the prediction error metrics (e.g., the mean square error (MSE) and mean absolute error (MAE)) that are obtained from applying the final model to the data from which it was derived tend to be overly optimistic when compared with applying the model to the external data sets (25). The random variable of interest is the "optimism" (OPT) for each of the metrics. OPT is the expected difference of the prediction error metric when the model is applied to its own

data compared to when the model is applied to the external data set (20,26). The OPT for each prediction error metric is calculated and added to the prediction error metric estimated from applying the final model to the original data to obtain the improved prediction error metric. The improved prediction error metric would then approach the value obtained when applying the final model to an external data set. When the OPT is relatively small (less than 0.15 times the improved prediction error metric), this indicates that the model is without substantial deficiency (20).

1.3.2 Simulation-based technique: The predictive check

The simulation-based techniques have been increasingly used for model evaluation in population PK/PD modeling. Yano et al. (27) introduced the application of a posterior predictive check (PPC) for the population pharmacokinetic model evaluation. In this approach, a summary feature of the observed data (called a statistic) is first computed, and then the adequacy of the developed model in explaining the observed data can be assessed by comparing the statistic computed from the observed data to its distribution obtained from the simulation based approach (27). The true PPC requires the drawing of random samples from the posterior distribution of the parameters which is a computationally burdensome procedure (28). However, Yano et al. (27) show that drawing random samples from the maximum likelihood parameter estimates performs as well as drawing samples from the posterior distribution itself. When random samples are drawn from the maximum likelihood estimations, PPC should be called a "predictive check (PC)" (29). Whereas the PPC focuses on comparing a statistic which can be derived from both the observed and simulated data, the visual predictive check (VPC),

originated from PPC, is based on a graphical comparison between the prediction intervals obtained from the simulations and the observed data (30). Both PPC and VPC are based on the premise that if the model derived from the observed data is adequate, it should generate similar data as the observed data when used in the simulation setting.

1.4 Pharmacokinetics of antiepileptic drugs

1.4.1 Pharmacokinetics of lamotrigine

Lamotrigine (LTG) is a new generation antiepileptic drug (AED). LTG blocks voltage-gated sodium channels and inhibits the release of glutamate which is the major excitatory neurotransmitter in the mammalian brain (31). LTG is a phenyltriazine and is chemically unrelated to any other established AED (32). It is approved as monotherapy and adjunctive treatment for the treatment of partial and generalized tonic-clonic seizures. Pharmacokinetics of LTG have been extensively studied in adult healthy volunteers, patients with renal impairment and chronic renal failure, and young patients with epilepsy (33-39).

1.4.1.1 Absorption and distribution

A study in healthy volunteers receiving single and multiple doses of LTG shows that LTG is rapidly absorbed after oral administration with the time to maximum concentration of 1-3 hours and an absolute bioavailability of 98% (33,40). Plasma protein binding of LTG in human was estimated to be 56% by an equilibrium analysis and was considered to be constant over its therapeutic concentrations (1-4 mcg/ml). Therefore, protein binding is not thought to be an issue. The apparent volume of distribution (V/F)

of LTG ranges from 77 to 133 L as reported in adult healthy volunteers and patients with epilepsy (33,35,38,39).

1.4.1.2 Metabolism and excretion

LTG is a weak base which is extensively metabolized by uridine 5'-diphosphate (UDP)-glucuronosyl-transferases. The studies of LTG metabolism identify a quaternary glucuronide at the N-2 position of the triazine ring as a major metabolite which can be found approximately 80% of the given dose (41-43). Another glucuronide conjugate, N-5 glucuronide, is a minor metabolite (10%). Only 10% of the dose is excreted unchanged in the urine (43). All of the metabolites are excreted in the urine in a pharmacologically inactive form.

The apparent clearance of LTG (CL/F) in adult healthy volunteers is reported to be between 1.6 and 2.6 L/hr corresponding to a half-life of 24 to 35 hours (32). LTG exhibits linear pharmacokinetics and the pharmacokinetics of LTG can be adequately described by a one compartment model with the first order absorption and first order elimination (35).

The pharmacokinetics of LTG can be affected by other AEDs i.e., phenytoin (PHT), carbamazepine (CBZ), phenobarbital (PB), primidone and valproic acid (VPA). LTG clearance significantly increases in patients co-medicated with other enzyme inducing drugs such as PHT, CBZ, PB, and primidone. The mean half life of LTG is decreased to approximately 14 hours in patients receiving LTG with other enzyme-inducing AEDs

(44). On the other hand, VPA competitively inhibits glucuronidation of LTG; therefore, co-administration with VPA substantially decreases LTG clearance by 50% resulting in a two-fold increase of the LTG half-life (45,46). However, the effect of the combination of an enzyme inducing AED and VPA on lamotrigine disposition appears to compensate each other effect and, therefore, gives the LTG half-life similar to those receiving LTG monotherapy (44).

1.4.1.3 Pharmacokinetics of lamotrigine in the elderly

The treatment of epilepsy in certain groups of patients requires particular care and special considerations due to physical and metabolic differences (47). In the elderly, epilepsy is common and the treatment in this patient population can be challenging. Changes in body composition, hepatic and renal function due to aging may impact drug's pharmacokinetics which may affect the safety and efficacy of drug therapy in this population. Moreover, the increasing number of co-medications used by this population increases the susceptibility of this population to drug-interactions. It has been thought that most cytochrome P450 (CYP) isoenzyme activities are decreased in older age; whereas, phase II enzyme activities are less affected by aging (48). LTG is primarily metabolized by glucuronidation; therefore, the effect of aging on its metabolism is believed to be minimal. LTG pharmacokinetics have been well studied in adult healthy volunteers and patients with epilepsy. However, the impact of age on LTG pharmacokinetics is not well described. Few studies have investigated the influence of age on LTG pharmacokinetics. Posner et al (49) evaluated the pharmacokinetics of LTG after a single oral dose of 150 mg of LTG in healthy volunteers aged 65-76 years (N=12)

as compared to a younger group of volunteers aged 26-38 years (N=12). They found a 37% decreased in the LTG clearance in the elderly groups. The mean LTG half-life was reported to be 31 hours in the elderly group and 25 hours in the younger adult volunteers. Surprisingly, population pharmacokinetic studies of LTG show no impact of aging on LTG pharmacokinetics (37-39). Therefore, the influence of advanced age on LTG pharmacokinetics needs to be further investigated to optimally treat elderly population.

1.4.2 Pharmacokinetics of carbamazepine

Carbamazepine (CBZ) is approved for the treatment of several types of seizures including partial and generalized tonic-clonic seizures and bipolar disorder (50). Also, it is the first drug of choice for trigeminal neuralgia treatment (51). The anticonvulsant property of CBZ is exerted by blocking the sodium channel; therefore, stabilizing the inactive form of the sodium channel (52,53). Moreover, recent studies show that CBZ can inhibit glutamatergic neurotransmission which may also contribute to its anticonvulsant activity (53). CBZ exhibits complicated pharmacokinetics including a high variability in absorption, a narrow therapeutic index, and an enzyme inducing property.

1.4.2.1 Absorption and distribution

The absorption of CBZ after oral administration is slow and unpredictable (54). The time to peak plasma concentration varies widely from 4 hour to as late as 24 hours (55-58). The delayed and irregular absorption is believed to be due to a slow dissolution rate (59). The absolute bioavailability of CBZ has not been determined due to the unavailability of an intravenous formulation. However, the oral bioavailability estimated from the use of

radio labeled CBZ is reported to be between 75% and 85% (54). CBZ is a highly protein-bound drug with approximately 75% of CBZ bound to plasma protein in the concentration range of 5-30 mcg/ml (60). Even though, CBZ is mainly bound to albumin, other proteins such as α_1-acid glycoprotein may be implicated (61,62). The apparent volume of distribution of CBZ ranges between 0.8 and 2.0 L/kg (51). These estimated numbers may be higher than the real value of CBZ volume of distribution due to the possibility of incomplete bioavailability.

1.4.2.2 Metabolism and excretion

CBZ is almost completely metabolized in humans with only 2% of the dose being excreted unchanged in the urine (63). The biotransformation of CBZ is mostly via two oxidative pathways: the epoxidation and aromatic hydroxylation. The epoxidation is the most important pathway yielding CBZ-10,11-epoxide (CBZ-E) as an active metabolite. CBZ-E is comparatively stable and has its own antiepileptic activity. However, only a small amount of CBZ-E (1-2 % of the dose) is found in the urine as it is enzymatically hydrolyzed to trans-10,11-dihydroxy-CBZ (CBZ-diol) before being excreted via the urine (64). CYP3A4 and CYP2C8 is a principle and minor enzyme responsible for biotransformation of CBZ to CBZ-E, whereas CYP1A2 is a major enzyme responsible for hydroxylation of CBZ (65).

1.4.2.3 Pharmacokinetics of carbamazepine in the elderly

The effect of age on CBZ pharmacokinetics is not well studied and still controversial. In a previous study (66), the pharmacokinetics of a single oral dose of CBZ were compared

between a group of six healthy young volunteers (aged 20-25 years) and five elderly healthy volunteers (aged 66-84 years). No significant differences of CBZ pharmacokinetics were observed between the young and elderly groups. Conversely, a population pharmacokinetic study by Graves et al (67) shows that CL/F decreased approximately 25% in patients aged 70 years or older. Moreover, a case-matched study by Battino et al (68) shows a 23% reduction of CBZ CL/F in elderly patient groups (aged 65 years and older) compared with younger patients (aged 20-50 years) receiving CBZ monotherapy of CBZ. However, few elderly patients were included in these studies and; thus, the influence of age on pharmacokinetics of CBZ needs to be further investigated.

1.5 Autoinduction/deinduction of carbamazepine

A previous CBZ pharmacokinetic study in adult healthy volunteers shows that CBZ half-life following a single dose administration ranges from 18 to 55 hours, whereas following multiple administrations of CBZ, the half-life was reported to be shorter (16.4-26.6 hours) (69). These results suggest that CBZ exhibits autoinduction, a phenomenon in which a drug's clearance increases with time after repeated administrations. This situation has been defined as time-dependent kinetics. It is well documented that CBZ is a potent inducer of other drugs' metabolism and it undergoes autoinduction leading to a complex pharmacokinetic profile (58,69,70). Previous studies demonstrate that both CBZ and its metabolite, CBZ-E, induce several enzymes including multiple CYP isoenzymes, conjugating enzymes, and transporters in human and rats (71,72). The mechanism of enzyme induction of CBZ involves *de novo* protein synthesis (73). An increase of the

specific protein levels is believed to be a consequence of an increasing gene transcription. Deinduction, a reverse process of autoinduction, occurs when chronic CBZ therapy is discontinued. Based on a current understanding of the autoinduction mechanism, deinduction is due to a decrease in enzyme synthesis resulting in a decrease of the amount of enzyme. The time course of autoinduction/deinduction is important to optimally adjust the CBZ dosage regimens and other co-medications during initiating or terminating CBZ therapy.

1.5.1 Pharmacokinetic model for autoinduction/deinduction: The application of an enzyme turnover model

Attempts to develop a pharmacokinetic model to characterize the time course of autoinduction/deinduction were made. Levy et al (74) proposed a model in which the drug clearance can be calculated at any time during the induction process as described by equation 1.1.

$$CL(t) = CL' - ((CL' - CL) \times e^{-k't}) \quad (1.1)$$

where CL(t) is the clearance at any time during the induction process, CL' is the clearance at the new steady state post-induction, CL is the pre-induction clearance, and k' represents the first-order degradation rate constant of the induced enzyme. This time dependent clearance model (described in equation 1.1) allows clearance to be increased mono-exponentially during the induction process.

The application of an enzyme turnover model where the concentration of the inducer is counter-balanced by the amount of the induced enzyme was first introduced by Scheyer et al (75). This model has been widely used to describe the time course of enzyme induction (76-79). The enzyme turnover model consists of a hypothetical enzyme compartment which is governed by a zero-order rate of enzyme synthesis ($k_{enz,\ in}$) and a first order rate constant of enzyme degradation ($k_{enz,\ out}$). Induction can be achieved by either increasing the rate of enzyme synthesis or decreasing the rate of enzyme degradation. Conversely, deinduction can be described by decreasing of the rate of enzyme synthesis or increasing of the rate of enzyme degradation. This model assumes that the amount of enzyme is proportional to drug clearance.

1.6 Aims of dissertation

The general aims of this dissertation were to quantitatively study the pharmacokinetics of LTG and CBZ in community-dwelling elderly epilepsy patients which provides useful information for dose optimization in this population and to identify and quantify important covariates affecting pharmacokinetic parameters of these drugs by nonlinear mixed effect modeling. During the covariate model building of LTG, a collinearity between blood urea nitrogen/serum creatinine ratio (BUN/CR) was observed. The simulation-based study was further performed to investigate the effect of collinearity on the power, bias and precision of parameter estimates. Furthermore, this dissertation also aimed to apply an enzyme turnover model to characterize the time course of CBZ deinduction in patients with epilepsy.

1.7 References

1. DiMasi JA, Hansen RW, Grabowski HG. The price of innovation: new estimates of drug development costs. *J Health Econ*. 2003;22(2):151-185.
2. Williams PJ, Ette EI. Pharmacometrics: Impacting Drug Development and Pharmacotherapy. In: Williams PJ, Ette EI, editors. *Pharmacometrics: The Science of Quantitative Pharmacology*, New Jersey: John Wiley&Sons, Inc., 2007.
3. Sheiner LB, Beal SL. Evaluation of methods for estimating population pharmacokinetic parameters. II. Biexponential model and experimental pharmacokinetic data. *J Pharmacokinet Biopharm*. 1981;9(5):635-651.
4. Sheiner LB, Beal SL. Evaluation of methods for estimating population pharmacokinetics parameters. I. Michaelis-Menten model: routine clinical pharmacokinetic data. *J Pharmacokinet Biopharm*. 1980;8(6):553-571.
5. Sheiner LB, Beal SL. Evaluation of methods for estimating population pharmacokinetic parameters. III. Monoexponential model: routine clinical pharmacokinetic data. *J Pharmacokinet Biopharm*. 1983;11(3):303-319.
6. Sheiner LB, Rosenberg B, Marathe VV. Estimation of population characteristics of pharmacokinetic parameters from routine clinical data. *J Pharmacokinet Biopharm*. 1977;5(5):445-479.
7. Sun H, Fadiran EO, Jones CD, et al. Population pharmacokinetics. A regulatory perspective. *Clin Pharmacokinet*. 1999;37(1):41-58.
8. Grasela TH, Sheiner BL. Pharmacostatistical Modeling for Observational Data. *J Pharmacokinet Biopharm*. 1991;19(3):25S-36S.
9. Sheiner BL, Grasela TH. An Introduction to Mixed Effect Modeling: Concepts, Definitions, and Justification. *J Pharmacokinet Biopharm*. 1991;19(3):11S-23S.
10. Ette EI, Williams PJ. Population pharmacokinetics I: background, concepts, and models. *Ann Pharmacother*. 2004;38(10):1702-1706.
11. Dartois C, Brendel K, Comets E, et al. Overview of model-building strategies in population PK/PD analyses: 2002-2004 literature survey. *Br J Clin Pharmacol*. 2007;64(5):603-612.

12. Mandema JW, Verotta D, Sheiner LB. Building population pharmacokinetic--pharmacodynamic models. I. Models for covariate effects. *J Pharmacokinet Biopharm*. 1992;20(5):511-528.
13. Jonsson EN, Karlsson MO. Automated covariate model building within NONMEM. *Pharm Res*. 1998;15(9):1463-1468.
14. Wahlby U, Jonsson EN, Karlsson MO. Comparison of stepwise covariate model building strategies in population pharmacokinetic-pharmacodynamic analysis. *AAPS PharmSci*. 2002;4(4):E27.
15. Ribbing J, Jonsson EN. Power, selection bias and predictive performance of the Population Pharmacokinetic Covariate Model. *J Pharmacokinet Pharmacodyn*. 2004;31(2):109-134.
16. Steyerberg EW, Eijkemans MJ, Habbema JD. Stepwise selection in small data sets: a simulation study of bias in logistic regression analysis. *J Clin Epidemiol*. 1999;52(10):935-942.
17. Miller AJ. Selection of subsets of regression variables. *J R Stat Soc Series A (General)*. 1984;147:389-425.
18. Hocking RR. Developments in Linear-Regression Methodology - 1959-1982. *Technometrics*. 1983;25(3):219-230.
19. Bonate PL. *Pharmacokinetic-Pharmacodynamic Modeling and Simulation*: Springer Science+Business Media, Inc. 2006.
20. Ette EI, Williams PJ, Kim YH, Lane JR, Liu MJ, Capparelli EV. Model appropriateness and population pharmacokinetic modeling. *J Clin Pharmacol*. 2003;43(6):610-623.
21. Brendel K, Dartois C, Comets E, et al. Are population pharmacokinetic and/or pharmacodynamic models adequately evaluated? A survey of the literature from 2002 to 2004. *Clin Pharmacokinet*. 2007;46(3):221-234.
22. Yafune A, Ishiguro M. Bootstrap approach for constructing confidence intervals for population pharmacokinetic parameters. I: A use of bootstrap standard error. *Stat Med*. 1999;18(5):581-599.
23. Efron B. Bootstrap methods: another look at the jackknife. *Ann Stat*. 1979;7:1-26.

24. Efron B. Estimating the error rate of a prediction rule: improvement on cross-validation. *J Am Stat Assoc*. 1983;78:316-331.
25. Efron B, Gong G. A leisurely look at the bootstrap, the jacknife, and cross-validation. *Am Stat*. 1983;37(1):36-48.
26. Ette EI. Stability and performance of a population pharmacokinetic model. *J Clin Pharmacol*. 1997;37(6):486-495.
27. Yano Y, Beal SL, Sheiner LB. Evaluating pharmacokinetic/pharmacodynamic models using the posterior predictive check. *J Pharmacokinet Pharmacodyn*. 2001;28(2):171-192.
28. Gelman A, Carlin JB, Stern H, Rubin DB. *Bayesian Data Analysis*, London: Chapman and Hall. 1995.
29. Jadhav PR, Gobburu JV. A new equivalence based metric for predictive check to qualify mixed-effects models. *Aaps J*. 2005;7(3):E523-531.
30. Holford NH. The Visual Predictive Check: Superior to Standard Diagnostic (Rorschanch) Plots. PAGE 14, 2005.
31. Leach MJ, Lees G, Riddall DR. Lamotrigine: Mechamism of Action. In: Levy RH, Mattson RH, Meldrum BS, editors. *Antiepileptic Drugs*, 4th ed., New York: Raven Press, 1995.
32. Garnett WR. Lamotrigine: pharmacokinetics. *J Child Neurol*. 1997;12 Suppl 1:S10-15.
33. Cohen AF, Land GS, Breimer DD, Yuen WC, Winton C, Peck AW. Lamotrigine, a new anticonvulsant: pharmacokinetics in normal humans. *Clin Pharmacol Ther*. 1987;42(5):535-541.
34. Fillastre JP, Taburet AM, Fialaire A, Etienne I, Bidault R, Singlas E. Pharmacokinetics of lamotrigine in patients with renal impairment: influence of haemodialysis. *Drugs Exp Clin Res*. 1993;19(1):25-32.
35. Ramsay RE, Pellock JM, Garnett WR, et al. Pharmacokinetics and safety of lamotrigine (Lamictal) in patients with epilepsy. *Epilepsy Res*. 1991;10(2-3):191-200.

36. Wootton R, Soul-Lawton J, Rolan PE, Sheung CT, Cooper JD, Posner J. Comparison of the pharmacokinetics of lamotrigine in patients with chronic renal failure and healthy volunteers. *Br J Clin Pharmacol*. 1997;43(1):23-27.
37. Chan V, Morris RG, Ilett KF, Tett SE. Population pharmacokinetics of lamotrigine. *Ther Drug Monit*. 2001;23(6):630-635.
38. Grasela TH, Fiedler-Kelly J, Cox E, Womble GP, Risner ME, Chen C. Population pharmacokinetics of lamotrigine adjunctive therapy in adults with epilepsy. *J Clin Pharmacol*. 1999;39(4):373-384.
39. Hussein Z, Posner J. Population pharmacokinetics of lamotrigine monotherapy in patients with epilepsy: retrospective analysis of routine monitoring data. *Br J Clin Pharmacol*. 1997;43(5):457-465.
40. Peck AW. Clinical pharmacology of lamotrigine. *Epilepsia*. 1991;32 Suppl 2:S9-12.
41. Magdalou J, Herber R, Bidault R, Siest G. In vitro N-glucuronidation of a novel antiepileptic drug, lamotrigine, by human liver microsomes. *J Pharmacol Exp Ther*. 1992;260(3):1166-1173.
42. Sinz MW, Remmel RP. Isolation and characterization of a novel quaternary ammonium-linked glucuronide of lamotrigine. *Drug Metab Dispos*. 1991;19(1):149-153.
43. Doig MV, Clare RA. Use of thermospray liquid chromatography-mass spectrometry to aid in the identification of urinary metabolites of a novel antiepileptic drug, Lamotrigine. *J Chromatogr*. 1991;554(1-2):181-189.
44. Jawad S, Yuen WC, Peck AW, Hamilton MJ, Oxley JR, Richens A. Lamotrigine: single-dose pharmacokinetics and initial 1 week experience in refractory epilepsy. *Epilepsy Res*. 1987;1(3):194-201.
45. Kanner AM, Frey M. Adding valproate to lamotrigine: a study of their pharmacokinetic interaction. *Neurology*. 2000;55(4):588-591.
46. Yau MK, Wargin WA, Wolf KB. Effect of valproate on the pharmacokinetics of lamotrigine at steady state. *Epilepsia*. 1992;33(Suppl 3):82.

47. Leppik IE. Treatment of epilepsy in 3 specialized populations. *Am J Manag Care*. 2001;7(7 Suppl):S221-226.
48. McLean AJ, Le Couteur DG. Aging biology and geriatric clinical pharmacology. *Pharmacol Rev*. 2004;56(2):163-184.
49. Posner J, Holdich T, Crome P. Comparison of lamotrigine pharmacokinetics in young and elderly healthy volunteers. *J Pharm Med*. 1991;1:121-128.
50. El-Mallakh R, Weisler RH, Townsend MH, Ginsberg LD. Bipolar II disorder: current and future treatment options. *Ann Clin Psychiatry*. 2006;18(4):259-266.
51. Bertilsson L. Clinical pharmacokinetics of carbamazepine. *Clin Pharmacokinet*. 1978;3(2):128-143.
52. Davies JA. Mechanisms of action of antiepileptic drugs. *Seizure*. 1995;4(4):267-271.
53. Kwan P, Sills GJ, Brodie MJ. The mechanisms of action of commonly used antiepileptic drugs. *Pharmacol Ther*. 2001;90(1):21-34.
54. Morselli PL. Carbamazepine: Absorption, Distribution, and Excretion. In: Levy RH, Mattson RH, Meldrum BS, editors. *Antiepileptic Drugs*, 4th ed., New York: Raven Press, 1995.
55. Cotter LM, Eadie MJ, Hooper WD, Lander CM, Smith GA, Tyrer JH. The pharmacokinetics of carbamazepine. *Eur J Clin Pharmacol*. 1977;12(6):451-456.
56. Rawlins MD, Collste P, Bertilsson L, Palmer L. Distribution and elimination kinetics of carbamazepine in man. *Eur J Clin Pharmacol*. 1975;8(2):91-96.
57. Smith GA, Hooper WD, Tyrer JH, Eadie MJ, Werth B. The comparative bioavailability of carbamazepine in 100 mg and 200 mg tablets. *Clin Exp Pharmacol Physiol*. 1979;6(1):37-40.
58. Geradin AP, Abadie FV, Campestrini JA, Theobald W. Pharmacokinetics of carbamazepine in normal humans after single and repeated oral doses. *J Pharmacokinet Biopharm*. 1976;4(6):521-535.
59. Levy RH, Pitlick WH, Troupin AS, Green JR, Neal JM. Pharmacokinetics of carbamazepine in normal man. *Clin Pharmacol Ther*. 1975;17(6):657-668.

60. Di Salle E, Pacifici GM, Morselli PL. Studies on plasma protein binding of carbamazepine. *Pharmacol Res Commun*. 1974;6(2):193-202.

61. Baruzzi A, Contin M, Perucca E, Albani F, Riva R. Altered serum protein binding of carbamazepine in disease states associated with an increased alpha 1-acid glycoprotein concentration. *Eur J Clin Pharmacol*. 1986;31(1):85-89.

62. Contin M, Riva R, Albani F, Perucca E, Lamontanara G, Baruzzi A. Alpha 1-acid glycoprotein concentration and serum protein binding of carbamazepine and carbamazepine-10,11 epoxide in children with epilepsy. *Eur J Clin Pharmacol*. 1985;29(2):211-214.

63. Faigle JW, Feldmann KF. Carbamazepine: Chemistry and Biotransformation. In: Levy RH, Mattson RH, Meldrum BS, editors. *Antiepileptic Drugs*, 4th ed., New York: Raven Press, 1995.

64. Baker KM, Csetenyi J, Frigerio A, Morselli PL, Parravicini F, Pifferi G. 10,11-Dihydro-10,11-dihydroxy-5H-dibenz(b,f)azepine-5-carboxamide, a metabolite of carbamazepine isolated from human and rat urine. *J Med Chem*. 1973;16(6):703-705.

65. Kerr BM, Thummel KE, Wurden CJ, et al. Human liver carbamazepine metabolism. Role of CYP3A4 and CYP2C8 in 10,11-epoxide formation. *Biochem Pharmacol*. 1994;47(11):1969-1979.

66. Hockings N, Pall A, Moody J, Davidson AV, Davidson DL. The effects of age on carbamazepine pharmacokinetics and adverse effects. *Br J Clin Pharmacol*. 1986;22(6):725-728.

67. Graves NM, Brundage RC, Wen Y, et al. Population pharmacokinetics of carbamazepine in adults with epilepsy. *Pharmacotherapy*. 1998;18(2):273-281.

68. Battino D, Croci D, Rossini A, Messina S, Mamoli D, Perucca E. Serum carbamazepine concentrations in elderly patients: a case-matched pharmacokinetic evaluation based on therapeutic drug monitoring data. *Epilepsia*. 2003;44(7):923-929.

69. Eichelbaum M, Ekbom K, Bertilsson L, Ringberger VA, Rane A. Plasma kinetics of carbamazepine and its epoxide metabolite in man after single and multiple doses. *Eur J Clin Pharmacol*. 1975;8(5):337-341.

70. Pitlick WH, Levy RH. Time-dependent kinetics I: Exponential autoinduction of carbamazepine in monkeys. *J Pharm Sci*. 1977;66(5):647-649.

71. Oscarson M, Zanger UM, Rifki OF, Klein K, Eichelbaum M, Meyer UA. Transcriptional profiling of genes induced in the livers of patients treated with carbamazepine. *Clin Pharmacol Ther*. 2006;80(5):440-456.

72. Tateishi T, Asoh M, Nakura H, et al. Carbamazepine induces multiple cytochrome P450 subfamilies in rats. *Chem Biol Interact*. 1999;117(3):257-268.

73. Okey AB. Enzyme induction in the cytochrome P-450 system. *Pharmacol Ther*. 1990;45(2):241-298.

74. Levy RH, Lai AA, Dumain MS. Time-dependent kinetics IV: Pharmacokinetic theory of enzyme induction. *J Pharm Sci*. 1979;68(3):398-399.

75. Scheyer RD, Cramer JA, Mattson RH. A pharmacodynamic approach to the estimate of carbamazepine autoinduction. *J Pharm Sci*. 1994;83(4):491-494.

76. Hassan M, Svensson US, Ljungman P, et al. A mechanism-based pharmacokinetic-enzyme model for cyclophosphamide autoinduction in breast cancer patients. *Br J Clin Pharmacol*. 1999;48(5):669-677.

77. Huitema AD, Mathot RA, Tibben MM, Rodenhuis S, Beijnen JH. A mechanism-based pharmacokinetic model for the cytochrome P450 drug-drug interaction between cyclophosphamide and thioTEPA and the autoinduction of cyclophosphamide. *J Pharmacokinet Pharmacodyn*. 2001;28(3):211-230.

78. Kerbusch T, Huitema AD, Ouwerkerk J, et al. Evaluation of the autoinduction of ifosfamide metabolism by a population pharmacokinetic approach using NONMEM. *Br J Clin Pharmacol*. 2000;49(6):555-561.

79. Magnusson MO, Dahl ML, Cederberg J, Karlsson MO, Sandstrom R. Pharmacodynamics of Carbamazepine-mediated Induction of CYP3A4, CYP1A2, and Pgp as Assessed by Probe Substrates Midazolam, Caffeine, and Digoxin. *Clin Pharmacol Ther*. 2007

CHAPTER 2

Population Pharmacokinetics of Lamotrigine in Elderly Patients

2.1 Background and aims of the study

The study comparing LTG, CBZ and GPB shows that LTG may be a good choice for treating epilepsy in the elderly community dwelling patients (1). However, dosing of lamotrigine in elderly patients is based largely on studies from younger adults and not evidence-based data from studies in elderly patients. Age-related changes in physiology may affect a drug's pharmacokinetics: absorption, distribution, metabolism, and elimination. Therefore, it is possible that LTG pharmacokinetic parameters and the interindividual variability in these parameters will be different in elderly than in younger patients. Even though the pharmacokinetics of LTG have been well studied in adult healthy volunteers and younger patients (2-5), the investigation of influence of age on LTG pharmacokinetics has been understudied (6,7). Moreover, few elderly patients were included in these past studies and the influence of age on LTG pharmacokinetics is still controversial. An understanding of LTG pharmacokinetics in elderly patients is essential for optimal LTG treatment in this population.

The aims of this study were to estimate the population pharmacokinetic parameters of LTG and their variability in an elderly population and to describe the relationship between patient specific covariates including age, weight, race, renal function, liver function, phenytoin (PHT) use, smoking, and alcohol use and pharmacokinetic parameters.

2.2 Subjects and methods

2.2.1 Patients and data collection

This study was approved by the University of Minnesota's Human Subject's Committee as an exempt study. Data were obtained from the Department of Veterans Affairs (VA) Cooperative Study 428, a randomized, double-blind, parallel group, monotherapy comparison study of LTG, gabapentin (GBP), and CBZ in elderly patients with epilepsy (N=593) (1). The VA Cooperative Study 428 was approved by the central VA Human Rights Committee and all local institutional review boards. Patients 60 years or older with newly diagnosed seizures were randomly assigned to one of the three treatment groups. Data from the LTG arm were used in this analysis. The LTG dose was titrated at 25 mg/day for 2 weeks, 50 mg/day for 2 weeks, 100 mg/day for 1 week, followed by 150 mg/day. Patients were allowed to enter the study while they were on PHT therapy; however, the PHT doses were gradually withdrawn during the 6-week titration phase of LTG. Clinical evaluations and blood concentrations were obtained at enrollment, biweekly to week 8, monthly to week 28, and bimonthly to the end of the study (week 52). Time of blood draw, dosing history including the actual time and drug amount of the last three doses before sampling time, and updated comedications were obtained at each clinic visit. Ninety-five percent of the patients were determined to be adherent via pill counts.

2.2.2 Population pharmacokinetic analysis

Data were analyzed by a nonlinear mixed effects modeling approach using the NONMEM system (version V Level 1.1, NONMEM Project Group, UCSF/Globomax

and PDx-Pop version 1.1j release 4). Xpose 3.1 (8) and S-PLUS 2000 (Insightful Corp, Seattle, WA, USA) were used for goodness of fit assessment and model evaluation. A one-compartment model with first-order absorption and elimination was used (subroutine ADVAN2 TRANS 2) (9). The first-order conditional estimation method with interaction (FOCE-I) was used for all analyses. The pharmacokinetic parameters obtained from the model were: apparent clearance (CL/F), apparent volume of distribution (V/F), and absorption rate constant (K_a). The interindividual variability (IIV) was modeled using an exponential error model as given in equation 2.1.

$$P_i = TVP \times \exp(\eta_i), \tag{2.1}$$

where P_i describes the individual pharmacokinetic parameter, TVP represents the mean (typical) value of the pharmacokinetic parameter in the population, and η_i represents the interindividual variability which is assumed to be normally distributed with a mean of zero and variance of ω^2. The residual unexplained variability (RUV) was modeled using a combined proportional and additive error model as given in equation 2.2.

$$C_{obs,\,ij} = C_{pred,\,ij} \times (1+\varepsilon_{1,\,ij}) + \varepsilon_{2,\,ij}, \tag{2.2}$$

where $C_{obs,ij}$ and $C_{pred,\,ij}$ describe the j^{th} observed and predicted plasma concentrations in the i^{th} individual and ε_{ij} is the residual unexplained variability which is assumed to have a normal distribution with a mean of zero and variance of σ^2.

Initially, the model was developed without including patient specific covariates (base pharmacokinetic model). Before the covariate model building was performed, hypotheses were formulated concerning body size measurements, age, race, comedications, liver function, smoking, alcohol use, and renal function and how they may affect LTG CL/F. These covariates were selected based on their possible effects on the pharmacokinetics due to aging (10) (body size, decreased liver function, decreased renal function, decreased albumin levels), the administration of comedication present in this population, and the effects on liver metabolism in general (smoking, alcohol use, comedications). Race was tested as a covariate based on previous population pharmacokinetic studies of LTG in younger adults (11,12). During stepwise covariate model building, 19 covariates including all body size measurements (weight, body mass index [BMI], body surface area [BSA], ideal body weight [IBW], and lean body weight [LBW]); race; study center; PHT use; smoking; alcohol use; age; albumin (ALB); blood urea nitrogen (BUN); BUN/serum creatinine ratio (BUN/CR ratio); serum creatinine (CR); creatinine clearance (CRCL) which was calculated using Cockcroft-Gault equation; aspartate aminotransferase; alanine aminotransferase; and duration of therapy (week) were considered in the analysis. Age was tested as both a continuous and a categorical covariate (age $\leq$ 80, and age > 80 years). Due to the small sample size of some race categories, race was evaluated as a dichotomous covariate (White and non-White).

The significance of the patient specific covariates was evaluated by the improvement in the goodness of fit using the likelihood ratio test and visual inspection of diagnostic plots. The covariate model was built in a stepwise fashion. Each covariate was added to the

base model one at a time during forward selection. A decrease in the objective function value (OFV) of at least 6.64 (χ^2, $p \leq 0.01$, df=1) was considered significant for adding a single covariate into the model. The full model was developed by incorporating all significant covariates. Each covariate from the full model was deleted one at a time to obtain the final model using backward deletion. An increase of OFV from the full model of at least 10.83 (χ^2, $p \leq 0.001$, df=1) was used as the chosen criterion for retaining the covariate in the model.

2.2.3 Randomization test

A covariate randomization test, also called a permutation test, was applied to obtain the actual significance levels for each covariate effect under a given data set and analysis method (13,14). The idea behind the randomization test is to repeatedly generate a data set that would arise under the null hypothesis (for example, null hypothesis = no covariate effect). Then, the empirical distribution of a statistic of interest under the null hypothesis is obtained. To perform the randomization test, first, each covariate vector in the final model was randomly permuted; therefore, breaking any existing relationship between the covariate and pharmacokinetic parameters. The reduced model (a model without a parameter-covariate relationship) was fitted to the original data. A full model (a model including a parameter-covariate relationship) was fitted to each of the permuted data. The difference in the objective function value (dOFV) between a full and a reduced model was calculated. This process was repeated 2000 times. Finally, 2000 dOFVs were obtained and were rank ordered. The values corresponding to the 0.1^{th} and 1^{st} percentile represent the cutoff of dOFVs for actual significance levels of 0.001 and 0.01,

respectively. The randomization test was performed for each of the covariates separately, as the actual significance levels can be different for each covariate. All the covariate randomization procedures were performed using the randomization test option in Wings for NONMEM (version 409d, http://wfn.sourcefourge.net).

2.2.4 Model evaluation: The nonparametric bootstrap and predictive check

2.2.4.1 The bootstrap confidence interval

The reliability of the final population pharmacokinetic model was confirmed by reestimating the model parameter estimates and their 95% confidence intervals (CI) using a nonparametric bootstrap approach. One thousand bootstrap data sets were generated by repeated sampling with replacement from the original data set using the bootstrap option in Wings for NONMEM (version 409d, http://wfn.sourcefourge.net). The final population pharmacokinetic model was fitted to each of these bootstrap data. One thousand parameter estimates obtained from the bootstrap data were rank ordered. The values at 2.5^{th} and 97.5^{th} percentile of the rank ordering values were used as the lower and upper boundary of the bootstrap 95% CI (15) and were then compared with the values obtained from NONMEM.

2.2.4.2 The bootstrap predictive performance assessment

The predictive performance of the final model was assessed by two prediction error metrics (P_1 and P_2)—the mean squared error (MSE=P_1), the average of the squared difference between the observed and model predicted concentrations, and the mean absolute error (MAE=P_2), the average of the absolute difference between the observed

and model predicted concentrations. In this current analysis, two hundred bootstrap data sets were used and the optimism (OPT) for each of the prediction error metrics was obtained from the following steps.

Step1:

Two hundred bootstrap data sets (D_i, i = 1, 2 … 200) with the same sample size as the original data (D_o) were generated using Wings for NONMEM (version 409d, http://wfn.sourcefourge.net).

Step2:

The final model derived from the original data set (M_o) was applied to each of the bootstrap data (D_i) resulting in a bootstrap model (M_i, i=1, 2 … 200). It should be noted that, in this step, all parameters (coefficients and random effects) were allowed to be estimated for each of the bootstrap data. For example, when M_o was applied to D_{11}, the bootstrap model obtained was M_{11} (M_{11}=F(M_o : D_{11})). Therefore, 200 bootstrap models (M_1 to M_{200}) were obtained in this step. The bootstrap apparent errors ($AE_{1,i}$ and $AE_{2,i}$: i = 1, 2 … 200) were calculated. Thus, one obtained $AE_{1,i}$ =[P_1(M_i : D_i)] and $AE_{2,i}$ = [P_2(M_i : D_i)]—the MSE and MAE obtained when the bootstrap models were applied to the bootstrap samples. All the apparent errors were calculated using S-PLUS 2000 (Insightful Corp, Seattle, WA, USA).

Step3:

The bootstrap models (M_i) obtained from Step 2 were applied to the original data set (D_o) In this process, the coefficients and random effects were fixed for M_1 to M_{200}. So, the bootstrap prediction error original ($PE_{1,i}$ and $PE_{2,i}$: i = 1, 2 … 200) were calculated. The $PE_{1,i}$ = [P_1(M_i : D_o)] and $PE_{2,i}$ = [P_2(M_i : D_o)] are the MSE and MAE obtained from

applying the bootstrap model to the original data set. All the prediction error metrics were calculated using S-PLUS 2000 (Insightful Corp, Seattle, WA, USA).

Step4:

The optimism (OPT) for each of the prediction error metrics was estimated by equation 2.3a and 2.3b.

$$OPT_{1,i} = PE_{1,i} - AE_{1,i} \quad (2.3a)$$

$$OPT_{2,i} = PE_{2,i} - AE_{2,i} \quad (2.3b)$$

$$i=1, 2 \ldots 200$$

where $OPT_{1,i}$ is the optimism for the mean square error and $OPT_{2,i}$ is the optimism for the mean absolute error.

Step5:

The average OPT for the mean square error and the mean absolute error ($\overline{OPT_1}$ and $\overline{OPT_2}$) were calculated from equation 2.4a and 2.4b.

$$\overline{OPT_1} = 1/200 \times \sum_{i=1}^{200} OPT_{1,i} \quad (2.4a)$$

$$\overline{OPT_2} = 1/200 \times \sum_{i=1}^{200} OPT_{2,i} \quad (2.4b)$$

Step6:

The improved estimates of the prediction error metrics were obtained by adding the average OPT obtained from Step 5 to the prediction error metric obtained from fitting the final model to the original data set, as presented in equation 2.5a and 2.5b.

$$MSEimp = P_1(M_o:D_o) + \overline{OPT_1} \quad (2.5a)$$

$$MAEimp = P_2(M_o:D_o) + \overline{OPT_2} \quad (2.5b)$$

2.2.4.3 The predictive check (PC)

The predictive check was performed to assess whether the final model provides a sufficient summary of the original data. In this study, the chosen statistics were quantiles of the concentration (10% to 90% quantiles). The general approach for the predictive check has 3 steps as described below.

Step1: Estimation step

The population model parameters ($\hat{\theta}$) were estimated by fitting the model to the observed data

Step2: Simulation step

A number of replicated data sets (y_i^{rep}, i = 1, 2 … Nrep) were simulated under the same design as the observed data by using $\hat{\theta}$

Step3: Evaluation step

A statistic form each of the replicated data ($T(y_i^{rep})$) was calculated and the histogram of a statistic distribution from all of the replicated data was compared to the same statistic calculated from the original data ($T(y^{obs})$). The predictive p-value (p^{pc}) can be derived by equation 2.6:

$$p^{pc} = \frac{1}{Nrep}\sum_{i=1}^{Nrep} I\left(T(y_i^{rep}) \geq T(y^{obs})\right) \qquad (2.6)$$

where *i* is simulation index (i = 1,2 … Nrep), $T(y_i^{rep})$ is a statistic from each replicated data, $T(y^{obs})$ is a statistic from the observed data, and I(·) describes the indicator function (taking value 1 when $T(y_i^{rep}) \geq T(y^{obs})$ and 0 when $T(y_i^{rep}) < T(y^{obs})$).

The ideal value of p^{pc} equals 0.5 suggesting the model performs adequately in term of a statistic, however, a p^{pc} value between 0.2-0.8 is generally acceptable (16). Two hundred replicated data sets were generated in this study (Nrep=200). S-PLUS 2000 was used to generate multiple control streams with a different seed number and they were transfered to NONMEM to simulate the replicated data. The output data from NONMEM were then collected by S-PLUS to calculate the statistics and generate the histograms of the statistic distribution against the observed statistics and also compute the p^{pc}.

2.3 Results

2.3.1 Model building

A total of 875 concentrations from 148 patients were available for the analysis. A summary of the patient characteristics is shown in Table 2.1. During the structural model development, the data did not contain enough information for accurate estimation of K_a and IIV for V/F. Therefore, K_a was fixed to a literature value of 3.5 hr^{-1} (17). The IIV for V/F and K_a were not estimated in this analysis. A scatterplot of measured LTG concentrations versus time after last dose for the patients receiving 150 mg/day LTG are shown in Figure 2.1. From this figure, it shows that the LTG concentrations for all patients were considerably constant over 24 hours.

Table 2.1 Patient characteristics (N=148)

Patient characteristics	Frequency (%)
Gender	
Male	143 (96.6)
Female	5 (3.4)
Race	
American Indian	3 (2)
Black, not of Hispanic origin	37 (25)
Hispanic	9 (6.1)
White, not of Hispanic origin	99 (66.9)
Concomittant antiepileptic drugs	
PHT*	36 (24.3)
Smokers	31 (20.9)
Alcohol use	24 (16.2)
	Mean
Age (year)	70.6 (60-92)
Weight (kg)	80.9 (40-123)
IBW (kg)	68.8 (50.1-82.4)
BMI (kg/m^2)	26.4 (14-48)
LBW (kg)	60.7 (36.4-79)
BSA (m^2)	1.96 (1.4-2.5)
Height (inches)	68.8 (59-76)
Albumin (mg%)	3.96 (2.3-5.3)
BUN (mg%)	18.7 (2-78)
Serum creatinine (mg%)	1.23 (0.5-4.10)
BUN/CR ratio	15.6 (2.3-36)
Creatinine clearance (mL/min)	68.8 (19.8-199)
Aspartate aminotransferase (mU/mL)	22.5 (8-117)
Alanine aminotransferase (mU/mL)	22.7 (2-131)
Duration of therapy (week)	18.5 (2-104)

*The patients used PHT before enrollment and PHT dose was gradually withdrawn during the 6-week titration phase of LTG.

IBW, ideal body weight; BMI, body mass index; LBW, lean body weight; BSA, body surface area; BUN, blood urea nitrogen; BUN/CR, blood urea nitrogen/serum creatinine ratio; PHT, phenytoin.

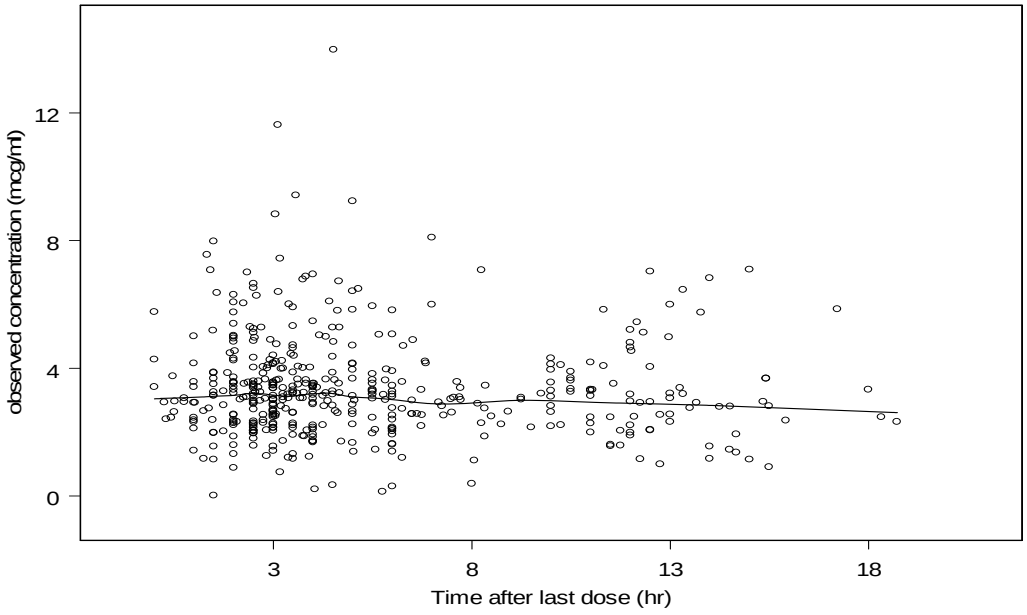

Figure 2.1 *Scatterplot of the observed concentrations (mcg/mL) versus time after last dose (hours) for patients receiving lamotrigine 150 mg/day.*

During the univariate analysis for clearance, all covariates of body size measurements were significant. However, weight was brought forward in the model for further model development because it caused the largest decrease in OFV and is commonly used in clinical practice for dose adjustment. Both BUN and BUN/CR ratio were also significant during univariate analysis but BUN/CR ratio was chosen to be incorporated into the model due to the larger drop in OFV. During forward selection analysis, BUN/CR ratio, weight, age (as a categorical covariate), and PHT use were significant covariates and were incorporated into the base model for clearance. When backward deletion was performed, age failed to reach a significance level. Therefore, BUN/CR ratio, weight and PHT use remained in the final model which can be represented by equation 2.7.

$$CL/F = (\theta_1 \times \text{BUN/CR ratio} + \theta_2 \times WT) \times \theta_3 \text{ (if patient taking phenytoin)} \quad (2.7)$$

Parameter estimates from NONMEM are given in Table 2.2. None of the covariates was found to be statistically significant for V/F. From the final model, the percent of coefficient of variation (%CV) for IIV for CL/F was 34.2%, the proportional and additive RUV were 19.8% and 0.31 mcg/ml, respectively. Goodness of fit plots from the base model and the final model are presented in Figure 2.2. The final model showed an improvement of fit compared with the base model. The results from the performed randomization tests are shown in Table 2.3. Based on a 2000 randomization procedure, the actual significance levels for each covariate were similar to the nominal levels.

2.3.2 Model evaluation

2.3.2.1 The nonparametric bootstrap

From 1000 bootstrap runs, two runs were terminated during minimization due to rounding errors. However, the results including these two runs were not different from when they were excluded. Therefore, these two runs that did not obtain a covariance matrix were included. Finally, all 1000 bootstrap runs were included in the bootstrap calculations. Table 2.2 shows the summary of the estimates and 95% CI from 1000 bootstrap data sets compared with the values from NONMEM. The parameter estimates for the fixed and the random effects from the bootstrap procedure were comparable and within 5%, and 10% of the estimates from NONMEM, which indicate that the final parameter estimates is reliable (18).

Table 2.2 Final parameter estimates and 95% confidence intervals (CI) from NONMEM and the bootstrap analysis

Parameter	NONMEM		Bootstrap Analysis	
	Estimate	95%CI*	Median	95%CI†
θ1 (L/hr)	0.0332	[0.0199,0.0465]	0.0333	[0.020,0.0469]
θ2 (L/hr/kg)	0.0268	[0.0238,0.0298]	0.0267	[0.0236,0.0295]
θ3 (L/hr)	1.59	[1.34,1.84]	1.59	[1.39,1.87]
V/F (L)	115	[81.9,148]	114	[88.0025,157]
IIV for CL/F (%CV)	34.2	[27.92,39.5]	33.8	[28.27,39.75]
RUV, proportional (%CV)	19.8	[16.2,22.9]	19.8	[16.58,23.02]
RUV, additive (SD, mcg/ml)	0.308	[0.219,0.3754]	0.3064	[0.2243,0.3768]

* (Estimate) ± 1.96 x (standard error of the estimate)

† 2.5^{th} and 97.5^{th} percentile values of the ranked bootstrap parameter estimates

SD, standard deviation

Table 2.3 Results from the randomization test of each covariate in the final model

Covariates	dOFV*	Actual significance level	p-value corresponding χ^2, df=1
Weight	10.621	0.001	0.0011
	5.148	0.01	0.0233
BUN/CR ratio	9.806	0.001	0.0017
	6.049	0.01	0.014
PHT	15.029	0.001	0.0001
	6.796	0.01	0.009

* dOFV corresponding to 0.1^{th} and 1^{st} percentile from 2000 randomly permuted data

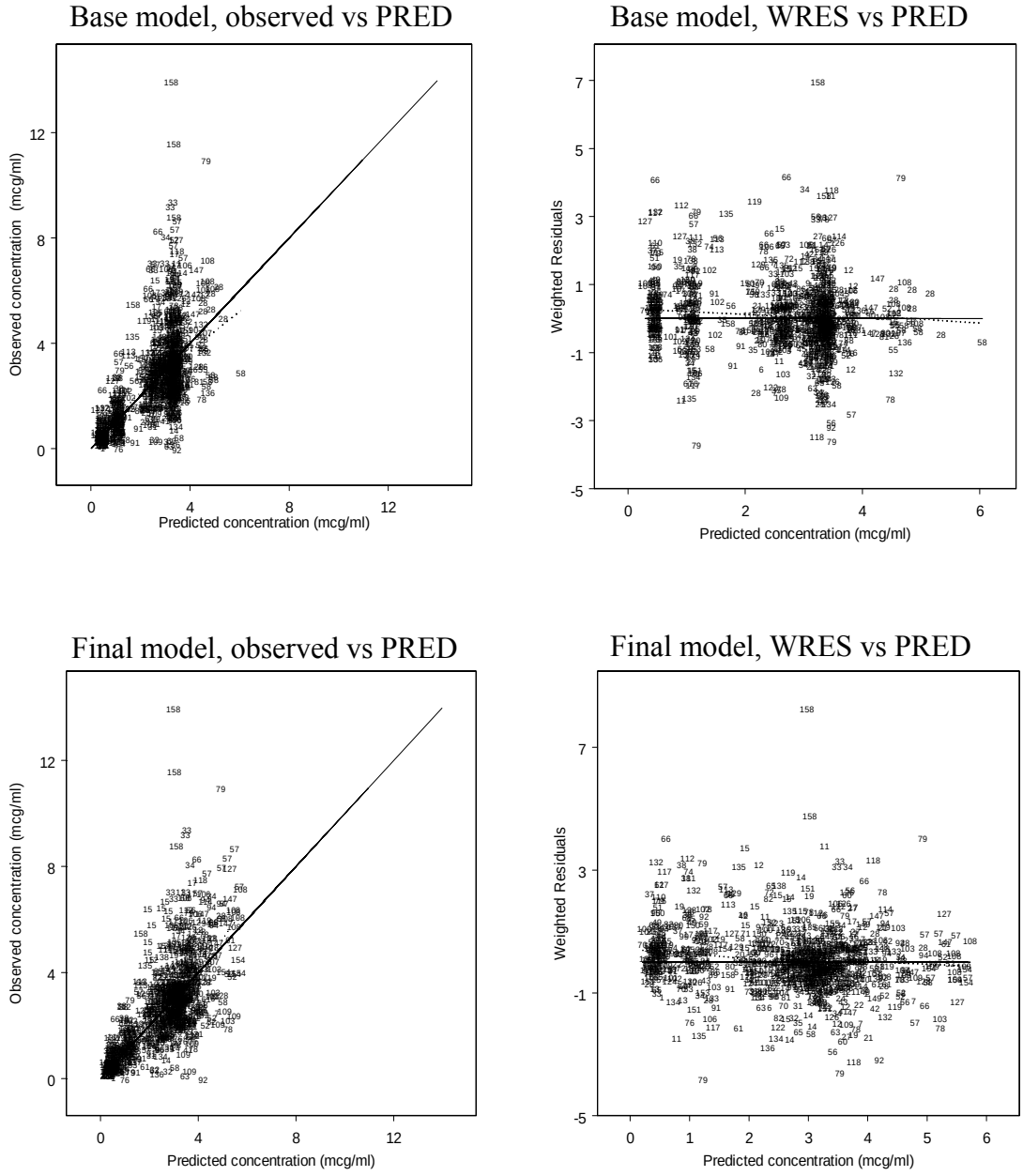

Figure 2.2 *Goodness of fit plots; the observed versus population model-predicted concentrations (PRED) and weighted residuals (WRES) versus population model-predicted concentrations (PRED) of the base model and the final model.*

The summary results from the bootstrap predictive performance assessment are shown in Table 2.4. The $\overline{OPT}_1$ and $\overline{OPT}_2$ were 0.03 mcg^2/ml^2 and 0.0063 mcg/ml, respectively. The average OPT for both MSE and MAE are small and less than 0.15 times MSEimp and MAEimp which indicates that the model is without substantial deficiencies.

Table 2.4 The bootstrap predictive performance assessment results

$P_1(M_o:D_o)$	$P_2(M_o:D_o)$	$\overline{OPT}_1$	$\overline{OPT}_2$	MSEimp	MAEimp
1.77	0.88	0.03	0.0063	1.804	0.8863

$P_1(M_o:D_o)$, a mean square error obtained from fitting the final model to the original data; $P_2(M_o:D_o)$, a mean absolute error obtained from fitting the final model to the original data; $\overline{OPT}_1$, the average OPT for MSE; $\overline{OPT}_2$, the average OPT for MAE; MSEimp, the improved mean square error; MAEimp, the improved mean absolute error

2.3.2.2 The predictive check

The results from the predictive check, the histograms of the statistic distribution (concentrations at each quantile) from 200 simulations versus the observed statistic (represented as a vertical line), are presented in Figure 2.3. A majority of the observed statistics fall within the predicted range returned by the simulations, indicating that important characteristics of the data seem to be captured in the final model. On the basis of this result, we conclude that the model performs adequately in term of the statistics.

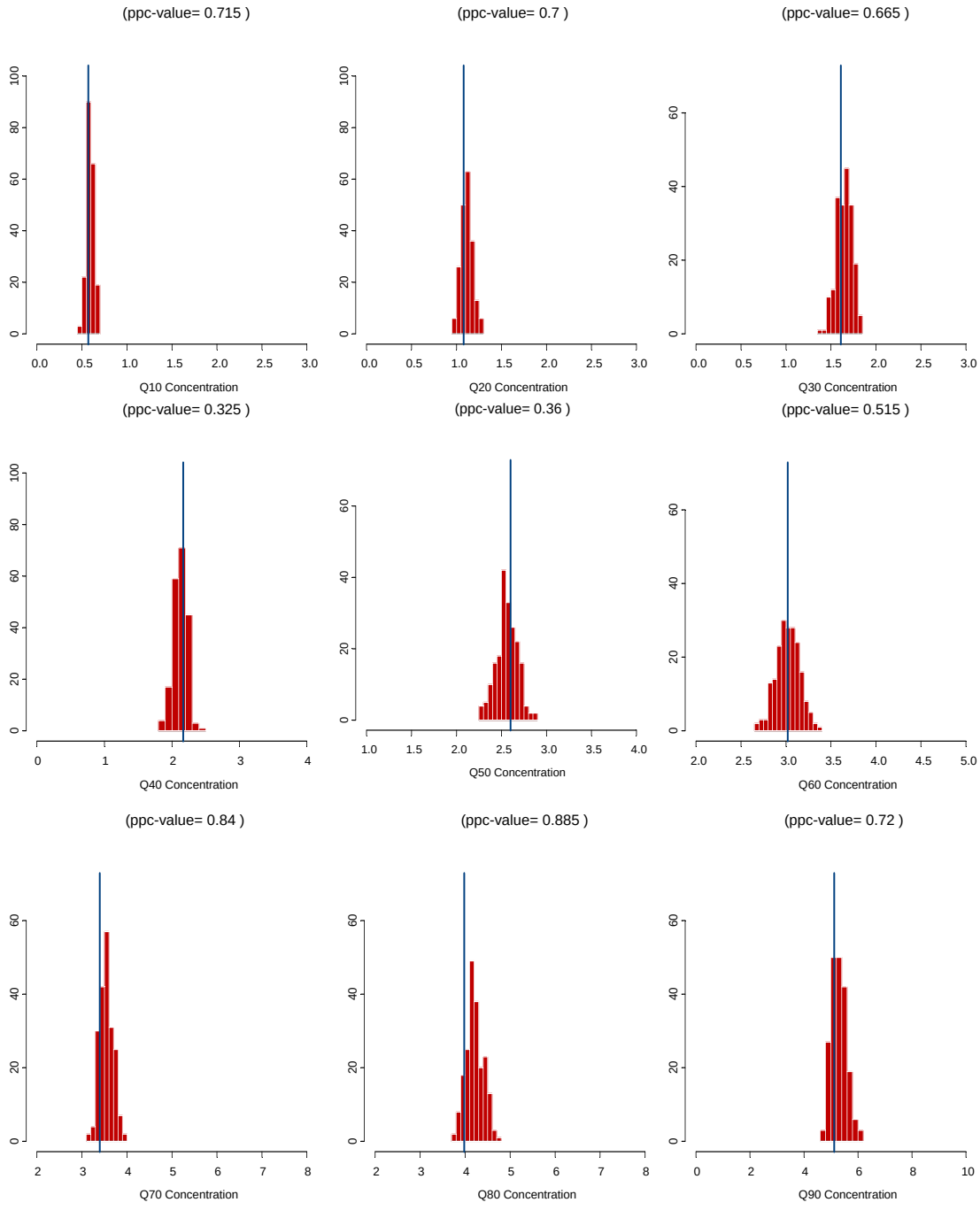

Figure 2.3 *The predictive check results. The histograms of the statistic distribution (concentrations at each quantile) from 200 simulated data sets versus the observed statistics (plotted as the vertical line).*

2.4 Discussion

This is the first prospective study to determine the population pharmacokinetics of LTG for a group of community-dwelling elderly epilepsy patients. A population mean CL/F for patients using LTG monotherapy in this study was estimated to be 2.64 L/hr for a patient having a BUN/CR ratio of 15 and weighing 80 kg (the mean BUN/CR ratio and weight of this study population) with an interindividual variability of 34%. The estimate of the population mean CL/F in this elderly population is in close agreement with those reported from other traditional and population pharmacokinetic studies of lamotrigine monotherapy in adult population (2.14-2.52 L/hr) (3,12,17). Moreover, the 34% interindividual variability of CL/F obtained from our study is similar to the values obtained from younger populations (32-38%) (11,12,17). The population mean V/F was estimated to be 115 L which is also consistent with previous population pharmacokinetic studies (11). Among 19 covariates evaluated in this analysis, only BUN/CR ratio, weight and PHT use were significant covariates for CL/F.

A previous study comparing lamotrigine pharmacokinetics in adult (aged 26 to 38 years) and elderly (aged 65 to 76 years) healthy volunteers found 37% lower in apparent clearance in the elderly group (7). Interestingly, the results from our study showed no difference of the estimated LTG pharmacokinetic parameters compared with the results previously reported in adult patients. Two population pharmacokinetic studies of lamotrigine show that age was not found to be a significant covariate for CL/F which is consistent with our study (11,12). Lamotrigine is primarily metabolized through Phase II enzymes, UDP-glucoronosyltransferases (UGTs), which has been found to be minimally affected by aging (19). Nonetheless, our study consisted of only elderly patients aged 60

years and older. The influence of age on LTG pharmacokinetics should be further investigated in a data set with wider age range.

Previous population pharmacokinetic studies of LTG show a difference in drug disposition among races. Grasela et al (11) found a 25% reduction in lamotrigine clearance in non-Caucasian patients compared with Caucasian patients. Hussein and Posner (12) show a significant reduction in lamotrigine clearance of 28.7% in Asian patients compared with Caucasian patients. In our study, race was not found to be a significant covariate. One possible reason could be a high correlation between race and BUN/CR ratio in this patient population. There is evidence of a significant difference of BUN/CR ratio among races in both general and renal disease patients (20,21). A significant difference of BUN/CR ratio among races was also observed in our data as shown in Figure 2.4.

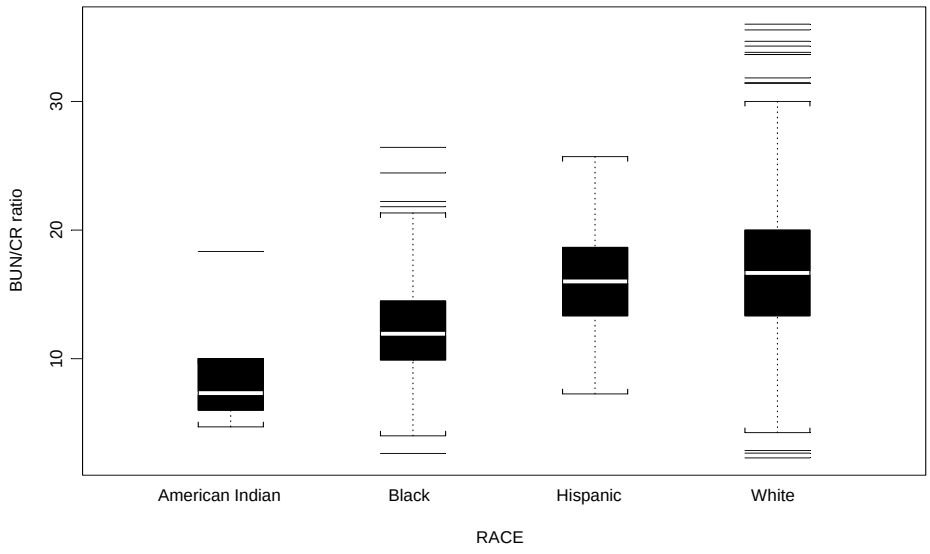

Figure 2.4 *Box plot of BUN/CR ratio among races.*

When two correlated variables are both included in a model, it could lead to artificial statistically non-significant parameter estimates (22). Even though there is documentation of race differences in cytochrome P450 enzyme activities, the race differences UGTs have not been well studied. As BUN/CR ratio is a numerically measurable predictor, whereas patients' self report of race can be subjective, using BUN/CR ratio as a predictor may obtain a more accurate estimation of LTG CL/F.

Enzyme-inducing comedications (i.e., PHT, CBZ, primidone and PB) can profoundly increase lamotrigine clearance (23,24). Due to the study design, only PHT could be tested in this analysis. The apparent clearance of LTG increases more than 50% when PHT is given as a comedication. The current guidelines for LTG dosing account for the enhanced clearance in patients when using other enzyme-inducing antiepileptic drugs.

The presence of autoinduction of LTG metabolism is still unclear. A pharmacokinetic study of LTG in normal volunteers receiving multiple doses of LTG over 7 days suggests the absence of autoinduction (3), whereas a previous population pharmacokinetic study shows a 17% increase in CL/F from the first dose over 48 weeks of therapy (12). In our study, duration of therapy (week) failed to be a significant covariate during covariate model building. Figure 2.5 shows the scatter plot of empirical Bayes estimates for CL/F under the base model against duration of therapy (week). This plot illustrates no relationship between CL/F and week of therapy. Thus, there is no evidence of autoinduction of LTG metabolism in our study. Total daily dose (TDD), a covariate normally used for indicating a degree of autoinduction of drug metabolism in population

pharmacokinetic studies, was not included in the covariate model building due to the possible inherent correlation between dose and CL/F in therapeutic drug monitoring settings (25). As the protocol of the VA Cooperative Study 428 allowed for adjustment of LTG dose based on seizure control or the occurrence of side effects, this could also introduce an inherent correlation between dose and CL/F in this data set and make conclusion of dose as a covariate inappropriate.

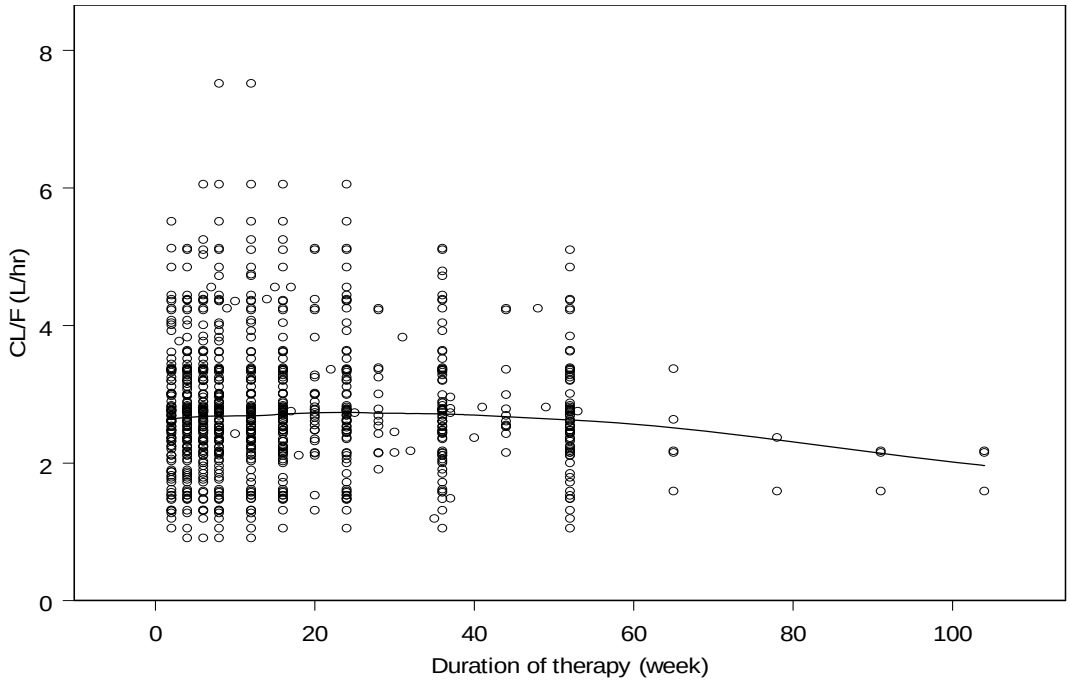

Figure 2.5 *Scatterplot of the empirical Bayes estimates of CL/F (L/hr) against duration of therapy (week) under the base model.*

The results from the randomization test showed that the actual significance levels were similar to the nominal levels which is expected when FOCE-I is used (14). When the bootstrap was applied to re-estimate the typical values and random effects, they were similar to those estimated from the NONMEM analysis. This indicates that the estimated population pharmacokinetic parameters are reliable. The results from the bootstrap predictive performance procedure indicated that the developed model is without substantive deficiencies. Furthermore, the results from the predictive check did not indicate a substantial difference between the observed statistic and the simulated statistic distribution (Figure 2.3).

In conclusion, this study presents a population pharmacokinetic model of LTG therapy in elderly community-dwelling patients with epilepsy. The results from this study showed that estimated population mean pharmacokinetic parameters in this elderly population are consistent with those previously reported in younger patients. From the analysis, BUN/CR ratio, weight and PHT use were significant covariates for LTG CL/F. The results from the bootstrap and predictive check confirm the reliability and predictive performance of the final model. The proposed model from this study can be useful to predict LTG concentrations and individualize dosing regimens in the elderly population.

2.5 References

1. Rowan AJ, Ramsay RE, Collins JF, et al. New onset geriatric epilepsy: a randomized study of gabapentin, lamotrigine, and carbamazepine. *Neurology*. 2005;64(11):1868-1873.
2. Ramsay RE, Pellock JM, Garnett WR, et al. Pharmacokinetics and safety of lamotrigine (Lamictal) in patients with epilepsy. *Epilepsy Res*. 1991;10(2-3):191-200.
3. Cohen AF, Land GS, Breimer DD, Yuen WC, Winton C, Peck AW. Lamotrigine, a new anticonvulsant: pharmacokinetics in normal humans. *Clin Pharmacol Ther*. 1987;42(5):535-541.
4. Fillastre JP, Taburet AM, Fialaire A, Etienne I, Bidault R, Singlas E. Pharmacokinetics of lamotrigine in patients with renal impairment: influence of haemodialysis. *Drugs Exp Clin Res*. 1993;19(1):25-32.
5. Wootton R, Soul-Lawton J, Rolan PE, Sheung CT, Cooper JD, Posner J. Comparison of the pharmacokinetics of lamotrigine in patients with chronic renal failure and healthy volunteers. *Br J Clin Pharmacol*. 1997;43(1):23-27.
6. Armijo JA, Bravo J, Cuadrado A, Herranz JL. Lamotrigine serum concentration-to-dose ratio: influence of age and concomitant antiepileptic drugs and dosage implications. *Ther Drug Monit*. 1999;21(2):182-190.
7. Posner J, Holdich T, Crome P. Comparison of lamotrigine pharmacokinetics in young and elderly healthy volunteers. *J Pharm Med*. 1991;1:121-128.
8. Jonsson EN, Karlsson MO. Xpose--an S-PLUS based population pharmacokinetic/pharmacodynamic model building aid for NONMEM. *Comput Methods Programs Biomed*. 1999;58(1):51-64.
9. Beal SL, Sheiner LB. *NONMEM User's Guides*. University of California, San Fransisco, CA, NONMEM project group. 1994.
10. Mangoni AA, Jackson SH. Age-related changes in pharmacokinetics and pharmacodynamics: basic principles and practical applications. *Br J Clin Pharmacol*. 2004;57(1):6-14.

11. Grasela TH, Fiedler-Kelly J, Cox E, Womble GP, Risner ME, Chen C. Population pharmacokinetics of lamotrigine adjunctive therapy in adults with epilepsy. *J Clin Pharmacol*. 1999;39(4):373-384.
12. Hussein Z, Posner J. Population pharmacokinetics of lamotrigine monotherapy in patients with epilepsy: retrospective analysis of routine monitoring data. *Br J Clin Pharmacol*. 1997;43(5):457-465.
13. Gobburu JV, Lawrence J. Application of resampling techniques to estimate exact significance levels for covariate selection during nonlinear mixed effects model building: some inferences. *Pharm Res*. 2002;19(1):92-98.
14. Wahlby U, Jonsson EN, Karlsson MO. Assessment of actual significance levels for covariate effects in NONMEM. *J Pharmacokinet Pharmacodyn*. 2001;28(3):231-252.
15. Ette EI, Williams PJ, Kim YH, Lane JR, Liu MJ, Capparelli EV. Model appropriateness and population pharmacokinetic modeling. *J Clin Pharmacol*. 2003;43(6):610-623.
16. Gobburu JV. Posterior Predictive Check: What, How and When? AAPS, Salt Lake City, Utah, 2003.
17. Chan V, Morris RG, Ilett KF, Tett SE. Population pharmacokinetics of lamotrigine. *Ther Drug Monit*. 2001;23(6):630-635.
18. Ette EI, Williams PJ, Lane JR. Population pharmacokinetics III: design, analysis, and application of population pharmacokinetic Studies. *Ann Pharmacother*. 2004;38(12):2136-2144.
19. Perucca E. Clinical pharmacokinetics of new-generation antiepileptic drugs at the extremes of age. *Clin Pharmacokinet*. 2006;45(4):351-363.
20. United State Renal Data System. 2006. Annual Data Report: Chapter three; patient characteristics. p 81-94.
21. Casey AE, Gilbert FW, Ratliff CR, Downey E. Race-sex values of serum creatine-phosphokinase, uric acid, urea nitrogen and creatinine. *Ala J Med Sci*. 1968;5(3):474-476.

22. Bonate PL. The effect of collinearity on parameter estimates in nonlinear mixed effect models. *Pharm Res*. 1999;16(5):709-717.
23. Garnett WR. Lamotrigine: pharmacokinetics. *J Child Neurol*. 1997;12 Suppl 1:S10-15.
24. Rambeck B, Wolf P. Lamotrigine clinical pharmacokinetics. *Clin Pharmacokinet*. 1993;25(6):433-443.
25. Ahn JE, Birnbaum AK, Brundage RC. Inherent correlation between dose and clearance in therapeutic drug monitoring settings: possible misinterpretation in population pharmacokinetic analyses. *J Pharmacokinet Pharmacodyn*. 2005;32(5-6):703-718.

CHAPTER 3

Population Pharmacokinetics of Carbamazepine in Community-Dwelling Elderly Patients

3.1 Background and aims of the study

The incidence of epilepsy is increasing in those over 60 years of age (1). Although lamotrigine and gabapentin have been shown to be more tolerable than carbamazepine in the elderly population (2), carbamazepine is still used frequently in the elderly epilepsy patients (3,4). In addition, elderly patients who are on CBZ and considered stable will most likely not switch to another antiepileptic drug. The population pharmacokinetics of CBZ has been extensively studied in the younger population (5-13); however, little information is available on CBZ pharmacokinetics in an elderly community-dwelling population. In addition, previous data are derived from retrospective clinical data in which medication adherence was not defined.

CBZ is extensively metabolized in man, mainly by CYP3A4 isoenzyme, yielding CBZ-10, 11-epoxide as a major metabolite. Not only is CBZ inducible by other enzyme-inducing co-medications, it also induces its own metabolism making this medication a challenge when administered as part of a polytherapy regimen. There is evidence that CYP3A4 shows a decrease in activity with increasing age (14). Moreover, it has been suggested that the inducible effect is less sensitive in the elderly than in younger patients (15,16). Due to complex pharmacokinetic properties of CBZ, including autoinduction, high variability in absorption, high protein binding, low therapeutic index, and enzyme

inducing property, it is necessary to obtain pharmacokinetic information in respective populations in order to optimize drug therapy in these patients.

The aims of this study were to determine the relevant pharmacokinetic parameters (apparent clearance, apparent volume of distribution, and absorption rate constant) and their variability in a community-based elderly population. The patient specific covariates that may influence pharmacokinetic parameters including age, body size measurements, race, renal function, liver function, PHT use, smoking, and alcohol were also investigated. These defined relationships can then be used to facilitate clinicians in individualizing CBZ therapy in elderly community-based patients.

3.2 Subjects and methods

3.2.1 Patients and data collection

This study was approved by the University of Minnesota's Human Subject's Committee as an exempt study. CBZ concentration data were obtained from the Department of Veterans Affairs (VA) Cooperative study 428, a randomized, double-blind, parallel group, monotherapy comparison study of LTG, GBP, and CBZ in the elderly patients with epilepsy (2). Data from CBZ arm were used in this analysis. CBZ dose was titrated by 200 mg every 2 weeks to 600 mg/day. The details of patients and data collection procedures were similar to those previously presented under section 2.2.1. Ninety-three percent compliance was report in this study via pill counts.

3.2.2 Population pharmacokinetic analysis

The population pharmacokinetic analyses were performed using NONMEM (version VI, NONMEM Project Group, UCSF/Globomax and PDx-Pop version 2.0). A one-compartment model with first order absorption and elimination (subroutine ADVAN2, TRANS2) was used (17). Therefore, CL/F, V/F and K_a were obtained from the model. The interindividual variability (IIV) was modeled using an exponential error model for all parameters which can be described by equation 3.1.

$$P_i = TVP \times \exp(\eta_i) \quad (3.1)$$

where P_i is the pharmacokinetic parameter for subject i, TVP is the typical value of pharmacokinetic parameter in the population, and η_i is the interindividual variability which is assumed to be normally distributed with a mean of zero and variance of ω^2.

The residual unexplained variability (RUV) which includes other unexplained variability (e.g., model misspecification, assay errors, and dosing history errors) was modeled using a proportional error model which can be described by equation 3.2.

$$C_{obs,\,ij} = C_{pred,\,ij} \times (1+ \varepsilon_{ij}) \quad (3.2)$$

where $C_{obs,\,ij}$ and $C_{pred,\,ij}$ are the j^{th} observed and predicted plasma concentrations in the i^{th} individual and ε_{ij} is the residual unexplained variability which is assumed to be normally distributed with a mean of zero and variance of σ^2.

The first-order conditional estimation method with interaction (FOCE-I) was used for all analyses. The goodness of fit of the model was graphically assessed by Xpose 3.1(18) and S-PLUS 2000 (Insightful Corp, Seattle, WA, USA)

The model was initially developed without including patient specific covariates (base pharmacokinetic model). To identify the significant covariates, 18 available covariates that could be important in elderly patients were considered in the covariate model building step. These covariates included measures of body size (weight, body mass index (BMI), body surface area (BSA), ideal body weight (IBW), lean body weight (LBW)) to determine if body size is a better predictor of pharmacokinetic parameters in elderly patients; demographic factors (race, age, study center); co-medication use of known metabolic inducers and inhibitors (PHT use); factors that could effect liver function (alcohol use, smoking, age, aspartate aminotransferase (AST), alanine aminotransferase (ALT)); factors that could effect protein binding (albumin (ALB), total protein); and kidney function indicators (blood urea nitrogen (BUN), serum creatinine (CR), creatinine clearance (CRCL) which was calculated using Cockroft-Gault equation) were tested. Due to a small sample size of some race categories, race was evaluated as a dichotomous covariate (White and non-White). Age was evaluated as both a continuous and categorical covariate (age $\leq$ 80, and age > 80 years). Age 80 years was considered as a possible break point based on the initial graphical analysis. Each covariate was added to the base model sequentially using a stepwise technique. All continuous covariates were introduced into the base model in a linear and non-linear manner. The significance of each covariate was evaluated by the likelihood ratio test and visual inspection of

diagnostic plots. A decrease in NONMEM objective function value (OFV) of at least 6.64 (χ^2, $p \leq 0.01$, df=1) and 10.83 (χ^2, $p \leq 0.001$, df=1) were used as cutoff values for forward selection and backward deletion, respectively.

3.2.3 Randomization test

Each covariate vector in the final model was randomly permuted 2000 times using Wings for NONMEM (Version 600, http://wfn.sourcefourge.net). The detailed methods of randomization test procedures are presented in section 2.2.3.

3.2.4 Model evaluation: The nonparametric bootstrap and predictive check

3.2.4.1 The bootstrap confidence interval

One thousand bootstrap data sets were generated using the bootstrap option in Wings for NONMEM (Version 600, http://wfn.sourcefourge.net) and were used to obtain the bootstrap 95% confidence intervals (CI) for each parameter estimate. The detailed methods of the bootstrap CI procedures are presented in section 2.2.4.1.

3.2.4.2 The bootstrap predictive performance assessment

Two hundred bootstrap data sets were generated using Wings for NONMEM (Version 600, http://wfn.sourcefourge.net) and were used to calculate $\overline{OPT_1}$ and $\overline{OPT_2}$. The detailed methods of the bootstrap approach for predictive performance assessment are presented in section 2.2.4.2.

3.2.4.3 The predictive check (PC)

The detailed methods of the predictive check are presented in section 2.2.4.3.

3.3 Results

3.3.1 Population pharmacokinetic modeling

A total of 555 plasma concentrations from 121 patients were used for this analysis. A summary of the patient characteristics is shown in Table 3.1. A scatterplot of CBZ plasma concentrations against the time after last dose for patients receiving CBZ 600 mg/day is shown in Figure 3.1.

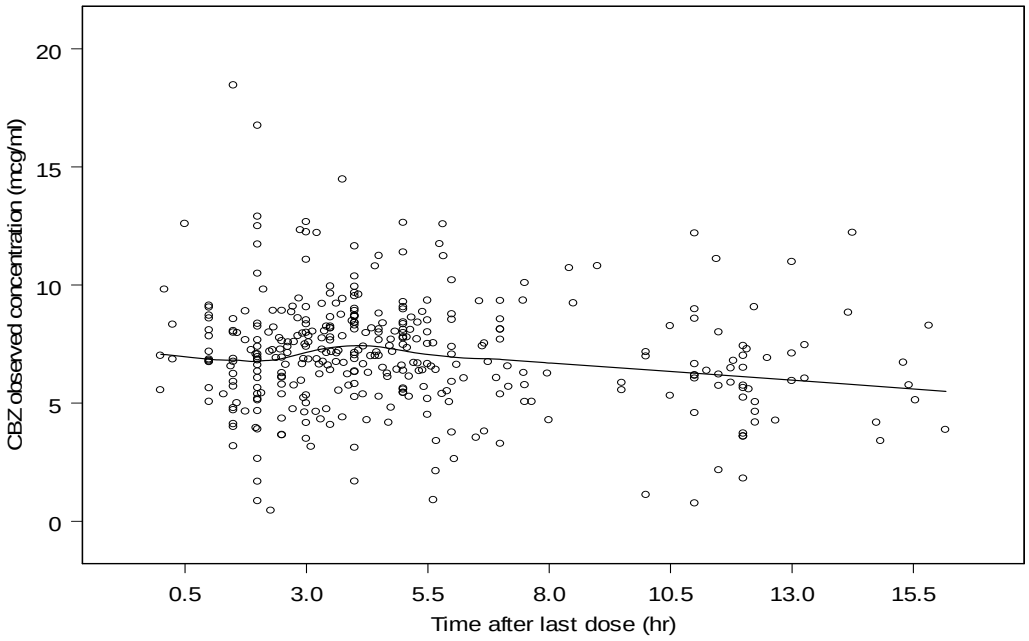

Figure 3.1 *Scatterplot of CBZ observed concentrations versus time after last dose(hours) for patients taking CBZ 600 mg/day*

Table 3.1 Patient characteristics (N=121)

Patient Characteristics	Frequencies (%)
Gender	
Male	118 (97.5)
Female	3 (2.5)
Race	
American Indian	3 (2.5)
Black	30 (24.8)
Hispanic	4 (3.3)
White	83 (68.6)
Other	1 (0.8)
Alcohol use	36 (29.8)
Smokers	31 (25.6)
PHT use*	20 (16.5)
	mean (range)
Age (year)	70.5 (60-96)
Weight (kg)	81.4 (50-129)
IBW (kg)	68.6 (37-82)
BMI (kg)	27 (17-38)
LBW (kg)	61 (39-80)
BSA (m^2)	1.96 (1.44-2.5)
Height (inches)	68.6 (52-76)
Creatinine Clearance (ml/min)	76.45 (5.45-174)
BUN (mg%)	18.4 (3-92)
Serum creatinine (mg%)	1.15 (0.6-11.5)
Albumin (mg%)	3.8 (2.1-5)
Aspartate aminotransferase (mU/ml)	24 (6-361)
Alanine aminotransferase (mU/ml)	27 (3-266)
Total protein (gm%)	7 (5.5-9)

* The patients used PHT before enrollment and PHT dose was gradually withdrawn during the 5-week titration phase of CBZ.

IBW, ideal body weight; BMI, body mass index; LBW, lean body weight; BSA, body surface area; BUN, blood urea nitrogen; PHT, phenytoin.

As the data are sparse and a number of samples collected in the absorption phase were limited, an accurate estimation of IIV for K_a cannot be obtained. Therefore, the IIV of K_a was not estimated in this analysis. During the forward selection process, the significant covariates for CL/F were PHT use and ALT, whereas PHT use and alcohol use were the significant covariates for V/F. When backward deletion was performed, ALT failed to reach a significance level for CL/F. Similarly, alcohol use and PHT use failed to reach a significance level for V/F. Finally, only PHT use was a significant covariate for CL/F as represented by equation 3.3, whereas none of the covariates were significant for V/F.

$$\text{CL/F (L/hr)} = \theta_1 \times \theta_2 \text{ (if taking phenytoin)} \tag{3.3}$$

The parameter estimates from NONMEM are summarized in Table 3.2. Based on these results, the estimate of CL/F for patients receiving CBZ monotherapy is 3.59 L/hr with an IIV of 18.1%. CL/F increases 23% in patients receiving PHT as a comedication. The goodness of fit plots from the base model and final model are presented in Figure 3.2.

The cutoff dOFV corresponding to the actual p-value of 0.01 and 0.001 based on a 2000 randomization procedure are presented in Table 3.3. The results from the randomization test show that the actual significance levels are similar to the nominal levels.

Table 3.2 Final parameter estimates and 95% confidence intervals (CI) from NONMEM and the bootstrap analysis[§]

Parameter	NONMEM		Bootstrap Analysis	
	Estimate	95% CI*	Median	95% CI[†]
CL/F (L/hr)	3.59	[3.39-3.79]	3.58	[3.39-3.80]
If taking PHT	1.23	[0.961-1.50]	1.26	[0.963-1.50]
V/F (L)	102	[37.1-167]	92.1	[19-189.6]
K_a (hr^{-1})	0.197	[0.0933-0.301]	0.19	[0.03-0.314]
IIV of CL/F (%CV)	18.1	[12.37-22.34]	17.92	[13.02-22.98]
IIV of V/F (%CV)	74.7	[21.1-103.44]	77.84	[1.06-121.24]
RUV, proportional (%CV)	25.1	[21.47-28.2]	24.6	[21.74-28.68]

[§] From 747 bootstrap runs with a successful minimization and successful covariance step

***** (Estimate) ± 1.96 x (standard error of the estimate)

[†] 2.5th and 97.5th percentile of the ranked bootstrap parameter estimates

Table 3.3 Results from the randomization test for the covariate in the final model

Covariates	dOFV*	Actual significance level	p-value corresponding χ^2, df=1
PHT	9.763	0.001	0.00178
	6.379	0.01	0.0115

***** dOFV corresponding to 0.1^{th} and 1^{st} percentiles from 2000 randomly permuted data

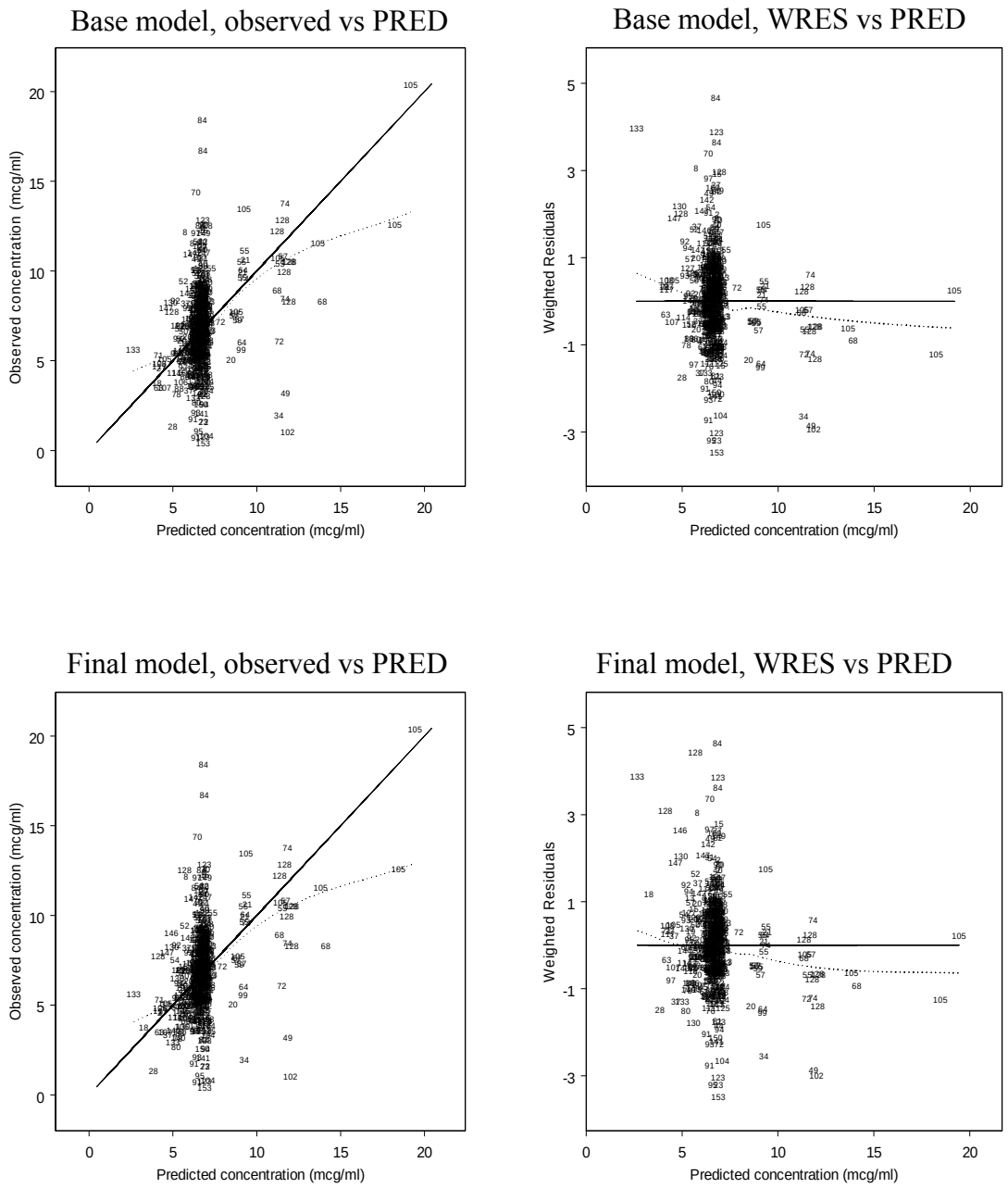

Figure 3.2 *Goodness of fit plots; the observed versus population model predicted concentrations (PRED), and weighted residuals (WRES) versus population model predicted concentrations (PRED) of the base and the final model*

3.3.2. Model evaluation

3.3.2.1 The nonparametric bootstrap

From 1000 bootstrap runs, 747 runs with a successful minimization and a successful covariance step were included in the bootstrap calculations. The summary of the parameter estimates and their 95% CI from NONMEM compared with the values from the bootstrap approach is shown in Table 3.2. The mean parameter estimates for the fixed effects and random effects from the bootstrap approach were comparable and within 10% of the estimates from NONMEM. Therefore, the parameter estimates from NONMEM were deemed reliable (19). The 95% CI for all parameters from the bootstrap approach are generally comparable with the estimates from NONMEM, except for the IIV of V/F.

The predictive performance of the final model was assessed by the bootstrap approach. The summary results from 200 bootstrap data sets are presented in Table 3.4. The average OPT for the mean square error ($\overline{OPT_1}$) and the mean absolute error ($\overline{OPT_2}$) were 0.03 $mcg^2/ml^2$and 0.009 mcg/ml, respectively. Both $\overline{OPT_1}$ and $\overline{OPT_2}$ are small and less than 0.15 times MSEimp and MAEimp. Therefore, the model is considered to be without substantial deficiencies.

Table 3.4 The bootstrap predictive performance assessment results

$P_1(M_o:D_o)$	$P_2(M_o:D_o)$	$\overline{OPT_1}$	$\overline{OPT_2}$	MSEimp	MAEimp
5.29	1.63	0.0334	0.0093	5.32	1.64

$P_1(M_o:D_o)$, mean square error obtained from fitting the final model to the original data set; $P_2(M_o:D_o)$, mean absolute error obtained from fitting the final model to the original data; $\overline{OPT_1}$, the average OPT for MSE; $\overline{OPT_2}$, the average OPT for MAE; MSEimp, the improved mean square error; MAEimp, the improved mean absolute error

3.3.2.2 The predictive check (PC)

Figure 3.3 shows the histogram of the statistic distribution (concentration at each quantile) versus the observed statistic (presented as a vertical line) and the p^{pc} values. The model adequately predicted the concentrations at the higher quantiles (Q70-Q90), as it reveals that the observed statistics fall within the histograms of the simulated statistic distribution. However, the model tends to underpredict the concentrations at the lower quantiles (Q10- Q60).

3.4 Discussion

Individualization of CBZ therapy in elderly patients is difficult due to its complicated pharmacokinetics and the lack of CBZ pharmacokinetic information in this population. This study presents the population pharmacokinetic modeling of CBZ which allows the estimation of the pharmacokinetic parameters and also the investigation of their relationship with patient specific covariates useful for optimizing CBZ therapy in the

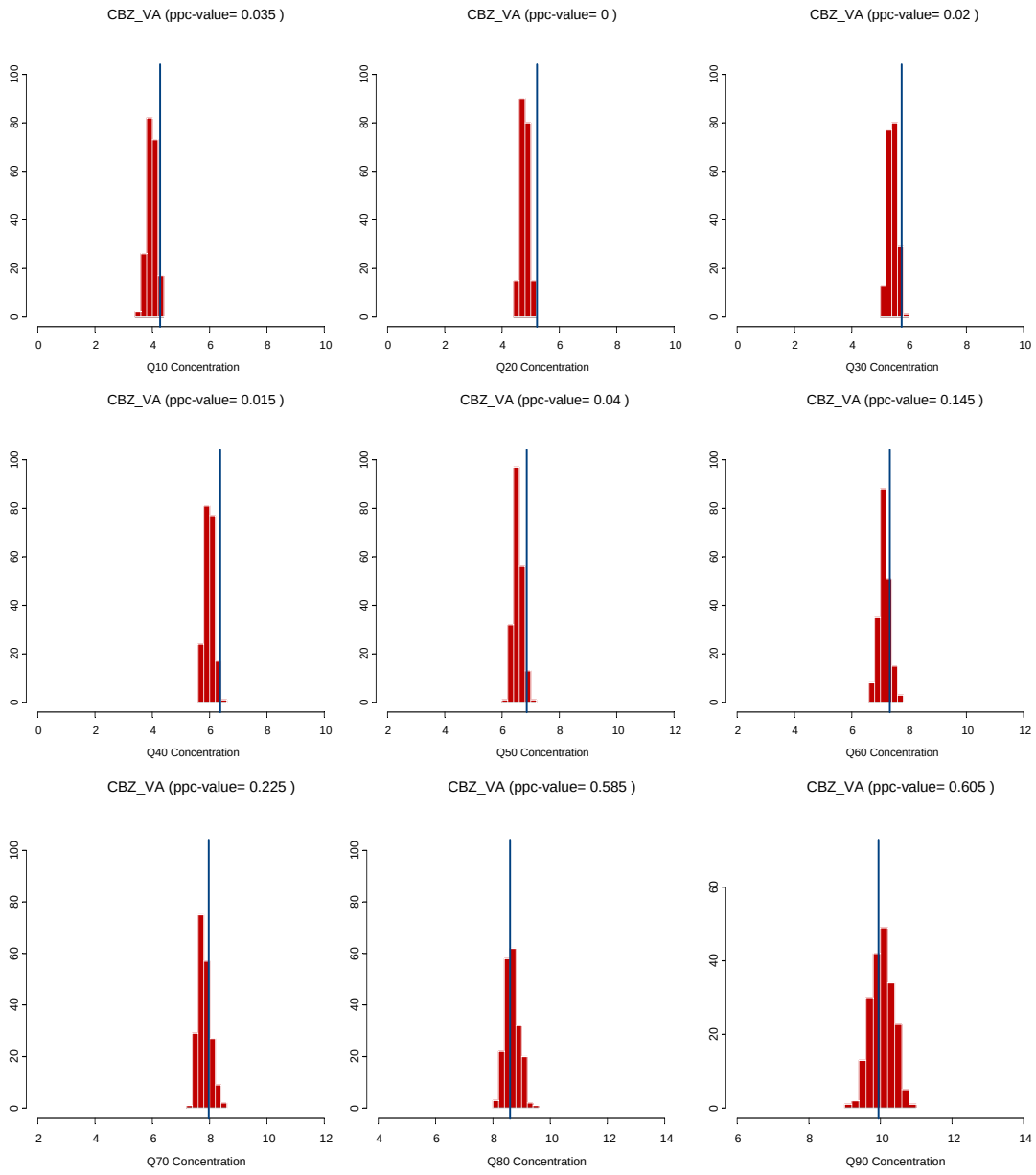

Figure 3.3 *The predictive check results. The histograms of the statistic distribution (concentrations at each quantile) from 200 simulated data sets versus the observed statistic (plotted as the vertical line).*

community-dwelling elderly patients. According to our results, the mean CL/F estimated from the model was 3.59 L/hr in patients receiving CBZ monotherapy with an interindividual variability of 18.1%. Among 18 covariates considered in this analysis, PHT use was the only covariate found to be significant for CL/F. The estimates of V/F and K_a were 102 L (IIV= 74%) and 0.197 hr^{-1}, respectively. Based on the parameter estimates from this model, CBZ half-life was approximately 19.7 hours in this community-dwelling elderly population.

The estimate of CL/F and its IIV from our study are comparable with previous reports from population pharmacokinetic studies of CBZ in adults and elderly patients (10,13,20,21). CYP3A4, which is a major enzyme responsible for the metabolism of CBZ, is known to decrease its capacity with increasing age (14). Whereas, there is evidence of decreasing CL/F of CBZ in elderly patients compared with adult patients (10,22), some studies show no age-dependent changes in CL/F of CBZ (21,23). In our study, the effect of age on CL/F of CBZ was not observed. However, this data set consists of only elderly epilepsy patients (age 60-96 years old) and a direct comparison to a young adult population was not made. In order to investigate the effect of age on CBZ pharmacokinetics and the difference of pharmacokinetic parameters between elderly and younger adults, further study in a data set with a wider range of age is required.

It is well documented that CBZ undergoes autoinduction. As the concentrations of CBZ in our study were measured at 2 weeks after changing dose and the autinduction of CBZ is reported to be completed within 2 weeks (24,25), these CBZ concentrations should

reflect the concentration at post-induction phase. Whereas the VA Cooperative data did not allow us to explore the autoinduction of CBZ, an investigation of CBZ deinduction yielding important parameters for characterizing the time course of CBZ autoinduction/deinduction using data from a separate study are presented in Chapter 4.

The metabolism of CBZ is highly inducible by other antiepileptic drugs including PHT, primidone, and phenobarbital (26,27). In this study, PHT increases CBZ clearance, but to a lesser extent than in previous studies in adult patients (23% compared to approximately 43%) (10,21). This difference in the effect of PHT on CBZ clearance may be due to the decreased sensitivity to enzyme induction in community-dwelling elderly patients (15,16). Therefore, dose adjustment of CBZ when comediation with PHT should be done carefully in this population due to the less effect of PHT induction on CBZ metabolism and the additive pharmacological effect from the combination of these two drugs. Clinical responses should be carefully monitored during CBZ dose adjustment.

Previous population pharmacokinetic studies show a positive association between CL/F and total daily dose (13,21). Several explanations are given for this association such as a change in bioavailability, hepatic enzyme activity, or the degree of autoinduction of CBZ metabolism (13,21). In medications where doses are adjusted based on therapeutic drug monitoring, clinical response or adverse effects, there is an inherent correlation between dose and drug clearance; this correlation does not necessarily imply a true relationship (28). The clinical management of CBZ in this elderly population would introduce an

inherent correlation between dose and CL/F in this data set. Therefore, total daily dose was not considered as a covariate in this study.

The results from the randomization test show that the actual significance levels are similar to the nominal levels which is expected when FOCE-I is used (29). The results from the bootstrap analysis (Table 3.3) show that the median parameter estimates obtained from a bootstrap procedure were generally comparable to the estimates from NONMEM indicating that the final parameter estimates are reliable (30). However, 95% CI of IIV for V/F obtained from the bootstrap approach was wider than the one obtained from NONMEM. This may be a result of the sparse sampling design used in this data. With a limited number of samples per individual, the ability to obtain an accurate and a precise estimate of IIV for V/F is often problematic (31). This contributes to a wider bootstrap 95% CI of IIV for V/F. The results from the predictive check indicate an underprediction at the lower concentrations. This could be consequences from excluding total daily dose as a covariate in the model deriving from the data set with a presence of TDM effect (28) or censoring data below the quantification limit of the assay (BQL) .

In conclusion, this study presents the application of nonlinear mixed effects modeling to obtain the important information of CBZ pharmacokinetics in community elderly patients from clinical trial data with a sparse-sample design. The results from this study can be used for individualization of CBZ dosage regimens in community-dwelling elderly patients. The final proposed model can be applied to estimate the recommended target dose of CBZ in this elderly population.

3.5 References

1. Hauser WA, Annegers JF, Kurland LT. Prevalence of epilepsy in Rochester, Minnesota: 1940-80. *Epilepsia*. 1991;32:429-445.
2. Rowan AJ, Ramsay RE, Collins JF, et al. New onset geriatric epilepsy: a randomized study of gabapentin, lamotrigine, and carbamazepine. *Neurology*. 2005;64(11):1868-1873.
3. Savica R, Beghi E, Mazzaglia G, et al. Prescribing patterns of antiepileptic drugs in Italy: a nationwide population-based study in the years 2000-2005. *Eur J Neurol*. 2007;14(12):1317-1321.
4. Cloyd JC, Lackner TE, Leppik IE. Antiepileptics in the elderly. Pharmacoepidemiology and pharmacokinetics. *Arch Fam Med*. 1994;3(7):589-598.
5. Bondareva IB, Sokolov AV, Tischenkova IF, Jelliffe RW. Population pharmacokinetic modelling of carbamazepine by using the iterative Bayesian (IT2B) and the nonparametric EM (NPEM) algorithms: implications for dosage. *J Clin Pharm Ther*. 2001;26(3):213-223.
6. Carlsson KC, Hoem NO, Glauser T, Vinks AA. Development of a population pharmacokinetic model for carbamazepine based on sparse therapeutic monitoring data from pediatric patients with epilepsy. *Clinical therapeutics*. 2005;27(5):618-626.
7. Chan E, Lee HS, Hue SS. Population pharmacokinetics of carbamazepine in Singapore epileptic patients. *Br J Clin Pharmacol*. 2001;51(6):567-576.
8. Deleu D, Aarons L, Ahmed IA. Population pharmacokinetics of free carbamazepine in adult Omani epileptic patients. *Eur J Clin Pharmacol*. 2001;57(3):243-248.
9. Delgado Iribarnegaray MF, Santo Bueldga D, Garcia Sanchez MJ, Otero MJ, Falcao AC, Dominguez-Gil A. Carbamazepine population pharmacokinetics in children: mixed-effect models. *Ther Drug Monit*. 1997;19(2):132-139.

10. Graves NM, Brundage RC, Wen Y, et al. Population pharmacokinetics of carbamazepine in adults with epilepsy. *Pharmacotherapy*. 1998;18(2):273-281.
11. Ismail R, Rahman AF. Estimation of population pharmacokinetics for carbamazepine in Malaysian patients using the OPT computer program. *J Clin Pharm Ther*. 1993;18(1):55-58.
12. Jiao Z, Zhong MK, Shi XJ, Hu M, Zhang JH. Population pharmacokinetics of carbamazepine in Chinese epilepsy patients. *Ther Drug Monit*. 2003;25(3):279-286.
13. Reith DM, Hooper WD, Parke J, Charles B. Population pharmacokinetic modeling of steady state carbamazepine clearance in children, adolescents, and adults. *J Pharmacokinet Pharmacodyn*. 2001;28(1):79-92.
14. Tanaka E. In vivo age-related changes in hepatic drug-oxidizing capacity in humans. *J Clin Pharm Ther*. 1998;23(4):247-255.
15. Salem SA, Rajjayabun P, Shepherd AM, Stevenson IH. Reduced induction of drug metabolism in the elderly. *Age and ageing*. 1978;7(2):68-73.
16. Twum-Barima Y, Finnigan T, Habash AI, Cape RD, Carruthers SG. Impaired enzyme induction by rifampicin in the elderly. *Br J Clin Pharmacol*. 1984;17(5):595-597.
17. Beal SL, Sheiner LB. *NONMEM Users Guide*: University of California, San Fransisco, CA, NONMEM project group. 1994.
18. Jonsson EN, Karlsson MO. Xpose--an S-PLUS based population pharmacokinetic/pharmacodynamic model building aid for NONMEM. *Comput Methods Programs Biomed*. 1999;58(1):51-64.
19. Ette EI, Williams PJ, Lane JR. Population pharmacokinetics III: design, analysis, and application of population pharmacokinetic Studies. *The Annals of pharmacotherapy*. 2004;38(12):2136-2144.
20. Bondareva IB, Jelliffe RW, Gusev EI, Guekht AB, Melikyan EG, Belousov YB. Population pharmacokinetic modelling of carbamazepine in epileptic elderly patients: implications for dosage. *J Clin Pharm Ther*. 2006;31(3):211-221.

21. Jiao Z, Shi XJ, Zhao ZG, Zhong MK. Population pharmacokinetic modeling of steady state clearance of carbamazepine and its epoxide metabolite from sparse routine clinical data. *J Clin Pharm Ther*. 2004;29(3):247-256.
22. Battino D, Croci D, Rossini A, Messina S, Mamoli D, Perucca E. Serum carbamazepine concentrations in elderly patients: a case-matched pharmacokinetic evaluation based on therapeutic drug monitoring data. *Epilepsia*. 2003;44(7):923-929.
23. Hockings N, Pall A, Moody J, Davidson AV, Davidson DL. The effects of age on carbamazepine pharmacokinetics and adverse effects. *Br J Clin Pharmacol*. 1986;22(6):725-728.
24. Kudriakova TB, Sirota LA, Rozova GI, Gorkov VA. Autoinduction and steady-state pharmacokinetics of carbamazepine and its major metabolites. *Br J Clin Pharmacol*. 1992;33(6):611-615.
25. Bertilsson L, Tomson T, Tybring G. Pharmacokinetics: time-dependent changes--autoinduction of carbamazepine epoxidation. *Journal of clinical pharmacology*. 1986;26(6):459-462.
26. Christiansen J, Dam M. Influence of phenobarbital and diphenylhydantoin on plasma carbamazepine levels in patients with epilepsy. *Acta neurologica Scandinavica*. 1973;49(4):543-546.
27. Rambeck B, May T, Juergens U. Serum concentrations of carbamazepine and its epoxide and diol metabolites in epileptic patients: the influence of dose and comedication. *Ther Drug Monit*. 1987;9(3):298-303.
28. Ahn JE, Birnbaum AK, Brundage RC. Inherent correlation between dose and clearance in therapeutic drug monitoring settings: possible misinterpretation in population pharmacokinetic analyses. *J Pharmacokinet Pharmacodyn*. 2005;32(5-6):703-718.
29. Wahlby U, Jonsson EN, Karlsson MO. Assessment of actual significance levels for covariate effects in NONMEM. *J Pharmacokinet Pharmacodyn*. 2001;28(3):231-252.

30. Ette EI, Williams PJ, Kim YH, Lane JR, Liu MJ, Capparelli EV. Model appropriateness and population pharmacokinetic modeling. *Journal of clinical pharmacology*. 2003;43(6):610-623.
31. al-Banna MK, Kelman AW, Whiting B. Experimental design and efficient parameter estimation in population pharmacokinetics. *J Pharmacokinet Biopharm*. 1990;18(4):347-360.

CHAPTER 4

Characterization of the Time Course of Carbamazepine Deinduction by an Enzyme Turnover Model

4.1 Background and aims of the study

Carbamazepine is a potent inducer of several drug transporters and drug-metabolizing enzymes including multiple cytochrome P450 and uridine 5'-diphosphate glucuronosyltransferases isoenzymes (1) which can affect the disposition of other agents. Moreover, CBZ is one of the few drugs that, after multiple doses, can stimulate the synthesis of enzymes that catalyze its own metabolism by a process known as autoinduction (2-4). An increase in gene transcription resulting in an elevated level of drug metabolizing enzymes is thought to be the major mechanism of autoinduction (5). Deinduction, the reverse process of autoinduction, occurs when chronic CBZ therapy is discontinued. An understanding of the time course of CBZ deinduction is necessary in order to optimally adjust CBZ and co-medication dosing regimens when terminating CBZ therapy.

An enzyme turnover model has been applied to several drugs in order to characterize the time course of autoinduction in man (6-10). This model allows the estimation of a turnover rate constant of the induced enzymes which is an important parameter for characterizing the time course of both the autoinduction and deinduction process (6,9,10).

The aim of this study was to develop a population pharmacokinetic-enzyme turnover model that would describe the time course of CBZ deinduction under clinical conditions. This was accomplished by using a novel stable-labeled CBZ formulation that could be administered intravenously. The use of an intravenous formulation avoids the problems associated with variable absorption whereas the stable-label provided us with the means to measure a tracer amount of drug over a very short period of time. This information can provide evidence-based guidelines for management of drug therapy when CBZ is discontinued.

4.2 Subjects and methods

4.2.1 Patients and treatments

Data from fifteen patients with epilepsy receiving oral CBZ therapy in whom CBZ was being discontinued were recruited from epilepsy clinics in Minneapolis, MN, Miami, FL, and Atlanta, GA metropolitan areas. All subjects provided signed consent. The study was approved by the human subjects committee at each of the study sites and at the University of Minnesota. Patients were excluded from the study if they were on co-medications that are known to interact with CBZ. On the day of the study, patients were admitted to a clinical research center at the respective sites. A 10-minute intravenous infusion of a 100 mg dose of an investigational, stable-labeled CBZ (SL-CBZ) formulation (5H-dibenz[*b,f*]azepine-5-^{13}C, ^{15}N-Carboxamide; ^{13}C, ^{15}N-CBZ) was administered on three occasions: 1) the morning after the last dose of oral CBZ, following two weeks at the final regimen (mean dose = 140 mg±50.7 mg), 2) 6-8 days after the last oral CBZ dose, and 3) 6-8 weeks after the last oral CBZ dose. Serial plasma

SL-CBZ concentrations were measured following SL-CBZ administration at each occasion.

4.2.2 Blood sampling and assays

Fourteen blood samples were collected prior to drug administration and at 0.083, 0.25, 0.5, 1, 2, 4, 6, 10, 12, 24, 48, 72, and 96 hours after the end of the SL-CBZ infusion. The blood samples were immediately centrifuged and plasma was stored frozen until analysis. SL-CBZ concentrations were determined using liquid chromatograph-mass spectrometry (Agilent 1100 LCMSD with Electrospray, G 1946). Briefly, prepared samples were dried and reconstituted with ammonium acetate buffer and methanol as a mobile phase. CBZ-d_{10} was used as an internal standard. The samples were then separated using a Zorbex LC8/LC18 column (Agilent Technologies). Data were generated using Agilent ChemStation software (Agilent Technologies, Palo Alto, CA) and quantified using deuterated CBZ-d_{10} internal standard via a validated assay in the research laboratory.

4.2.3 Population pharmacokinetic analysis

Plasma SL-CBZ concentrations were fitted to a one-compartment model with a hypothetical enzyme compartment (6,8) to describe CBZ deinduction pharmacokinetics as shown in Figure 4.1.

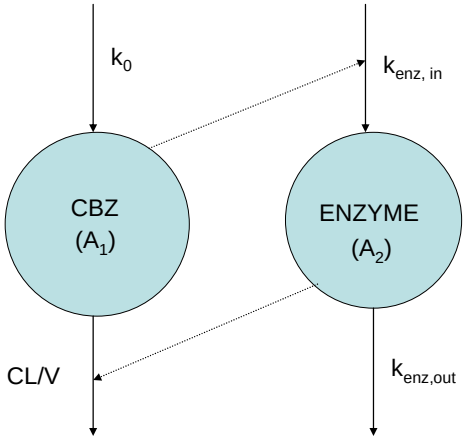

Figure 4.1 *Pharmacokinetic model of CBZ deinduction. The model represents a one-compartment model with a hypothetical enzyme compartment. The amount of CBZ (A_1) is determined by rate of infusion (k_0) and elimination rate constant (CL/V). The amount of enzymes (A_2) in a hypothetical enzyme compartment is governed by the rate constant of enzyme production ($k_{enz,\ in}$) and the rate constant of enzyme degradation ($k_{enz,\ out}$). The enzyme compartment is linked to the drug compartment by allowing CBZ clearance to be affected by amount of enzymes in a hypothetical enzyme compartment. At the same time, the absence/presence of CBZ affects the rate of enzyme synthesis.*

The change in the amount of CBZ (A_1, mg) over time can be described by equation 4.1.

$$\frac{dA_1}{dt} = k_o - CL \times Cp \times A_2, \quad (4.1)$$

where k_o is the rate of infusion (mg/hr), CL is CBZ clearance (L/hr), Cp is CBZ plasma concentration (mg/L). A_2 is the proportion of enzymes at time t relative to the amount of total enzymes at time zero in a hypothetical enzyme compartment. CBZ clearance is considered proportional to the amount of enzyme in a hypothetical enzyme compartment.

The deinduction process is often the result of a decrease in the rate of enzyme production, a reverse process of induction, leading the decrease amount of enzymes (11). Therefore, the chosen model was the model in which the change in the relative amount of enzymes in a hypothetical enzyme compartment (A_2) can be characterized by equation 4.2.

$$\frac{dA_2}{dt} = k_{enz,\,in} \times (1 - FACTOR) - k_{enz,\,out} \times A_2, \quad (4.2)$$

where $k_{enz,\,in}$ (relative amount/time) is the zero-order rate of enzyme production, $k_{enz,\,out}$ ($time^{-1}$) is the first-order rate constant of enzyme degradation, and FACTOR describes the fractional decrease of enzyme production rate. The apparent half-life of the CBZ deinduction process was estimated by dividing ln(2) by $k_{enz,\,out}$. Before the deinduction process (t = 0), the enzyme amount was assumed to be at steady state and was normalized to 1; therefore, the rate of enzyme production was equal to the rate of enzyme degradation. In this model, the deinduction process was assumed to begin at the first SL-CBZ administration (the next morning after the last dose of CBZ). It is possible that the

starting time of the deinduction process may impact the estimate of the half-life of the induced enzymes. Therefore, a sensitivity analysis, from time 0 (the start of SL-CBZ infusion) to 48 hours was performed to determine the effect of various starting times of the deinduction process on the estimate of $k_{enz,\ out}$. The models with the assumed starting time of the deinduction process at 0, 5, 10, 15, 20, 24, and 48 hours after the start of SL-CBZ infusion were fit to the data and the estimates of $k_{enz,\ out}$ were recorded.

Data from all three occasions were analyzed using the nonlinear mixed-effect modeling program (NONMEM), subroutine ADVAN 6 (version VI, NONMEM Project Group, UCSF/Globomax and PDx-Pop version 2.0). The first-order conditional estimation method with interaction (FOCE-I) was used for all analyses. Inter-individual variability (IIV) was modeled using an exponential error model for all parameters. The residual unexplained variability (RUV) was modeled using a proportional error model. Discrimination between hierarchical models was determined based on the difference in objective function value using the likelihood ratio test and visual inspection of diagnostic plots. A drop in objective function value of at least 10.83 (χ^2, $p < 0.001$, $df = 1$) after adding one parameter was considered statistically significant.

Initially, the model was developed without any covariates (base pharmacokinetic model). Due to the small sample size in this study, only weight was tested as a covariate. The covariate model was built in a stepwise fashion. Weight, centering at a convenience weight of 80 kg, was added on each estimated parameter (CL, V, and $k_{enz,\ out}$) one at a time using a linear covariate model. A decrease in OFV of at least 6.64 (χ^2, $p < 0.01$, df

= 1) was used to determine the inclusion of weight on each estimated parameter. The full model was developed by including all significant weight-parameter relationships. From the full model, weight was deleted from each parameter one at a time to obtain the final model. An increase of OFV from the full model of at least 10.83 (χ^2, $p \leq 0.001$, df=1) was used as the chosen criteria for retaining weight-parameter relationships in the covariate model. Xpose (12) and S-plus 2000 (Insightful Corp, Seattle, WA, USA) were used for graphical model diagnostics.

Several possible models other than the chosen model were considered (Table 4.1): i) a model where the deinduction process was characterized by increasing the rate of enzyme degradation rather than decreasing the rate of enzyme production, ii) a model describing autoinduction of CBZ in which an increase of enzyme amount is described by a linear relationship between CBZ concentrations and the rate of enzyme production, and iii) a model describing autoinduction of CBZ in which an increase of enzyme amount is described by an Emax relationship between CBZ concentrations and the rate of enzyme production.

4.2.4 Model evaluation

4.2.4.1 The bootstrap confidence interval

Five hundred bootstrap data sets were generated using Wings for NONMEM program (Version 600, http://wfn.sourcefourge.net) and were used for calculating the bootstrap 95% confidence intervals (CI). The detailed methods of the bootstrap confidence interval procedures are presented in section 2.2.4.1

4.2.4.2 The visual predictive check (VPC)

The visual predictive check was used as a diagnostic tool to assess the adequacy of the final model (13,14). The VPC is a graphical assessment to determine whether the proposed model is able to reproduce the variability in the observed data from which it was originated. Five hundred data sets were simulated with the same study design as the observed data using the final model parameter estimates obtained from NONMEM. The median and 90% prediction intervals (5^{th} and 95^{th} percentile) of the simulated concentrations were calculated at each time point and plotted against the observed concentrations.

4.3 Results

4.3.1 Model building

A total of 524 SL-CBZ concentration-time points from fifteen patients were used in this study. Six women and nine men with a mean weight of 78 kg, and age of 39 years participated in the study. Fourteen patients completed all three occasions of the study, whereas one patient only completed the first two occasions. Data from all fifteen patients were included in the analyses. Figure 4.2 presents the observed SL-CBZ concentration-time curves and variability for each individual at each occasion.

Of the model explored, the chosen model that described the deinduction process by a fractional decrease in the rate of enzyme production best described the data. A model where the deinduction process was characterized by an increasing rate of enzyme degradation described the data as well as the chosen model based on the OFV and

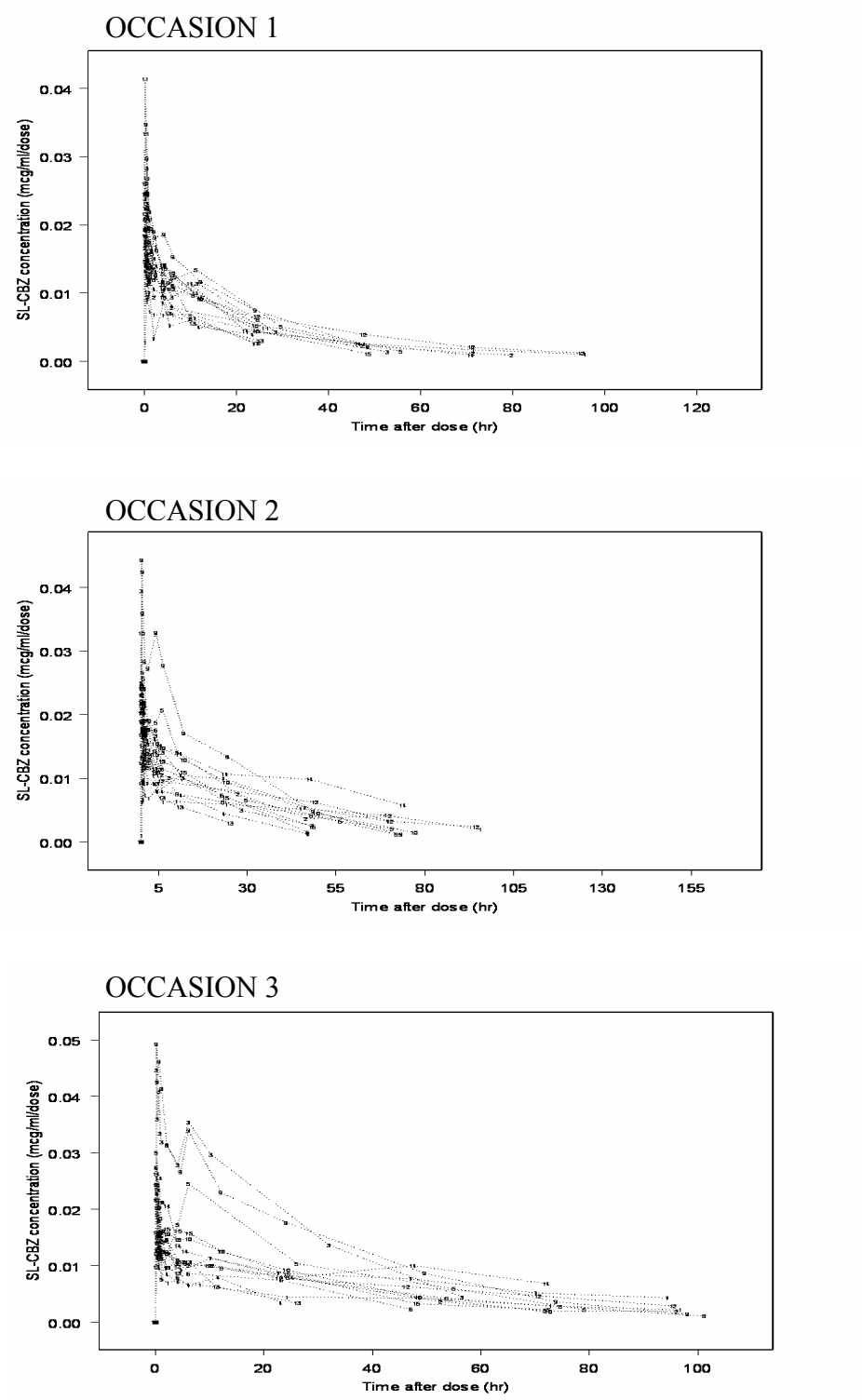

Figure 4.2 *The individual observed concentration time curves of SL-CBZ at each occasion*

goodness-of-fit plots. However, this model is not as physiologically plausible as the chosen model. The concentration-dependent autoinduction models, both linear and Emax models, were not able to fit the data. The model with the linear increase in the rate of enzyme production resulted in unreasonable parameter estimates and it was not possible to obtain the parameter estimates from the Emax type model. The results from the fit of all tested models are shown in Table 4.1

Table 4.1 The results from the fit of all models tested in this analysis

Model	Differential equation describing the change of amount of enzymes during deinduction process	Results
1	$\frac{dA_2}{dt} = k_{enz,\,in} \times (1 - FACTOR) - k_{enz,\,out} \times A_2$	Chosen model
2	$\frac{dA_2}{dt} = k_{enz,\,in} - k_{enz,\,out} \times (1 - FACTOR) \times A_2$	Described the data as well as the chosen model
3	$\frac{dA_2}{dt} = k_{enz,\,in} \times (1 + Slope \times Cp) - k_{enz,\,out} \times A_2$	Obtained unreasonable parameter estimates
4	$\frac{dA_2}{dt} = k_{enz,\,in} \times (1 + \frac{Emax \times Cp}{EC_{50} + Cp}) - k_{enz,\,out} \times A_2$	Unable to obtain the parameter estimates

Cp, SL-CBZ concentration; Emax, the maximum induction effect; EC_{50}, the concentration producing one-half of the maximum induction effect

Weight was tested as a covariate on V, CL, and $k_{enz,\ out}$. V was the only parameter indicated to have a significant relationship with weight. The addition of weight to V resulted in a drop in OFV from the base model (the difference in OFV = -19.7) and an improvement in the goodness-of-fit plots compared with the base pharmacokinetic model was observed (Figure 4.3). Therefore, the effect of weight on V was included in the final model. The final parameter estimates are presented in Table 4.2. Based on the $k_{enz,\ out}$ estimate of 0.00805 hr^{-1}, the model predicted apparent half-life of the deinduction process was 86 hours (3.6 days). Adding IIV into $k_{enz,\ out}$ or FACTOR did not improve the fit. Therefore, $k_{enz,\ out}$ and FACTOR were estimated without an estimate of IIV. Not being able to determine variability for an estimated parameter is not unusual if the data are limited and do not allow partitioning of the variability. The results from the sensitivity analysis showed that when the starting time of the deinduction process was varied from 0 to 48 hours, the estimated rate constants for the enzyme degradation were not different (the estimated $k_{enz,\ out}$ ranging from 0.008 to 0.0087 were obtained). These results indicate that the assumed starting time points have a small impact on the estimation of $k_{enz,\ out}$.

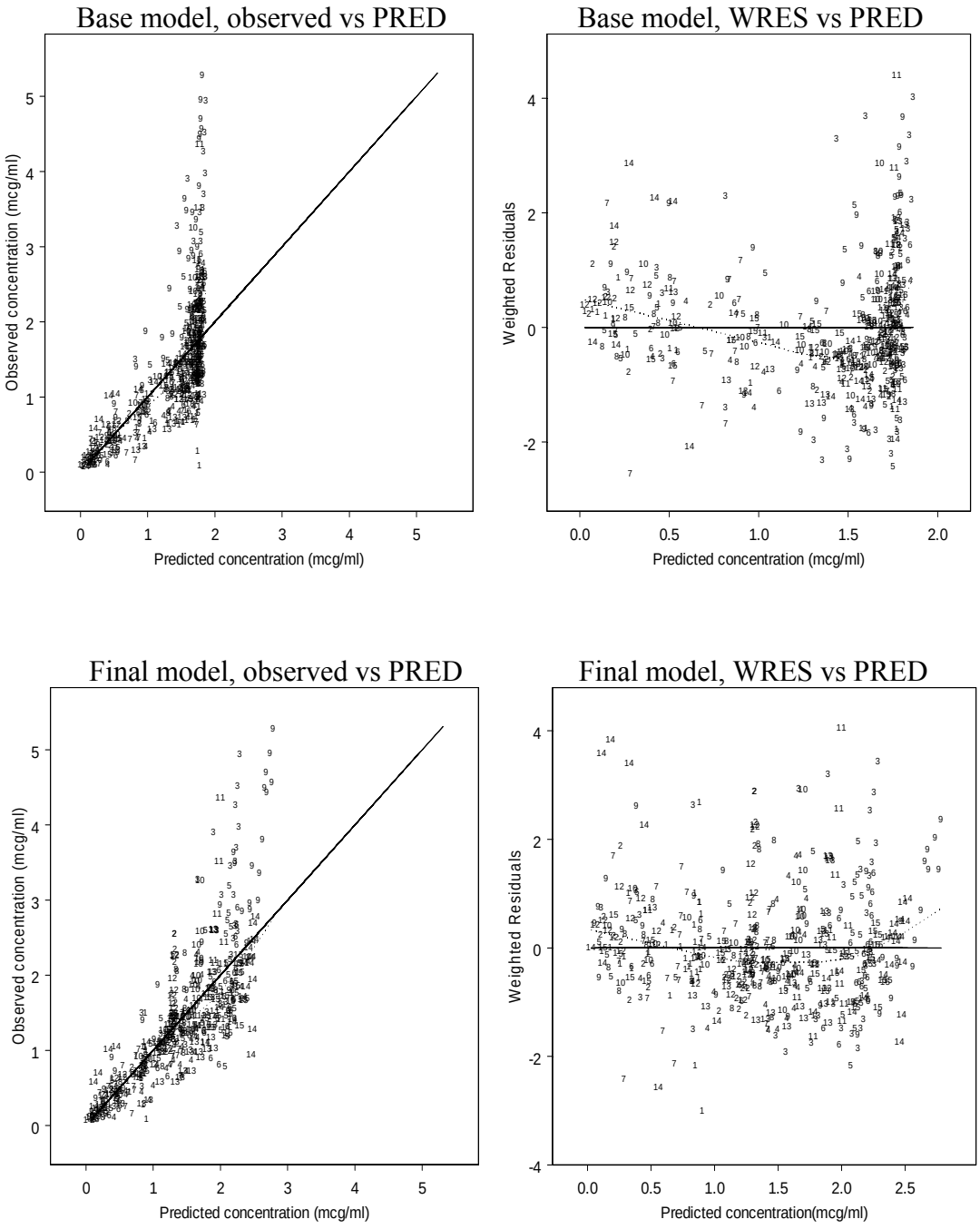

Figure 4.3 *The goodness of fit plot; the observed versus population model predicted concentrations (PRED) and weighted residuals (WRES) versus population model predicted concentrations (PRED) of the base model and the final model (adding weight into V)*

Table 4.2 Final model parameter estimates and 95% confidence intervals (CI) from NONMEM and the bootstrap analysis[§]

Parameters	NONMEM		Bootstrap Analysis	
	Estimates	95%CI[*]	Median	95% CI[†]
Initial clearance (L/hr)	3.05	[2.62, 3.48]	3.06	[2.67, 4.93]
V (L)	64.3	[59.2-69.4]	64.1	[58.54, 70.63]
Coefficient of weight on V	0.869	[0.57-1.17]	0.863	[0.5, 1.22]
First order rate constant for enzyme degradation ($k_{enz, out}$)	0.00805	[0.003-0.0128]	0.0082	[0.005,0.066]
FACTOR	0.494	[0.438-0.55]	0.497	[0.43,0.7]
IIV for initial clearance (%CV)	31.6	[19.52-40.52]	30	[18.4,39.8]
IIV for V (%CV)	17.5	[12.57-21.4]	16.16	[9.54, 20.86]
RUV, proportional (%CV)	26.9	[24.7-29.77]	26.7	[23.48, 29.79]

[§] From 493 bootstrap runs with a successful minimization and successful covariance step

[*] Estimate ± 1.96 × (standard error of the estimate)

[†] Values at 2.5th and 97.5th percentile of the ranked bootstrap parameter estimates

4.3.2 Model evaluation

4.3.2.1 The bootstrap confidence interval

From 500 bootstrap runs, 493 runs with a successful minimization and successful covariance step were included in the bootstrap analysis. The median parameter estimates and their 95% CI obtained from the bootstrap approach were comparable to the estimates obtained from NONMEM (Table 4.2). However, the 95% CI of $k_{enz,\ out}$ obtained from the bootstrap approach was wider than the one obtained from NONMEM. This situation is common when the size of sample is small (15). As the 95% CI obtained from NONMEM assumes the asymptotic normality, this assumption is true when the sample size is large enough. Therefore, in a small data set, the bootstrap 95% CI can be wider than the one obtained from NONMEM.

4.3.2.2 The visual predictive check

Figure 4.4 (a-c) presents the visual predictive check plots. These plots show that most of the observed concentrations on all three occasions fell within the 90% prediction intervals obtained from the simulated data represented by the shaded area. Less than 10% of the observed concentrations lie outside the specific prediction intervals. The results from the visual predictive check show that the final model adequately describes the majority of the observed data in this population.

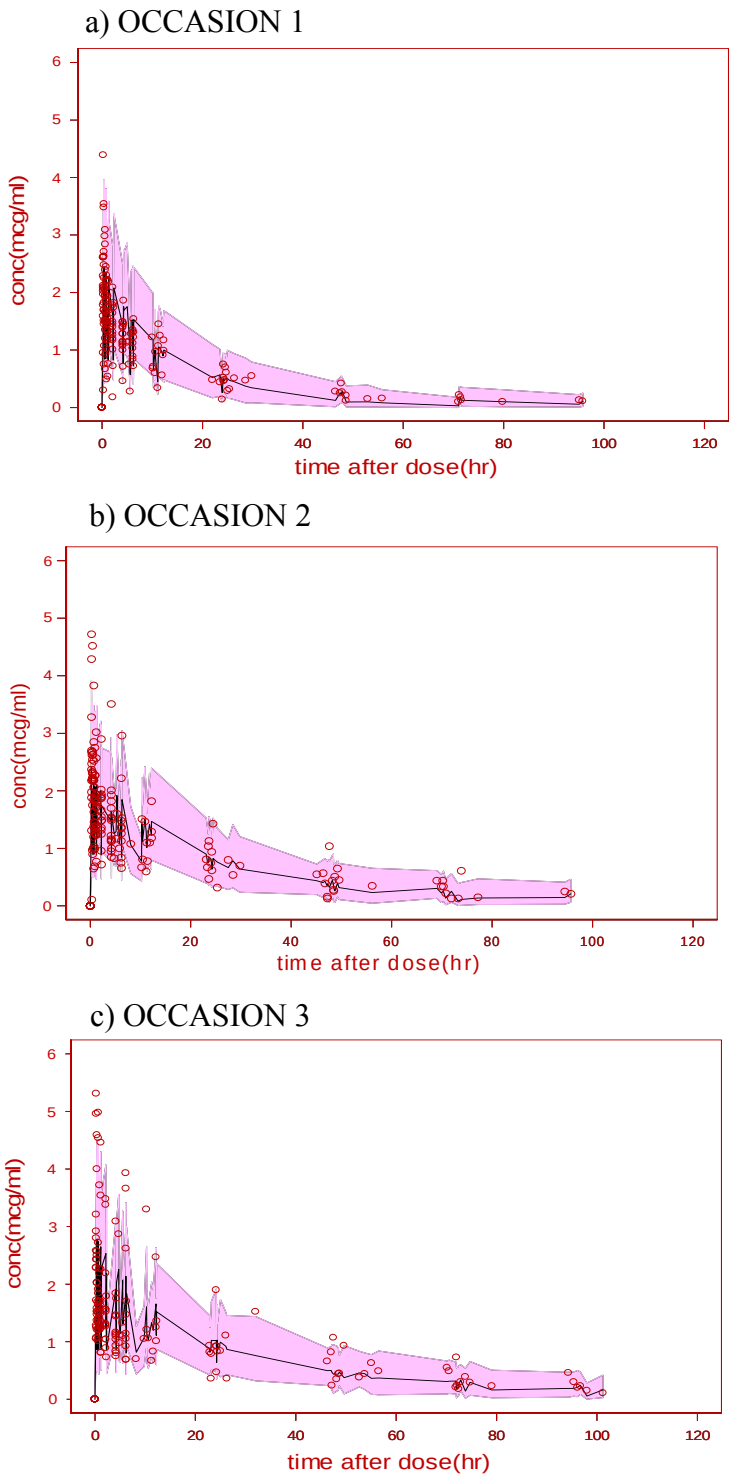

Figure 4.4 The visual predictive check plots for occasion 1 (a), occasion 2 (b), and occasion 3 (c). The solid lines and shaded area represent median and 90% prediction interval from 500 simulated data. The circles represent the observed concentrations.

4.4 Discussion

This study is the first to use an intravenous formulation to characterize the deinduction half-life of CBZ in patients with epilepsy. This use of an intravenous formulation avoided issues associated with variable absorption of the drug. Furthermore, our results demonstrate that the time course of CBZ deinduction can be adequately described by an enzyme turnover model. This model yields an estimate of the degradation half-life of the induced enzymes from which the time course of CBZ deinduction can be determined. It should be noted that this estimated half-life of enzyme turnover is a hybrid value encompassing all isoenzymes involved in CBZ metabolism rather than any particular isoenzyme.

The mechanism underlying autoinduction/deinduction of CBZ is not well understood. It has been postulated that autoinduction of CBZ metabolism occurs by increasing the synthesis of enzyme (*de novo* protein synthesis) (1). There is evidence that both CBZ and CBZ-E can activate the nuclear receptor, PXR (pregnane X receptor), resulting in a higher expression level of mRNA of numerous enzymes including several CYP genes, conjugated enzymes, and transporters (1). Deinduction is believed to occur via the reverse process of autoinduction. Based on current understanding of the mechanism of CBZ deinduction, the model used in this study, which is based on a decreasing rate of enzyme production is more physiologically plausible than a model with an increasing rate of enzyme degradation. Even though, the later model described the data as well as the chosen model. In order to apply a concentration-dependent autoinduction model (the linear and Emax model), drug concentrations should be measured during the induction

process (6,8,10). However the data used in this study were collected during the deinduction process of CBZ and models that describe the deinduction process are more applicable to fit this data than concentration-dependent autoinduction models (Table 4.1).

In the situations in which the elimination half-life of an inducer is similar to or longer than the induced enzymes, the pharmacokinetics of the inducer may impact the accurate estimation of a half-life of the induction/deinduction process; therefore, pharmacokinetics of the inducer cannot be ignored (16). However, in the case that the elimination half-life of an inducer is considerably faster than the half-life of the induced enzymes, the kinetics of the inducer will have minimal effect on the estimated half-life of the induction/deinduction process. Hence, the time course of the induction and deinduction processes is determined by the same rate constant of enzyme degradation (16). The rate constant for the enzyme degradation estimated from our model was 0.00805 hr^{-1}, corresponding to an overall enzyme half-life of 3.6 days (86.1 hours), whereas the elimination rate constant of CBZ in the induced state was estimated to be 0.048 hr^{-1}, corresponding to a CBZ half-life of 15 hours. These values are consistent with the enzyme half-life reported in previous studies of CBZ autoinduction/deinduction (10,17-19). Based on the proposed final model, the relative amount of enzymes in a hypothetical enzyme compartment predicted by this model is shown in Figure 4.5

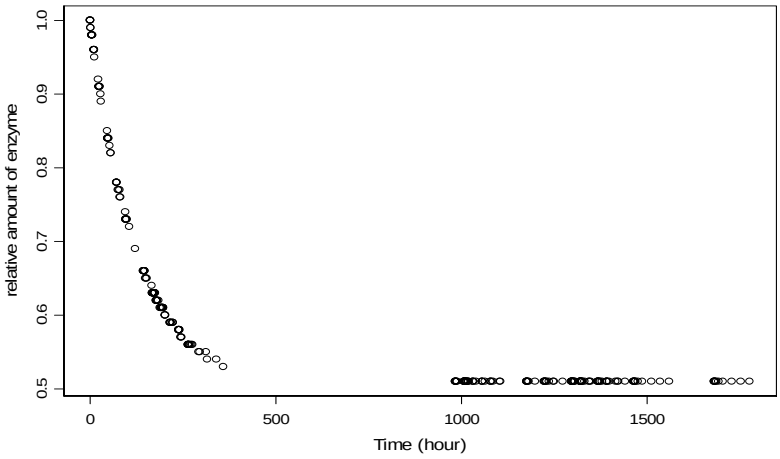

Figure 4.5 *The relative amount of enzyme in a hypothetical enzyme compartment with the initial amount of enzyme is normalized to 1*

In this study, the estimate of CBZ half-life is much faster than the estimated induced enzyme half-life; therefore, the all-or-none model used in our study, where the pharmacokinetics of the inducer was not incorporated in the model, should adequately describe the data. It is possible that a longer half-life of CBZ during the deinduced state may be observed and may affect the estimated half-life of the deinduction process. However, even if the half-life of CBZ doubled it would still be much shorter than the half-life of the induced enzymes. Therefore, with the relatively rapid elimination of CBZ during the deinduction process compared with the turnover half-life of the enzymes, the effect of CBZ kinetics on the estimate of the enzyme degradation rate constant should be negligible. A previous study that used probe substrates to determine the CBZ-mediated induction of CYP3A4 and CYP1A2 separately obtained the estimated half-lives of CYP3A4 and CYP1A2 of 70 and 105 hours, respectively (10). The estimated half-life of

enzymes obtained from our study following administration of an intravenous formulation is within this range.

The model used in this analysis assumed that the deinduction process started when the first dose of SL-CBZ was given (t=0). Bernus et al (20) speculates a 1-2 day lag time in the deinduction process of CBZ. Therefore, different starting times of the deinduction process, varying from time 0-48 hours, were tested in the sensitivity analysis. The results from the sensitivity analysis indicate that the time that deinduction begins has a minimal effect in the estimate of $k_{enz,\ out}$. It is also possible that the first two doses of SL-CBZ may delay the deinduction process causing a slight increase in the deinduction half-life; however, this effect should be minimal.

In summary, a population pharmacokinetic model characterizing the time course of CBZ deinduction was developed using an enzyme turnover model. The bootstrap approach and visual predictive check confirmed the reliability and adequacy of the final model. Based on a $k_{enz,\ out}$ estimate of 0.00805 hr^{-1}, induction of CBZ metabolizing enzymes is reduced by half at 3.6 days and by three-fourths at 7.2 days after CBZ is completely discontinued. Therefore, the deinduction process should be completed within 2 weeks after discontinuation of CBZ therapy. There are several clinical implications that arise from our results. The doses of a number of important drugs such as hormonal contraceptives may need to be adjusted within 3-6 days following discontinuation of CBZ. Also, it is common to discontinue CBZ during monitoring of persons with epilepsy in inpatient

diagnostic units. The results from this study can be important in estimating the optimal doses of CBZ when it is reintroduced after being held for seizure monitoring.

4.5 References

1. Oscarson M, Zanger UM, Rifki OF, Klein K, Eichelbaum M, Meyer UA. Transcriptional profiling of genes induced in the livers of patients treated with carbamazepine. *Clin Pharmacol Ther*. 2006;80(5):440-456.
2. Eichelbaum M, Ekbom K, Bertilsson L, Ringberger VA, Rane A. Plasma kinetics of carbamazepine and its epoxide metabolite in man after single and multiple doses. *Eur J Clin Pharmacol*. 1975;8(5):337-341.
3. Pitlick WH, Levy RH. Time-dependent kinetics I: Exponential autoinduction of carbamazepine in monkeys. *J Pharm Sci*. 1977;66(5):647-649.
4. Warren JWJ, Benmaman JD, Wannamaker BB, Levy RH. Kinetics of a carbamazepine-ethosuximide interaction. *Clin Pharmacol Ther*. 1980;28(5):646-651.
5. Okey AB. Enzyme induction in the cytochrome P-450 system. *Pharmacol Ther*. 1990;45(2):241-298.
6. Hassan M, Svensson US, Ljungman P, et al. A mechanism-based pharmacokinetic-enzyme model for cyclophosphamide autoinduction in breast cancer patients. *Br J Clin Pharmacol*. 1999;48(5):669-677.
7. Huitema AD, Mathot RA, Tibben MM, Rodenhuis S, Beijnen JH. A mechanism-based pharmacokinetic model for the cytochrome P450 drug-drug interaction between cyclophosphamide and thioTEPA and the autoinduction of cyclophosphamide. *J Pharmacokinet Pharmacodyn*. 2001;28(3):211-230.
8. Kerbusch T, Huitema AD, Ouwerkerk J, et al. Evaluation of the autoinduction of ifosfamide metabolism by a population pharmacokinetic approach using NONMEM. *Br J Clin Pharmacol*. 2000;49(6):555-561.
9. Gordi T, Xie R, Huong NV, Huong DX, Karlsson MO, Ashton M. A semiphysiological pharmacokinetic model for artemisinin in healthy subjects incorporating autoinduction of metabolism and saturable first-pass hepatic extraction. *Br J Clin Pharmacol*. 2005;59(2):189-198.

10. Magnusson MO, Dahl ML, Cederberg J, Karlsson MO, Sandstrom R. Pharmacodynamics of Carbamazepine-mediated Induction of CYP3A4, CYP1A2, and Pgp as Assessed by Probe Substrates Midazolam, Caffeine, and Digoxin. *Clin Pharmacol Ther*. 2007;
11. Fuhr U. Induction of drug metabolising enzymes: pharmacokinetic and toxicological consequences in humans. *Clin Pharmacokinet*. 2000;38(6):493-504.
12. Jonsson EN, Karlsson MO. Xpose--an S-PLUS based population pharmacokinetic/pharmacodynamic model building aid for NONMEM. *Comput Methods Programs Biomed*. 1999;58(1):51-64.
13. Fang L, Holford NH, Hinkle G, et al. Population pharmacokinetics of humanized monoclonal antibody HuCC49deltaCH2 and murine antibody CC49 in colorectal cancer patients. *J Clin Pharmacol*. 2007;47(2):227-237.
14. Yano Y, Beal SL, Sheiner LB. Evaluating pharmacokinetic/pharmacodynamic models using the posterior predictive check. *J Pharmacokinet Pharmacodyn*. 2001;28(2):171-192.
15. Yafune A, Ishiguro M. Bootstrap approach for constructing confidence intervals for population pharmacokinetic parameters. I: A use of bootstrap standard error. *Stat Med*. 1999;18(5):581-599.
16. Abramson FP. Kinetic models of induction: I. Persistence of the inducing substance. *J Pharm Sci*. 1986;75(3):223-228.
17. Korth-Bradley JM, Ludden TM. Carbamazepine pharmacokinetics during induction and reversal of induction. *Pharmacotherapy*. 1991;11(3):272.
18. Mikati MA, Browne TR, Collins JF. Time course of carbamazepine autoinduction. The VA Cooperative Study No.118 Group. *Neurology*. 1989;39(4):592-594.
19. Schaffler L, Bourgeois BF, Luders HO. Rapid reversibility of autoinduction of carbamazepine metabolism after temporary discontinuation. *Epilepsia*. 1994;35(1):195-198.

20. Bernus I, Dickinson RG, Hooper WD, Eadie MJ. Early stage autoinduction of carbamazepine metabolism in humans. *Eur J Clin Pharmacol*. 1994;47(4):355-360.

CHAPTER 5

The Effect of Collinearity on Power, Bias and Precision of Parameter Estimates in a Population Pharmacokinetic Covariate Model

5.1 Background and aims of the study

In the population pharmacokinetic/pharmacodynamic (PK/PD) analysis, one of the goals is to explain part of the parameter variability by using a covariate model that describes the relationship between patient specific covariates and pharmacokinetic parameters. It is common that in most situations more than covariate will be considered in the covariate model building step. A literature survey of model building strategies in population PK/PD analysis during 2002-2004 reported a median of 6 covariates tested in the covariate model building (1). As a number of covariates increases, a well-known problem that may arise is the collinearity among covariates in the data set. Several problems arise when two or more highly correlated covariates are simultaneously entered into a model (2-7). A study by Bonate (3) shows that high correlation between covariates affects the efficiency of the parameter estimates. Although the results indicated that the accuracy and precision of the parameter estimates decreased with a higher degree of collinearity, only one simulated data set was generated at each degree of collinearity in this study. Thus, the conclusions of the effect of collinearity on power and accuracy of the parameter estimates can not be drawn. Another simulation study investigated the effect of correlation between two covariates on the power of selecting a true covariate, bias, and predictive performance where the correlation was considered to be the correlation between the true and false covariates (8).

However, in a real practical situation, it is, most of the time, unable to distinguish which covariate is the true and which is the false covariate. More often, both of them could be true covariates and carry unique information on the parameter. The influence of the correlation between two true covariates on power and accuracy of the parameter estimates has not yet been studied. Our study, therefore, aimed to investigate the effect of collinearity between two true continuous covariates, sample sizes, and magnitude of covariate coefficient on power, bias, and precision of the parameter estimates in the population pharmacokinetic analysis. The results from this study could be useful to guide modelers on how and to what extent the collinearity could affect parameter estimates in covariate model building and when further action should be performed to avoid the consequent problems that may arise.

5.2 Methods

5.2.1 Simulation of covariate data sets

Covariate data consisting of five random covariate vectors (X_1, $X_{2\,(1)}$, $X_{2\,(2)}$, $X_{2\,(3)}$, and $X_{2\,(4)}$) were simulated from a multivariate normal distribution with the arbitrary mean of 100 and standard deviation of 20 for all covariates. In order to obtain the desired correlation between covariates, the correlation matrix used in the simulation was defined as:

	X_1	$X_{2\,(1)}$	$X_{2\,(2)}$	$X_{2\,(3)}$,	$X_{2\,(4)}$
X_1	1	0	0.15	0.5	0.85
$X_{2\,(1)}$	0	1	0	0	0
$X_{2\,(2)}$	0.15	0	1	0	0
$X_{2\,(3)}$	0.5	0	0	1	0
$X_{2\,(4)}$	0.85	0	0	0	1

Based on this correlation matrix, the correlation between X_1 and $X_{2\,(i)}$ (i=1 to 4) can be viewed as a correlation between two covariates which varied from 0 to 0.85. For each simulated covariate data set, *all* of the correlations between X_1 and the other four covariates ($X_{2\,(i)}$) should not deviate more than 0.05 from the values defined in the correlation matrix. Therefore, the correlation between X_1 and $X_{2\,(1)}$, X_1 and $X_{2\,(2)}$, X_1 and $X_{2\,(3)}$, and X_1 and $X_{2\,(4)}$, must be in the range of -0.05 to 0.05, 0.10 to 0.20, 0.45 to 0.55, and 0.80 to 0.90, respectively. If one or more of the correlations between these covariates were not within the desired range, that data set was discarded and replaced with a new set. As only a pair of covariates, X_1 and $X_{2\,(i)}$, was used later in the pharmacokinetic data simulations and data analysis, the correlations among covariates $X_{2(i)}$ were not of concern and no attempt was made to constrain them to be within the desired range. The covariate data sets for the sample size of 20, 50, 100, and 500 were generated. For each sample size, 500 covariate data sets were replicated. All covariate data were generated using S-PLUS 7 (Insightful Corp, Seattle, WA, USA).

5.2.2 Study design and pharmacokinetic data simulations

Plasma concentrations were simulated using NONMEM (version VI, NONMEM Project Group, UCSF/Globomax and PDx-Pop version 2.0). The drug pharmacokinetics were

assumed to follow a one-compartment model with a single i.v. bolus administration as described by equation 5.1:

$$C_{ij} = \frac{Dose}{V_i} \times e^{-(CLi/Vi)\times tj} \quad (5.1)$$

where C_{ij} represents the expected plasma concentrations of the i^{th} individual at time j, CL_i and V_i are the clearance and volume of distribution of the i^{th} individual. One thousand milligrams of a hypothetical drug was given to all individuals. Four plasma samples were collected at time 0.1, 1, 3 and 4 hour post dose for all subjects in all simulations. A linear relationship between the typical value of clearance (TVCL) and two of the covariates, X_1 and $X_{2\,(i)}$ (i = 1 to 4), as presented by equation 5.2a to 5.2d was used to describe the population mean clearance.

$$TVCL = \theta_1 + \theta_2 \times X_1 + \theta_3 \times X_{2\,(1)} \quad (5.2a)$$

$$TVCL = \theta_1 + \theta_2 \times X_1 + \theta_3 \times X_{2\,(2)} \quad (5.2b)$$

$$TVCL = \theta_1 + \theta_2 \times X_1 + \theta_3 \times X_{2\,(3)} \quad (5.2c)$$

$$TVCL = \theta_1 + \theta_2 \times X_1 + \theta_3 \times X_{2\,(4)} \quad (5.2d)$$

where θ_1 is the intercept, θ_2 is coefficient for covariate X_1, and θ_3 is coefficient for covariate $X_{2\,(i)}$. The value of θ_1 was set to be 10 for all simulation settings. In model I (default model), both θ_2 and θ_3 were set to be 0.3. The inter-individual variability (IIV) of

CL and V was modeled with an exponential error model as described by equation 5.3 and 5.4:

$$CL_i = TVCL \times \exp(\eta_{i,CL}) \quad (5.3)$$

$$V_i = TVV \times \exp(\eta_{i,V}) \quad (5.4)$$

where TVCL and TVV is the typical value of clearance and the typical value of volume of distribution in the population, and $\eta_{i,CL}$ and $\eta_{i,V}$ is the inter-individual variability which is assumed to be normally distributed with a mean of zero and variance of ω_{CL}^2 and ω_V^2. The residual unexplained variability was modeled with a proportional error model as described by equation 5.5:

$$C_{obs,ij} = C_{ij} \times (1 + \varepsilon_{ij}) \quad (5.5)$$

where $C_{obs,ij}$ and C_{ij} are the observed and expected concentrations for the i^{th} individual at time j, and ε_{ij} is the residual unexplained variability which is normally distributed with a mean of zero and variance of σ^2.

It must be kept in mind that each covariate data set consisted of five covariate vectors, and four pairs of the covariates representing four different correlations (0 to 0.85) were used for simulation of pharmacokinetic data as described by equation 5.2a to 5.2d *one at a time*. Therefore, for each covariate data set, four different pairs of covariates were used

in the simulation generating four simulated data sets with different levels of correlation. The simulations were repeated for all 500 covariate data sets previously generated in Section 5.2.1. Ultimately, for each size of sample, a total of 2000 simulated data sets (500 simulated data sets for each degree of correlation) were generated.

The impact of the covariate coefficient magnitude on the power of selecting the true covariates was further investigated. This investigation was performed for a sample size of 500. An alteration from model I was made. In this model (model II), the value for θ_3 was set to be 0.15 which is half of the value used in model I. The population pharmacokinetic parameter values used in the simulations for both model I and II are summarized in Table 5.1. The covariate data, structural, inter-individual variability and residual error model were kept the same as it was used in model I; only the parameter values were changed according to the values set for model II and the different random seeds from model I were used in this simulation setting. The simulations were repeated for all 500 covariate data for N=500.

Table 5.1 The population pharmacokinetic parameter values for simulations in model I and model II

PK parameters	Values	
	Model I	Model II[§]
θ_1	10	10
θ_2	0.3	0.3
θ_3	0.3	*0.15*
TVV	100	100
ω_{CL}^2	0.09	0.09
ω_V^2	0.09	0.09
σ^2	0.1	0.1

[§] Simulations were done in N=500

5.2.3 Data analysis

5.2.3.1 Power estimation and assessment of parameter estimates

All simulated data from model I and model II were analyzed using NONMEM. The first-order conditional estimation method with interaction (FOCE-I) was used for all analyses. For each simulated data set, two covariates (X_1 and $X_{2(i)}$) corresponding to the model of the TVCL used for simulating pharmacokinetic data, were tested to be included into the base model (the model without any covariates) using a stepwise forward selection procedure. For example, if the pharmacokinetic data were simulated using equation 5.2a, X_1 and $X_{2(1)}$ were tested to be included into the base model. Similarly, if equation 5.2b, 5.2c, or 5.2d was used in pharmacokinetic data simulation, X_1 and $X_{2(2)}$, X_1 and $X_{2(3)}$, or X_1 and $X_{2(4)}$ were tested to be included into the base model, respectively. In general, the stepwise forward selection starts with the base model. Then, each covariate is tested to be added into the base model one at a time. The most significant covariate is selected to be included into the base model. The remaining covariates are tested and, then, the most significant covariate is further added into the model with one covariate already selected. This process is then repeated until none of the remaining covariates are significant. A flow chart of the stepwise forward selection procedure is presented in Figure 5.1. The details of the analyses of a simulated data are described in the following steps:

Step 1: Each simulated data set was fitted to the base model (the model without any covariate). The objective function value (OFV) obtained from each fit was recorded.

Step 2: X_1 was added into the base model by assuming a linear relationship with TVCL as presented in equation 5.6. Each of the simulated data sets was then fitted to this model. The decrease in OFV from the base model ($dOFV_{(X_1)}$) was recorded.

$$TVCL = \theta_1 + \theta_2 \times X_1 \quad (5.6)$$

Step 3: Each of the simulated data sets was fitted to the model in which $X_{2\,(i)}$ was added linearly to the base model as presented in equation 5.7. As mentioned earlier, the covariate $X_{2(i)}$ was added corresponding to the model of the TVCL used for the simulation of pharmacokinetic data. For example, if the pharmacokinetic data were simulated using equation 5.2a, $X_{2(1)}$ was added into the base model in this step. The decrease in OFV from the base model ($dOFV_{(X_{2(i)})}$) was calculated and recorded.

$$TVCL = \theta_1 + \theta_2 \times X_{2\,(i)} \quad (5.7)$$

Step 4: The significance of covariate X_1 and $X_{2(i)}$ was assessed using the likelihood ratio test. A decrease in OFV of at least 3.84 from the base model was considered significant ($p=0.05$, χ^2, $df=1$). The most significant covariate between the two was brought forward into the base model. Therefore, either X_1, $X_{2\,(i)}$ or neither were added into the base model in this step based on its significance.

Step 5: The models with either a significant X_1 or $X_{2\,(i)}$ were further analyzed in this step. The remaining covariate was tested for including into the model with one covariate previously added. TVCL was modeled as a linear function of both X_1 and $X_{2(i)}$ as presented in equation 5.8.

$$TVCL = \theta_1 + \theta_2 \times X_1 + \theta_3 \times X_{2\,(i)} \quad (5.8)$$

The model in equation 5.8 was considered significantly better than the model with one covariate added, if the decrease in OFV of at least 3.84 (p=0.05, χ^2, df=1) was obtained. Step 1-5 were repeated for all simulated data. A summary flow chart of the simulation and data analysis is presented in Figure 5.2. The frequency of selecting the true covariate model (having both X_1 and $X_{2\,(i)}$ as significant covariates) was recorded and the estimated covariate coefficients for X_1 and $X_{2\,(i)}$ ($\hat{\theta}_2$ and $\hat{\theta}_3$) were extracted.

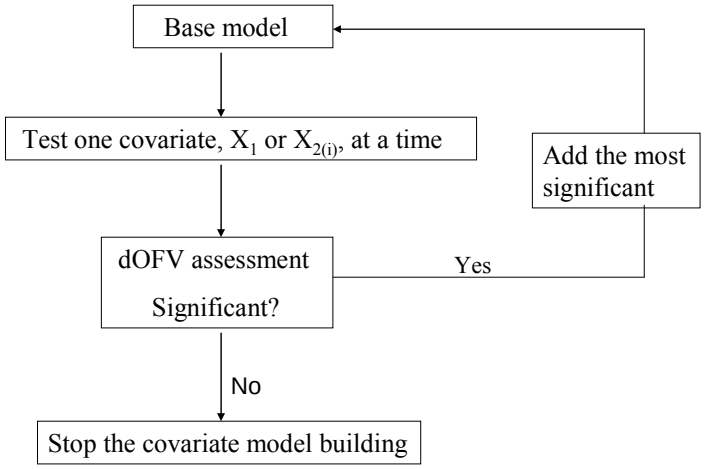

Figure 5.1 *Flow chart of stepwise forward selection procedure.*

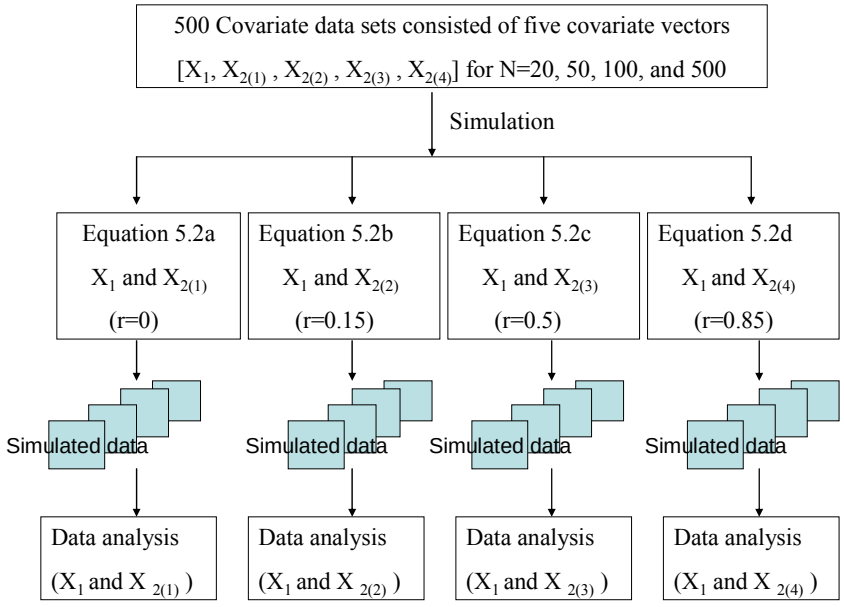

Figure 5.2 *A summary of the simulations and data analysis in the study. Five hundred covariate data sets consisted of five covariate vectors with different degrees of correlation were generated for a sample size of 20, 50, 100, and 500. Then, pharmacokinetic data sets were simulated assuming a linear relationship between the typical value of clearance (TVCL) and two of the covariates (X_1 and $X_{2(i)}$) as presented in equation 5.2a-5.2d. The simulated pharmacokinetic data sets were analyzed using the stepwise forward selection procedure. Two covariates (X_1 and $X_{2(i)}$) corresponding to the model of the TVCL used for simulating pharmacokinetic data were tested for including into the base model using the stepwise forward selection procedure.*

For each size of sample and degree of correlation, a percent power of selecting the true covariates was calculated from 500 simulations. Only the runs with successful minimization (with or without successful covariance matrix) were considered. The ratio of the number of replicates selecting the true covariate model to the total number of successfully minimized replicates multiplied by 100 was the estimated percent power.

The estimated covariate coefficients ($\hat{\theta}_2$ and $\hat{\theta}_3$) from model I were evaluated by comparison with the true values set for simulations. The mean percent prediction error (MPPE) which represents bias and the mean percent absolute error (MPAE) which represents precision were calculated as a relative value (9). Using θ_2 as an example, the MPPE and MPAE was calculated as

$$\text{MPPE} = \frac{\sum_{n=1}^{500} I \times [(\hat{\theta}_2 - \theta_2) / \theta_2]}{\sum_{n=1}^{500} I} \times 100 \qquad (5.9)$$

$$\text{MPAE} = \frac{\sum_{n=1}^{500} I \times |(\hat{\theta}_2 - \theta_2) / \theta_2|}{\sum_{n=1}^{500} I} \times 100 \qquad (5.10)$$

where n is a total number of replicated data sets with a successful minimization. $\hat{\theta}_2$ is the estimated covariate coefficient for X_1, θ_2 is the true value of covariate coefficient for X_1, and I is the indicator function (I=1, if the true covariate model was selected and I=0, if otherwise)

5.2.3.2 Standard error of parameter estimates

It is widely known that when two correlated covariates are simultaneously included into the model, the estimated coefficients tend to have large standard errors. In this study, the effect of the degree of collinearity on the standard error of parameter estimates was investigated in the sample size of 50 and 500. All simulated data sets from model I were analyzed by fitting the data to equation 5.8, regardless of a significance of any covariates.

The runs with a successful minimization and successful covariance step were included in this analysis. The absolute standard errors of the estimated covariate coefficients ($SE_{(\hat{\theta}_2)}$and $SE_{(\hat{\theta}_3)}$) were extracted and summarized.

5.3 Results

5.3.1 Power estimation and assessment of parameter estimates

The effect of the correlation between two covariates and sample size on percent power of selecting the true covariate model (selecting both X_1 and $X_{2(i)}$) from model I is shown in Figure 5.3.

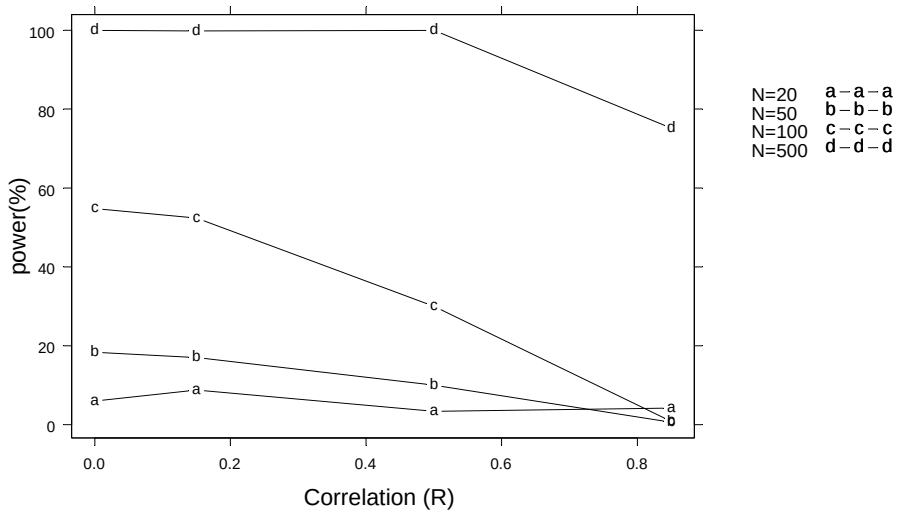

Figure 5.3 *The percent power of selecting the true covariate model at the different sample sizes (N=20, 50, 100, and 500) and degree of correlation (r=0, 0.15, 0.5, 0.85) from model I*

Figure 5.3 clearly shows that the percent power of selecting the true covariate model increases as the size of the sample increases. For the data set of 500 subjects, the percent

power is greater than 75 percent, even when both covariates are highly correlated (r=0.85). Within the same sample size, the effect of the degree of correlation between two covariates is observed. When the correlation between two covariates increases, the percent power is certainly diminished. In most size of samples, when the correlation between covariates is greater than 0.15, a loss of power is clearly observed. However, for a large sample size (N=500), a loss of percent power is not observed until the correlation is greater than 0.5. When the coefficients of the covariates are not equal (the value of θ_3 was set to be 0.15 instead of 0.3 according to model II) referring to one covariate having a stronger relationship with a parameter than the other, the loss of power along with the increase of a correlation as observed in the model I is still illustrated. Moreover, at all levels of correlation, the power of model II is substantially lower than observed in model I as presented in Figure 5.4.

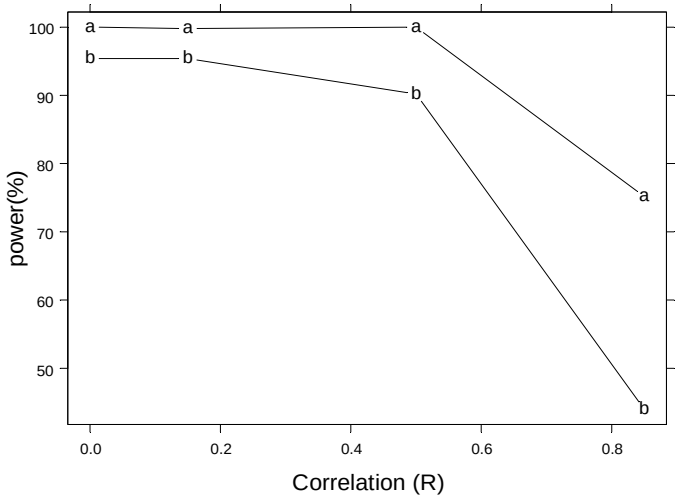

Figure 5.4 *Plot of percent power of selecting the true covariate model for N=500 vs. correlations compared between model I (a) and model II (b)*

The mean percentage prediction error (MPPE) and the mean percentage absolute error (MPAE) of the estimated covariate coefficients ($\hat{\theta}_2$ and $\hat{\theta}_3$) obtained from model I are presented in Figure 5.5. This figure shows that sample size and correlation affect bias and precision of the estimated covariate coefficients. Both MPPE and MPAE are generally decreased and approach zero when the sample size increases. As can be seen, within the same sample size, MPAE increases substantially when the correlation between covariate X_1 and $X_{2(i)}$ is greater than 0.5. Whereas the increase of MPAE is more prominent in a small data set ($N \leq 100$), the degree of correlation has a limited effect on MPAE when the sample size is considerably large ($N = 500$). Interestingly, effect of correlation on MPPE is less predictable.

5.3.2 Standard error of parameter estimates

Figure 5.6 presents the box-plots of the absolute standard error of $\hat{\theta}_2$ and $\hat{\theta}_3$ which were obtained from the analyses of N=50 and N=500. Both the sample size and correlations between two covariates affect the uncertainty of the parameter estimates which are represented by the standard error of the covariate coefficients. As expected, a larger sample size results in a smaller standard error of the estimated coefficients. Additionally, from this figure, it shows that an increase of the covariate coefficient standard errors is not clearly observed at a low correlation ($r \leq 0.15$); however, at a higher correlation ($r \geq 0.5$), the standard errors of covariate coefficients significantly increase.

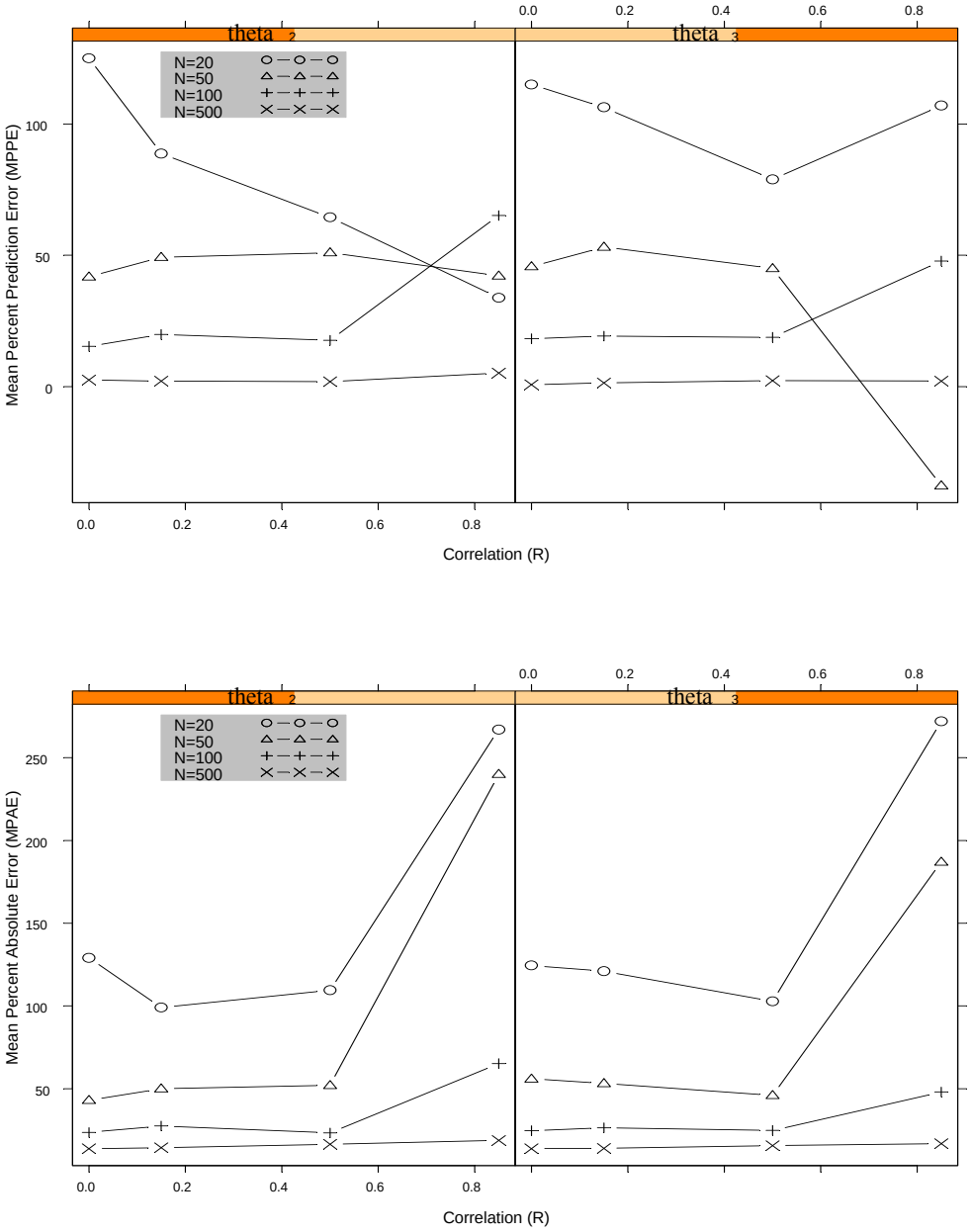

Figure 5.5 *The mean percent prediction error (MPPE) and mean percent absolute error (MPAE) of the estimated covariate coefficients ($\hat{\theta}_2$ and $\hat{\theta}_3$).*

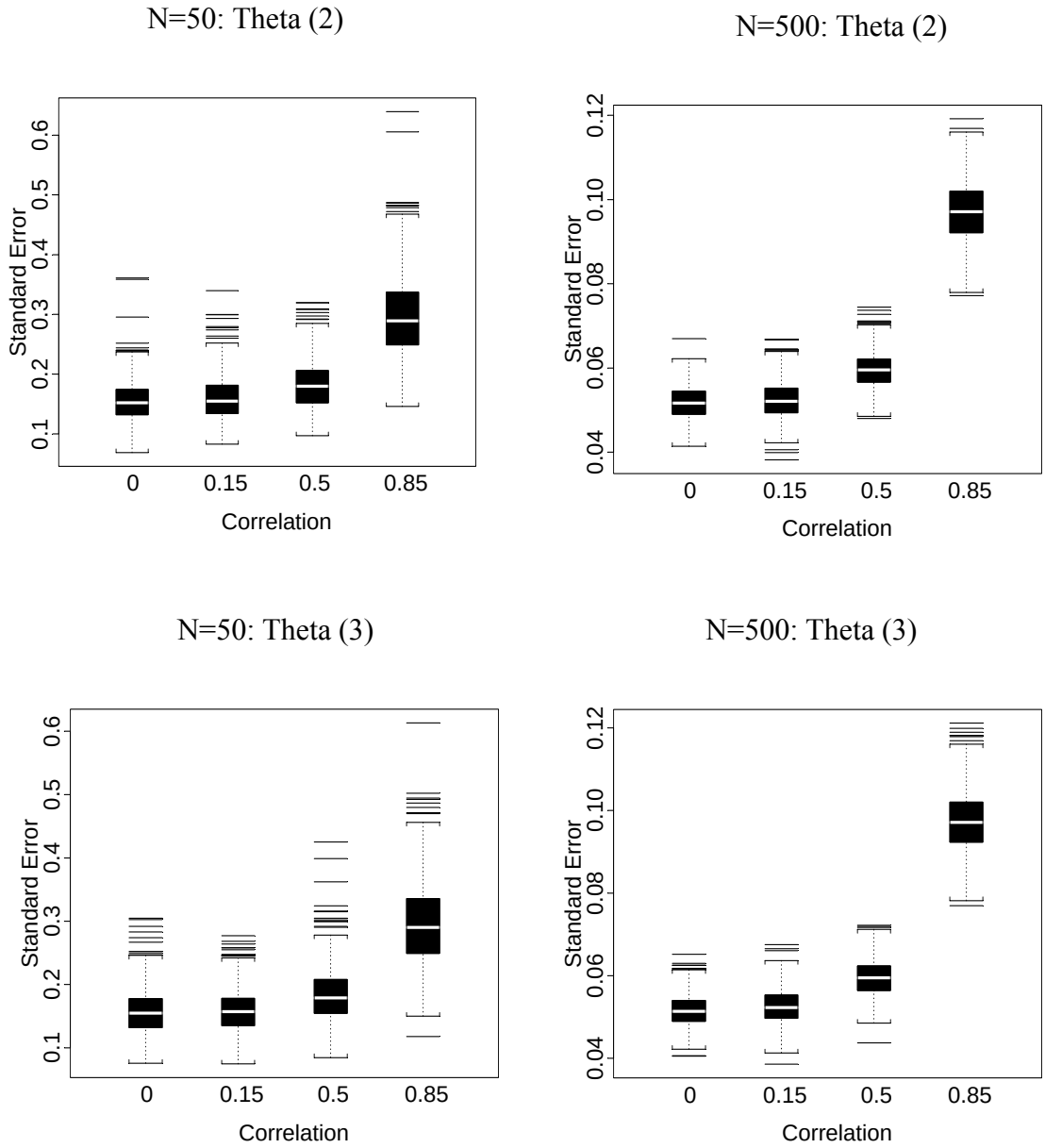

Figure 5.6 *Box-plots of the standard error of* $\hat{\theta}_2$ *and* $\hat{\theta}_3$ *as a function of correlation between* X_1 *and* $X_{2(i)}$ *from N=50 and N=500.*

5.4 Discussion

Collinearity, a condition where the predictor variables (covariates) are not independent, i.e., some variables are correlated with others, has been of great concern in population PK/PD analyses (10-14). Correlation among covariates is not uncommon, especially when several covariates are considered in covariate model building. It has been widely known that collinearity among covariates can seriously mislead the interpretation of a model. This simulation study illustrates that several factors (i.e., size of samples, degree of correlation, and magnitude of covariate coefficients) influence the power of selecting the true covariates, accuracy, and precision of the covariate coefficients in the covariate model building step. It is important to notice that both covariates (X_1 and $X_{2\,(i)}$, i=1 to 4) are the true covariates in this simulation study, yet a correlation between them was varied from 0 to 0.85, and both were tested to be included into the base model using the stepwise forward selection procedure.

Regardless of the size of samples, as the correlation between these two covariates increases, the power of obtaining the true covariate model decreases (Figure 1). A large sample size and large magnitude of covariate coefficients not only increases the power, but also increases a resistance to the loss of power when the correlation is rising. The loss of power would be a consequence of the inflation of a standard error related to the covariate coefficients. When the correlation between covariates increases, the standard error associated with one or both covariates is inflated and, at some point, covariates associated become statistically non-significant. This conclusion was confirmed by the results from the standard error evaluation. It is interesting to point out that the power of

selecting two true covariates using stepwise forward selection is fairly low. For data with a sample size of 100, which is a common sample size for population pharmacokinetic data analysis, the power of selecting the true covariate model was 55%, even with no correlation between covariates (r=0). A limited power to select authentic covariates of the stepwise selection procedure has been criticized (15,16). Thus, further investigation should be performed to investigate performance of a stepwise selection procedure in the population pharmacokinetic covariate model. However, even in the case that, both of the true covariates remain statistically significant, the precision and bias of the covariate coefficients need to be of concern. The precision of the covariate coefficients as represented by MPAE is considerably influenced by the correlation between covariates, especially in a small data set (Figure 5.5).

A stepwise procedure is frequently employed in the covariate model building (1). First, it includes significant covariates into the base model in a forward fashion and later re-evaluates the relationship via backward elimination (17). One of the well-known problems occurring from a stepwise procedure is called selection bias, which refers to an upward bias or overestimation of the effects of the selected covariates (18-20). In our study, it is best to investigate a selection bias when the correlation between covariates equals to zero. A collinearity between covariates could lead to biased coefficient estimates and, moreover, those coefficient estimates may exhibit an incorrect sign (3,21,22). With the fact that the calculated MPPE has a problem that it has a sign (positive or negative value) (9), these consequences from a higher collinearity may complicate the interpretation of a selection bias. Figure 5.5 shows that at a zero

correlation, the covariate coefficients tend to have a larger magnitude than their true value for all sample sizes which, therefore, yield a positive value of MPE, indicating the presence of selection bias. Previous studies show that selection bias directly depends on statistical power (8,19). It is not surprising that selection bias generally decreases when a larger size of sample is used in simulations. It should be pointed out that a decrease of MPPE along with an increase in correlation in some simulation settings does not imply a decrease in bias (Figure 5.5), though it is a result of a change in sign of the coefficient estimates to a negative value which can offset the calculated MPPE.

Our study has some limitations. This simulation study is limited to a case with two true covariates, whereas in a real situation of covariate model building in population PK/PD modeling, several covariates may carry unique information on a parameter. If several correlated covariates are to be tested, the conclusion may be somewhat different from our study. Further studies should investigate the influence of degree of correlation among covariates when more than two true covariates are considered in the covariate model building. Moreover, possible ways to remove correlation among covariates when it is presented is not investigated in this study. Several solutions such as the principal component, bias estimation techniques such as ridge regression, or transformation of the correlated covariates to a new variable (3,23,24) have been suggested when collinearity among covariates is detected. However, further studies need to be performed to provide modelers the optimal solutions to overcome the problems of collinearity.

In conclusion, in the situation in which two true covariates are selected to be incorporated into the base model using forward selection, the power of selecting the true covariates

depends on sample size, degree of correlation, and the magnitude of the covariate coefficients. Moreover, this study shows that degree of correlation could lead to biased and imprecise covariate coefficient estimates. Hence, the initial exploration of the correlation among covariates in a data set is recommended before the covariate model building step is performed. Based on our study, attention should be paid to when correlation between covariates is found to be greater or equal to 0.5, especially when a small to moderate data sets ($N \leq 100$) are used in the analyses.

5.5 References

1. Dartois C, Brendel K, Comets E, et al. Overview of model-building strategies in population PK/PD analyses: 2002-2004 literature survey. *Br J Clin Pharmacol*. 2007;64(5):603-612.
2. Shieh YY, Fouladi RT. The Effect of multicollinearity on multilevel modeling parameter estimates and standard errors. *Educational and Psychological Measurement*. 2003;63:951-985.
3. Bonate PL. The effect of collinearity on parameter estimates in nonlinear mixed effect models. *Pharm Res*. 1999;16(5):709-717.
4. Mason CH, Perreault WD. Collinearity, power, and interpretation of multiple regression analysis. *Journal of Marketing Research*. 1991;28:268-280.
5. Slinker BK, Glantz SA. Multiple regression for physiological data analysis: the problem of multicollinearity. *Am J Physiol*. 1985;249(1 Pt 2):R1-12.
6. Stewart GW. Collinearity and least squares regression. *Stat Sci*. 1987;1:68-100.
7. Tu YK, Kellett M, Clerehugh V, Gilthorpe MS. Problems of correlations between explanatory variables in multiple regression analyses in the dental literature. *Br Dent J*. 2005;199(7):457-461.
8. Ribbing J, Jonsson EN. Power, selection bias and predictive performance of the Population Pharmacokinetic Covariate Model. *J Pharmacokinet Pharmacodyn*. 2004;31(2):109-134.
9. Sheiner LB, Beal SL. Some suggestions for measuring predictive performance. *J Pharmacokinet Biopharm*. 1981;9(4):503-512.
10. Sheiner LB, Rosenberg B, Marathe VV. Estimation of population characteristics of pharmacokinetic parameters from routine clinical data. *J Pharmacokinet Biopharm*. 1977;5(5):445-479.
11. Nedelman JR. On some "disadvantages" of the population approach. *Aaps J*. 2005;7(2):E374-382.
12. Meibohm B, Laer S, Panetta JC, Barrett JS. Population pharmacokinetic studies in pediatrics: issues in design and analysis. *Aaps J*. 2005;7(2):E475-487.

13. Wahlby U, Jonsson EN, Karlsson MO. Comparison of stepwise covariate model building strategies in population pharmacokinetic-pharmacodynamic analysis. *AAPS PharmSci*. 2002;4(4):E27.
14. Bonate PL. Recommended reading in population pharmacokinetic pharmacodynamics. *Aaps J*. 2005;7(2):E363-373.
15. Derksen S, Keselman HJ. Backward, Forward and Stepwise Automated Subset-Selection Algorithms - Frequency of Obtaining Authentic and Noise Variables. *British Journal of Mathematical & Statistical Psychology*. 1992;45:265-282.
16. Steyerberg EW, Eijkemans MJ, Harrell FE, Jr., Habbema JD. Prognostic modeling with logistic regression analysis: in search of a sensible strategy in small data sets. *Med Decis Making*. 2001;21(1):45-56.
17. Jonsson EN, Karlsson MO. Automated covariate model building within NONMEM. *Pharm Res*. 1998;15(9):1463-1468.
18. Miller AJ. Selection of subsets of regression variables. *J R Stat Soc Series A (General)*. 1984;147:389-425.
19. Steyerberg EW, Eijkemans MJ, Habbema JD. Stepwise selection in small data sets: a simulation study of bias in logistic regression analysis. *J Clin Epidemiol*. 1999;52(10):935-942.
20. Vach K, Sauerbrei W, Schumacher M. Variable selection and shrinkage: comparison of some approaches. *Statistica Neerlandica*. 2001;55(1):53-75.
21. Hocking RR. Developments in Linear Regression Methodology:1959-1982. *Technometrics*. 1983;25(3)
22. Belsley DA, Kuh E, Welsch RE. *Regression Diagnostics: Identifying Influential Data and Sources of Collinearity*, New York: John Wiley and Sons, Inc. 1980.
23. Golberg MA, Cho HA. *Introduction to Regression Analysis*, Billerica, MA: WIT Press. 2004.
24. Hoerl RW, Schuenemeyer JH, Hoerl AE. A Simulation of biased estimation and subset selection regression techniques. *Technometrics*. 1986;28:369-380.

CHAPTER 6

Conclusions

The main objective of this dissertation is to characterize the pharmacokinetics of two antiepileptic drugs in community-dwelling elderly epilepsy patients (i.e., lamotrigine and carbamazepine) by means of nonlinear mixed effects modeling. Highlights from all studies in this dissertation and some suggestions for future investigations are presented in this chapter.

In Chapters 2 and 3, the population pharmacokinetic models of LTG and CBZ in the community-dwelling elderly patients were developed. The results from these two studies provided a better understanding of the pharmacokinetics of LTG and CBZ in the elderly epilepsy patients which can help us understand how to use these drugs more effectively in this population. The proposed models can be useful in practical circumstances to guide clinicians in individualizing LTG and CBZ dose in this population. One of the key aspects from these two studies is that the estimated population mean pharmacokinetic parameters for both LTG and CBZ in this community-dwelling elderly epilepsy population are consistent with those previously reported in younger patients. Moreover, age was not found to be a significant covariate for CL/F of either drug. Nonetheless, the data used in these studies consisted of only elderly patients aged 60 years and older and a direct comparison with younger patients was not made. Thus, the influence of age on CL/F of LTG and CBZ requires further investigation in a wider age range data.

The data used in the analyses of LTG and CBZ were data collected during a clinical trial study (The Department of Veteran Affairs (VA) Cooperative Study 428). The VA Cooperative data are unique in several aspects including 1) a prospective data collection, 2) adherence measures via pill counts, and 3) records of actual time and amount of the last three doses before blood sampling time. However, a single blood sample was drawn from each patient at each clinic visit with convenient sampling times (without controlling the times at which blood samples were taken). The sparse sampling and lack of time control of samples in the design lead to imprecise estimations of some pharmacokinetic parameters in the population pharmacokinetic models in these studies.

Autoinduction/deinduction of CBZ is an important characteristic of this drug and is of clinical concern. However, information concerning CBZ autoinduction/deinduction could not be obtained with the VA Cooperative data. Therefore, data from a study specifically designed to address CBZ deinduction was used to gain information about autoinduction/deinduction of CBZ. An enzyme turnover model was successfully applied to characterize the time course of CBZ deinduction in patients with epilepsy (Chapter 4). With this model, the half-life of the induced enzymes which is an important parameter for determining the time course of autoinduction/deinduction of CBZ under clinical conditions can be estimated. The use of a stable-labeled intravenous formulation allowed the possibility to measure a tracer amount of drug in the body and avoided the issues associated with high variability of CBZ absorption. The knowledge of the time course of CBZ deinduction is of great importance for optimal management of CBZ dosage regimens. Also of importance is how to manage both the addition and withdrawal of CBZ

from regimens that include comedications that are also substrates of the enzymes induced by CBZ.

An interesting problem occurred during the covariate model building for CL/F of LTG involving the presence of collinearity between blood urea nitrogen/serum creatinine ratio and race. The effect of collinearity on covariate model building is among one of the most frequent concerns raised by pharmacometricians (1-3), as its consequences could mislead the interpretation of a model. In Chapter 5, the effect of collinearity on power, bias, and precision of the parameter estimates in the population covariate model is illustrated. The results from this simulation study confirmed that the power of selecting the true covariates depends on the size of samples, degree of correlation between covariates, and the magnitude of the covariate effects. When two covariates are highly correlated and one does not have prior knowledge of which covariate does indeed belong to the model, using a stepwise procedure to select important covariates could lead to a loss of power of including true covariates into the model. What was not included in this dissertation is what should be done when collinearity does present. Several approaches have been proposed to deal with collinearity such as a ridge regression, a transformation of the correlated covariates, and a principal component. However, the most suitable way to handle the problem of collinearity in the population covariate model building remains understudied.

This dissertation provided the most detailed analyses available to date for the antiepileptic drugs in community-dwelling epilepsy patients. The knowledge obtained

from this dissertation could provide in-depth information on lamotrigine and carbamazepine pharmacokinetics which can be used for individualization of dosage regimens of these drugs in this special population.

6.1 References

1. Meibohm B, Laer S, Panetta JC, Barrett JS. Population pharmacokinetic studies in pediatrics: issues in design and analysis. *Aaps J*. 2005;7(2):E475-487.
2. Nedelman JR. On some "disadvantages" of the population approach. *Aaps J*. 2005;7(2):E374-382.
3. Sheiner LB, Rosenberg B, Marathe VV. Estimation of population characteristics of pharmacokinetic parameters from routine clinical data. *J Pharmacokinet Biopharm*. 1977;5(5):445-479.

Bibliography

Abramson FP. Kinetic models of induction: I. Persistence of the inducing substance. *J Pharm Sci*. 1986;75(3):223-228.

Ahn JE, Birnbaum AK, Brundage RC. Inherent correlation between dose and clearance in therapeutic drug monitoring settings: possible misinterpretation in population pharmacokinetic analyses. *J Pharmacokinet Pharmacodyn*. 2005;32(5-6):703-718.

al-Banna MK, Kelman AW, Whiting B. Experimental design and efficient parameter estimation in population pharmacokinetics. *J Pharmacokinet Biopharm*. 1990;18(4):347-360.

Armijo JA, Bravo J, Cuadrado A, Herranz JL. Lamotrigine serum concentration-to-dose ratio: influence of age and concomitant antiepileptic drugs and dosage implications. *Ther Drug Monit*. 1999;21(2):182-190.

Baker KM, Csetenyi J, Frigerio A, Morselli PL, Parravicini F, Pifferi G. 10,11-Dihydro-10,11-dihydroxy-5H-dibenz(b,f)azepine-5-carboxamide, a metabolite of carbamazepine isolated from human and rat urine. *J Med Chem*. 1973;16(6):703-705.

Baruzzi A, Contin M, Perucca E, Albani F, Riva R. Altered serum protein binding of carbamazepine in disease states associated with an increased alpha 1-acid glycoprotein concentration. *Eur J Clin Pharmacol*. 1986;31(1):85-89.

Battino D, Croci D, Rossini A, Messina S, Mamoli D, Perucca E. Serum carbamazepine concentrations in elderly patients: a case-matched pharmacokinetic evaluation based on therapeutic drug monitoring data. *Epilepsia*. 2003;44(7):923-929.

Beal SL, Sheiner LB. *NONMEM User's Guides*. University of California, San Fransisco, CA: NONMEM project group. 1994.

Belsley DA, Kuh E, Welsch RE. *Regression Diagnostics: Identifying Influential Data and Sources of Collinearity*, New York: John Wiley and Sons, Inc. 1980.

Bernus I, Dickinson RG, Hooper WD, Eadie MJ. Early stage autoinduction of carbamazepine metabolism in humans. *Eur J Clin Pharmacol*. 1994;47(4):355-360.

Bertilsson L. Clinical pharmacokinetics of carbamazepine. *Clin Pharmacokinet*. 1978;3(2):128-143.

Bertilsson L, Tomson T, Tybring G. Pharmacokinetics: time-dependent changes--autoinduction of carbamazepine epoxidation. *Journal of clinical pharmacology*. 1986;26(6):459-462.

Bonate PL. The effect of collinearity on parameter estimates in nonlinear mixed effect models. *Pharm Res*. 1999;16(5):709-717.

Bonate PL. Recommended reading in population pharmacokinetic pharmacodynamics. *Aaps J*. 2005;7(2):E363-373.

Bonate PL. *Pharmacokinetic-Pharmacodynamic Modeling and Simulation*: Springer Science+Business Media, Inc. 2006.

Bondareva IB, Jelliffe RW, Gusev EI, Guekht AB, Melikyan EG, Belousov YB. Population pharmacokinetic modelling of carbamazepine in epileptic elderly patients: implications for dosage. *J Clin Pharm Ther*. 2006;31(3):211-221.

Bondareva IB, Sokolov AV, Tischenkova IF, Jelliffe RW. Population pharmacokinetic modelling of carbamazepine by using the iterative Bayesian (IT2B) and the nonparametric EM (NPEM) algorithms: implications for dosage. *J Clin Pharm Ther*. 2001;26(3):213-223.

Brendel K, Dartois C, Comets E, et al. Are population pharmacokinetic and/or pharmacodynamic models adequately evaluated? A survey of the literature from 2002 to 2004. *Clin Pharmacokinet*. 2007;46(3):221-234.

Carlsson KC, Hoem NO, Glauser T, Vinks AA. Development of a population pharmacokinetic model for carbamazepine based on sparse therapeutic monitoring data from pediatric patients with epilepsy. *Clinical therapeutics*. 2005;27(5):618-626.

Casey AE, Gilbert FW, Ratliff CR, Downey E. Race-sex values of serum creatine-phosphokinase, uric acid, urea nitrogen and creatinine. *Ala J Med Sci*. 1968;5(3):474-476.

Chan E, Lee HS, Hue SS. Population pharmacokinetics of carbamazepine in Singapore epileptic patients. *Br J Clin Pharmacol*. 2001;51(6):567-576.

Chan V, Morris RG, Ilett KF, Tett SE. Population pharmacokinetics of lamotrigine. *Ther Drug Monit*. 2001;23(6):630-635.

Christiansen J, Dam M. Influence of phenobarbital and diphenylhydantoin on plasma carbamazepine levels in patients with epilepsy. *Acta neurologica Scandinavica*. 1973;49(4):543-546.

Cloyd JC, Lackner TE, Leppik IE. Antiepileptics in the elderly. Pharmacoepidemiology and pharmacokinetics. *Arch Fam Med*. 1994;3(7):589-598.

Cohen AF, Land GS, Breimer DD, Yuen WC, Winton C, Peck AW. Lamotrigine, a new anticonvulsant: pharmacokinetics in normal humans. *Clin Pharmacol Ther*. 1987;42(5):535-541.

Contin M, Riva R, Albani F, Perucca E, Lamontanara G, Baruzzi A. Alpha 1-acid glycoprotein concentration and serum protein binding of carbamazepine and carbamazepine-10,11 epoxide in children with epilepsy. *Eur J Clin Pharmacol*. 1985;29(2):211-214.

Cotter LM, Eadie MJ, Hooper WD, Lander CM, Smith GA, Tyrer JH. The pharmacokinetics of carbamazepine. *Eur J Clin Pharmacol*. 1977;12(6):451-456.

Dartois C, Brendel K, Comets E, et al. Overview of model-building strategies in population PK/PD analyses: 2002-2004 literature survey. *Br J Clin Pharmacol*. 2007;64(5):603-612.

Davies JA. Mechanisms of action of antiepileptic drugs. *Seizure*. 1995;4(4):267-271.

Deleu D, Aarons L, Ahmed IA. Population pharmacokinetics of free carbamazepine in adult Omani epileptic patients. *Eur J Clin Pharmacol*. 2001;57(3):243-248.

Delgado Iribarnegaray MF, Santo Bueldga D, Garcia Sanchez MJ, Otero MJ, Falcao AC, Dominguez-Gil A. Carbamazepine population pharmacokinetics in children: mixed-effect models. *Ther Drug Monit*. 1997;19(2):132-139.

Derksen S, Keselman HJ. Backward, Forward and Stepwise Automated Subset-Selection Algorithms - Frequency of Obtaining Authentic and Noise Variables. *British Journal of Mathematical & Statistical Psychology*. 1992;45:265-282.

Di Salle E, Pacifici GM, Morselli PL. Studies on plasma protein binding of carbamazepine. *Pharmacol Res Commun*. 1974;6(2):193-202.

DiMasi JA, Hansen RW, Grabowski HG. The price of innovation: new estimates of drug development costs. *J Health Econ*. 2003;22(2):151-185.

Doig MV, Clare RA. Use of thermospray liquid chromatography-mass spectrometry to aid in the identification of urinary metabolites of a novel antiepileptic drug, Lamotrigine. *J Chromatogr*. 1991;554(1-2):181-189.

Efron B. Bootstrap methods: another look at the jackknife. *Ann Stat*. 1979;7:1-26.

Efron B. Estimating the error rate of a prediction rule: improvement on cross-validation. *J Am Stat Assoc*. 1983;78:316-331.

Efron B, Gong G. A leisurely look at the bootstrap, the jacknife, and cross-validation. *Am Stat*. 1983;37(1):36-48.

Eichelbaum M, Ekbom K, Bertilsson L, Ringberger VA, Rane A. Plasma kinetics of carbamazepine and its epoxide metabolite in man after single and multiple doses. *Eur J Clin Pharmacol*. 1975;8(5):337-341.

El-Mallakh R, Weisler RH, Townsend MH, Ginsberg LD. Bipolar II disorder: current and future treatment options. *Ann Clin Psychiatry*. 2006;18(4):259-266.

Ette EI. Stability and performance of a population pharmacokinetic model. *J Clin Pharmacol*. 1997;37(6):486-495.

Ette EI, Williams PJ. Population pharmacokinetics I: background, concepts, and models. *Ann Pharmacother*. 2004;38(10):1702-1706.

Ette EI, Williams PJ, Kim YH, Lane JR, Liu MJ, Capparelli EV. Model appropriateness and population pharmacokinetic modeling. *J Clin Pharmacol*. 2003;43(6):610-623.

Ette EI, Williams PJ, Lane JR. Population pharmacokinetics III: design, analysis, and application of population pharmacokinetic Studies. *The Annals of pharmacotherapy*. 2004;38(12):2136-2144.

Faigle JW, Feldmann KF. Carbamazepine: Chemistry and Biotransformation. In: Levy RH, Mattson RH, Meldrum BS, editors. *Antiepileptic Drugs*, 4th ed., New York: Raven Press, 1995.

Fang L, Holford NH, Hinkle G, et al. Population pharmacokinetics of humanized monoclonal antibody HuCC49deltaCH2 and murine antibody CC49 in colorectal cancer patients. *J Clin Pharmacol*. 2007;47(2):227-237.

Fillastre JP, Taburet AM, Fialaire A, Etienne I, Bidault R, Singlas E. Pharmacokinetics of lamotrigine in patients with renal impairment: influence of haemodialysis. *Drugs Exp Clin Res*. 1993;19(1):25-32.

Fuhr U. Induction of drug metabolising enzymes: pharmacokinetic and toxicological consequences in humans. *Clin Pharmacokinet*. 2000;38(6):493-504.

Garnett WR. Lamotrigine: pharmacokinetics. *J Child Neurol*. 1997;12 Suppl 1:S10-15.

Gelman A, Carlin JB, Stern H, Rubin DB. *Bayesian Data Analysis*. ed., London: Chapman and Hall. 1995.

Geradin AP, Abadie FV, Campestrini JA, Theobald W. Pharmacokinetics of carbamazepine in normal humans after single and repeated oral doses. *J Pharmacokinet Biopharm*. 1976;4(6):521-535.

Gobburu JV. Posterior Predictive Check: What, How and When? AAPS, Salt Lake City, Utah, 2003.

Gobburu JV, Lawrence J. Application of resampling techniques to estimate exact significance levels for covariate selection during nonlinear mixed effects model building: some inferences. *Pharm Res*. 2002;19(1):92-98.

Golberg MA, Cho HA. *Introduction to Regression Analysis*, Billerica, MA: WIT Press. 2004.

Gordi T, Xie R, Huong NV, Huong DX, Karlsson MO, Ashton M. A semiphysiological pharmacokinetic model for artemisinin in healthy subjects incorporating autoinduction of metabolism and saturable first-pass hepatic extraction. *Br J Clin Pharmacol*. 2005;59(2):189-198.

Grasela TH, Fiedler-Kelly J, Cox E, Womble GP, Risner ME, Chen C. Population pharmacokinetics of lamotrigine adjunctive therapy in adults with epilepsy. *J Clin Pharmacol*. 1999;39(4):373-384.

Grasela TH, Sheiner BL. Pharmacostatistical Modeling for Observational Data. *J Pharmacokinet Biopharm*. 1991;19(3):25S-36S.

Graves NM, Brundage RC, Wen Y, et al. Population pharmacokinetics of carbamazepine in adults with epilepsy. *Pharmacotherapy*. 1998;18(2):273-281.

Hassan M, Svensson US, Ljungman P, et al. A mechanism-based pharmacokinetic-enzyme model for cyclophosphamide autoinduction in breast cancer patients. *Br J Clin Pharmacol*. 1999;48(5):669-677.

Hauser WA, Annegers JF, Kurland LT. Prevalence of epilepsy in Rochester, Minnesota: 1940-80. *Epilepsia*. 1991;32:429-445.

Hocking RR. Developments in Linear Regression Methodology:1959-1982. *Technometrics*. 1983;25(3)

Hockings N, Pall A, Moody J, Davidson AV, Davidson DL. The effects of age on carbamazepine pharmacokinetics and adverse effects. *Br J Clin Pharmacol*. 1986;22(6):725-728.

Hoerl RW, Schuenemeyer JH, Hoerl AE. A Simulation of biased estimation and subset selection regression techniques. *Technometrics*. 1986;28:369-380.

Holford NH. The Visual Predictive Check: Superior to Standard Diagnostic (Rorschanch) Plots. PAGE 14, 2005.

Huitema AD, Mathot RA, Tibben MM, Rodenhuis S, Beijnen JH. A mechanism-based pharmacokinetic model for the cytochrome P450 drug-drug interaction between cyclophosphamide and thioTEPA and the autoinduction of cyclophosphamide. *J Pharmacokinet Pharmacodyn*. 2001;28(3):211-230.

Hussein Z, Posner J. Population pharmacokinetics of lamotrigine monotherapy in patients with epilepsy: retrospective analysis of routine monitoring data. *Br J Clin Pharmacol*. 1997;43(5):457-465.

Ismail R, Rahman AF. Estimation of population pharmacokinetics for carbamazepine in Malaysian patients using the OPT computer program. *J Clin Pharm Ther*. 1993;18(1):55-58.

Jadhav PR, Gobburu JV. A new equivalence based metric for predictive check to qualify mixed-effects models. *Aaps J*. 2005;7(3):E523-531.

Jawad S, Yuen WC, Peck AW, Hamilton MJ, Oxley JR, Richens A. Lamotrigine: single-dose pharmacokinetics and initial 1 week experience in refractory epilepsy. *Epilepsy Res*. 1987;1(3):194-201.

Jiao Z, Shi XJ, Zhao ZG, Zhong MK. Population pharmacokinetic modeling of steady state clearance of carbamazepine and its epoxide metabolite from sparse routine clinical data. *J Clin Pharm Ther*. 2004;29(3):247-256.

Jiao Z, Zhong MK, Shi XJ, Hu M, Zhang JH. Population pharmacokinetics of carbamazepine in Chinese epilepsy patients. *Ther Drug Monit*. 2003;25(3):279-286.

Jonsson EN, Karlsson MO. Automated covariate model building within NONMEM. *Pharm Res*. 1998;15(9):1463-1468.

Jonsson EN, Karlsson MO. Xpose--an S-PLUS based population pharmacokinetic/pharmacodynamic model building aid for NONMEM. *Comput Methods Programs Biomed*. 1999;58(1):51-64.

Kanner AM, Frey M. Adding valproate to lamotrigine: a study of their pharmacokinetic interaction. *Neurology*. 2000;55(4):588-591.

Kerbusch T, Huitema AD, Ouwerkerk J, et al. Evaluation of the autoinduction of ifosfamide metabolism by a population pharmacokinetic approach using NONMEM. *Br J Clin Pharmacol*. 2000;49(6):555-561.

Kerr BM, Thummel KE, Wurden CJ, et al. Human liver carbamazepine metabolism. Role of CYP3A4 and CYP2C8 in 10,11-epoxide formation. *Biochem Pharmacol*. 1994;47(11):1969-1979.

Korth-Bradley JM, Ludden TM. Carbamazepine pharmacokinetics during induction and reversal of induction. *Pharmacotherapy*. 1991;11(3):272.

Kudriakova TB, Sirota LA, Rozova GI, Gorkov VA. Autoinduction and steady-state pharmacokinetics of carbamazepine and its major metabolites. *Br J Clin Pharmacol*. 1992;33(6):611-615.

Kwan P, Sills GJ, Brodie MJ. The mechanisms of action of commonly used antiepileptic drugs. *Pharmacol Ther*. 2001;90(1):21-34.

Leach MJ, Lees G, Riddall DR. Lamotrigine: Mechamism of Action. In: Levy RH, Mattson RH, Meldrum BS, editors. *Antiepileptic Drugs*, 4th ed., New York: Raven Press, 1995.

Leppik IE. Treatment of epilepsy in 3 specialized populations. *Am J Manag Care*. 2001;7(7 Suppl):S221-226.

Levy RH, Lai AA, Dumain MS. Time-dependent kinetics IV: Pharmacokinetic theory of enzyme induction. *J Pharm Sci*. 1979;68(3):398-399.

Levy RH, Pitlick WH, Troupin AS, Green JR, Neal JM. Pharmacokinetics of carbamazepine in normal man. *Clin Pharmacol Ther*. 1975;17(6):657-668.

Magdalou J, Herber R, Bidault R, Siest G. In vitro N-glucuronidation of a novel antiepileptic drug, lamotrigine, by human liver microsomes. *J Pharmacol Exp Ther*. 1992;260(3):1166-1173.

Magnusson MO, Dahl ML, Cederberg J, Karlsson MO, Sandstrom R. Pharmacodynamics of Carbamazepine-mediated Induction of CYP3A4, CYP1A2, and Pgp as Assessed by Probe Substrates Midazolam, Caffeine, and Digoxin. *Clin Pharmacol Ther*. 2007

Mandema JW, Verotta D, Sheiner LB. Building population pharmacokinetic--pharmacodynamic models. I. Models for covariate effects. *J Pharmacokinet Biopharm*. 1992;20(5):511-528.

Mangoni AA, Jackson SH. Age-related changes in pharmacokinetics and pharmacodynamics: basic principles and practical applications. *Br J Clin Pharmacol*. 2004;57(1):6-14.

Mason CH, Perreault WD. Collinearity, power, and interpretation of multiple regression analysis. *Journal of Marketing Research*. 1991;28:268-280.

McLean AJ, Le Couteur DG. Aging biology and geriatric clinical pharmacology. *Pharmacol Rev*. 2004;56(2):163-184.

Meibohm B, Laer S, Panetta JC, Barrett JS. Population pharmacokinetic studies in pediatrics: issues in design and analysis. *Aaps J*. 2005;7(2):E475-487.

Mikati MA, Browne TR, Collins JF. Time course of carbamazepine autoinduction. The VA Cooperative Study No.118 Group. *Neurology*. 1989;39(4):592-594.

Miller AJ. Selection of subsets of regression variables. *J R Stat Soc Series A (General)*. 1984;147:389-425.

Morselli PL. Carbamazepine: Absorption, Distribution, and Excretion. In: Levy RH, Mattson RH, Meldrum BS, editors. *Antiepileptic Drugs*, 4th ed., New York: Raven Press, Ltd., 1995.

Nedelman JR. On some "disadvantages" of the population approach. *Aaps J*. 2005;7(2):E374-382.

Okey AB. Enzyme induction in the cytochrome P-450 system. *Pharmacol Ther*. 1990;45(2):241-298.

Oscarson M, Zanger UM, Rifki OF, Klein K, Eichelbaum M, Meyer UA. Transcriptional profiling of genes induced in the livers of patients treated with carbamazepine. *Clin Pharmacol Ther*. 2006;80(5):440-456.

Peck AW. Clinical pharmacology of lamotrigine. *Epilepsia*. 1991;32 Suppl 2:S9-12.

Perucca E. Clinical pharmacokinetics of new-generation antiepileptic drugs at the extremes of age. *Clin Pharmacokinet*. 2006;45(4):351-363.

Pitlick WH, Levy RH. Time-dependent kinetics I: Exponential autoinduction of carbamazepine in monkeys. *J Pharm Sci*. 1977;66(5):647-649.

Posner J, Holdich T, Crome P. Comparison of lamotrigine pharmacokinetics in young and elderly healthy volunteers. *J Pharm Med*. 1991;1:121-128.

Rambeck B, May T, Juergens U. Serum concentrations of carbamazepine and its epoxide and diol metabolites in epileptic patients: the influence of dose and comedication. *Ther Drug Monit*. 1987;9(3):298-303.

Rambeck B, Wolf P. Lamotrigine clinical pharmacokinetics. *Clin Pharmacokinet*. 1993;25(6):433-443.

Ramsay RE, Pellock JM, Garnett WR, et al. Pharmacokinetics and safety of lamotrigine (Lamictal) in patients with epilepsy. *Epilepsy Res*. 1991;10(2-3):191-200.

Rawlins MD, Collste P, Bertilsson L, Palmer L. Distribution and elimination kinetics of carbamazepine in man. *Eur J Clin Pharmacol*. 1975;8(2):91-96.

Reith DM, Hooper WD, Parke J, Charles B. Population pharmacokinetic modeling of steady state carbamazepine clearance in children, adolescents, and adults. *J Pharmacokinet Pharmacodyn*. 2001;28(1):79-92.

Ribbing J, Jonsson EN. Power, selection bias and predictive performance of the Population Pharmacokinetic Covariate Model. *J Pharmacokinet Pharmacodyn*. 2004;31(2):109-134.

Rowan AJ, Ramsay RE, Collins JF, et al. New onset geriatric epilepsy: a randomized study of gabapentin, lamotrigine, and carbamazepine. *Neurology*. 2005;64(11):1868-1873.

Salem SA, Rajjayabun P, Shepherd AM, Stevenson IH. Reduced induction of drug metabolism in the elderly. *Age and ageing*. 1978;7(2):68-73.

Savica R, Beghi E, Mazzaglia G, et al. Prescribing patterns of antiepileptic drugs in Italy: a nationwide population-based study in the years 2000-2005. *Eur J Neurol*. 2007;14(12):1317-1321.

Schaffler L, Bourgeois BF, Luders HO. Rapid reversibility of autoinduction of carbamazepine metabolism after temporary discontinuation. *Epilepsia*. 1994;35(1):195-198.

Scheyer RD, Cramer JA, Mattson RH. A pharmacodynamic approach to the estimate of carbamazepine autoinduction. *J Pharm Sci*. 1994;83(4):491-494.

Sheiner LB, Beal SL. Evaluation of methods for estimating population pharmacokinetics parameters. I. Michaelis-Menten model: routine clinical pharmacokinetic data. *J Pharmacokinet Biopharm*. 1980;8(6):553-571.

Sheiner LB, Beal SL. Evaluation of methods for estimating population pharmacokinetic parameters. II. Biexponential model and experimental pharmacokinetic data. *J Pharmacokinet Biopharm*. 1981;9(5):635-651.

Sheiner LB, Beal SL. Some suggestions for measuring predictive performance. *J Pharmacokinet Biopharm*. 1981;9(4):503-512.

Sheiner LB, Beal SL. Evaluation of methods for estimating population pharmacokinetic parameters. III. Monoexponential model: routine clinical pharmacokinetic data. *J Pharmacokinet Biopharm*. 1983;11(3):303-319.

Sheiner LB, Grasela TH. An Introduction to Mixed Effect Modeling: Concepts, Definitions, and Justification. *J Pharmacokinet Biopharm*. 1991;19(3):11S-23S.

Sheiner LB, Rosenberg B, Marathe VV. Estimation of population characteristics of pharmacokinetic parameters from routine clinical data. *J Pharmacokinet Biopharm*. 1977;5(5):445-479.

Shieh YY, Fouladi RT. The Effect of multicollinearity on multilevel modeling parameter estimates and standard errors. *Educational and Psychological Measurement*. 2003;63:951-985.

Sinz MW, Remmel RP. Isolation and characterization of a novel quaternary ammonium-linked glucuronide of lamotrigine. *Drug Metab Dispos*. 1991;19(1):149-153.

Slinker BK, Glantz SA. Multiple regression for physiological data analysis: the problem of multicollinearity. *Am J Physiol*. 1985;249(1 Pt 2):R1-12.

Smith GA, Hooper WD, Tyrer JH, Eadie MJ, Werth B. The comparative bioavailability of carbamazepine in 100 mg and 200 mg tablets. *Clin Exp Pharmacol Physiol*. 1979;6(1):37-40.

Stewart GW. Collinearity and least squares regression. *Stat Sci*. 1987;1:68-100.

Steyerberg EW, Eijkemans MJ, Habbema JD. Stepwise selection in small data sets: a simulation study of bias in logistic regression analysis. *J Clin Epidemiol*. 1999;52(10):935-942.

Steyerberg EW, Eijkemans MJ, Harrell FE, Jr., Habbema JD. Prognostic modeling with logistic regression analysis: in search of a sensible strategy in small data sets. *Med Decis Making*. 2001;21(1):45-56.

Sun H, Fadiran EO, Jones CD, et al. Population pharmacokinetics. A regulatory perspective. *Clin Pharmacokinet*. 1999;37(1):41-58.

Tanaka E. In vivo age-related changes in hepatic drug-oxidizing capacity in humans. *J Clin Pharm Ther*. 1998;23(4):247-255.

Tateishi T, Asoh M, Nakura H, et al. Carbamazepine induces multiple cytochrome P450 subfamilies in rats. *Chem Biol Interact*. 1999;117(3):257-268.

Tu YK, Kellett M, Clerehugh V, Gilthorpe MS. Problems of correlations between explanatory variables in multiple regression analyses in the dental literature. *Br Dent J*. 2005;199(7):457-461.

Twum-Barima Y, Finnigan T, Habash AI, Cape RD, Carruthers SG. Impaired enzyme induction by rifampicin in the elderly. *Br J Clin Pharmacol*. 1984;17(5):595-597.

United State Renal Data System. 2006. Annual Data Report: Chapter three; patient characteristics. p 81-94.

Vach K, Sauerbrei W, Schumacher M. Variable selection and shrinkage: comparison of some approaches. *Statistica Neerlandica*. 2001;55(1):53-75.

Wahlby U, Jonsson EN, Karlsson MO. Assessment of actual significance levels for covariate effects in NONMEM. *J Pharmacokinet Pharmacodyn*. 2001;28(3):231-252.

Wahlby U, Jonsson EN, Karlsson MO. Comparison of stepwise covariate model building strategies in population pharmacokinetic-pharmacodynamic analysis. *AAPS PharmSci*. 2002;4(4):E27.

Warren JWJ, Benmaman JD, Wannamaker BB, Levy RH. Kinetics of a carbamazepine-ethosuximide interaction. *Clin Pharmacol Ther*. 1980;28(5):646-651.

Williams PJ, Ette EI. Pharmacometrics: Impacting Drug Development and Pharmacotherapy. In: Williams PJ, Ette EI, editors. *Pharmacometrics: The Science of Quantitative Pharmacology*, New Jersey: John Wiley&Sons, Inc., 2007.

Wootton R, Soul-Lawton J, Rolan PE, Sheung CT, Cooper JD, Posner J. Comparison of the pharmacokinetics of lamotrigine in patients with chronic renal failure and healthy volunteers. *Br J Clin Pharmacol*. 1997;43(1):23-27.

Yafune A, Ishiguro M. Bootstrap approach for constructing confidence intervals for population pharmacokinetic parameters. I: A use of bootstrap standard error. *Stat Med*. 1999;18(5):581-599.

Yano Y, Beal SL, Sheiner LB. Evaluating pharmacokinetic/pharmacodynamic models using the posterior predictive check. *J Pharmacokinet Pharmacodyn*. 2001;28(2):171-192.

Yau MK, Wargin WA, Wolf KB. Effect of valproate on the pharmacokinetics of lamotrigine at steady state. *Epilepsia*. 1992;33(Suppl 3):82.

Appendix A

NONMEM control stream for the final model of the population pharmacokinetics of lamotrigine in elderly patients (relevant to Chapter 2)

```
$PROB RUN# 704
$INPUT  C  ID  CT  WEEK=DROP  DUR  DATE=DROP  TIME  AMT
        DV  MDV  EVID  II  SS  AGE  AGE2  WT  IBW=DROP
        BSA=DROP  LBW=DROP  BMI=DROP  RACE  ALC=DROP  AST
        SMK=DROP  PHT  ALB  BUN=DROP  CR=DROP  BNCR  ALT
        CRCL=DROP
$DATA   LTG_VA.CSV   IGNORE=C
$SUBROUTINES  ADVAN2
$PK
   IF (PHT.EQ.0) THEN
   TVCL = THETA(1)*BNCR+THETA(2)*WT
   ELSE
   TVCL = (THETA(1)*BNCR+THETA(2)*WT)*THETA(3)
   ENDIF
   CL = TVCL*EXP(ETA(1))
   IF (CL.LE.0) EXIT 1 100
   TVV = THETA(4)
   V = TVV
   IF (V.LE.0) EXIT 1 200
   TVKA = THETA(5)
   KA = TVKA
   K = CL/V
   S2 = V
$ERROR
   DEL = 0
   IF(F.EQ.0) DEL = 0.1
   W = F
   IPRED = F
   IRES = DV-IPRED
   IWRES = IRES/(W+DEL)
   Y= F+F * ERR(1)+ERR(2)
$THETA
 (0, 0.5)   ; THETA 1
 (0, 0.2)   ; THETA 2
 (0.5)      ; THETA 3
 (0, 120)   ; THETA 4
 (3.5 FIXED); THETA 5
$OMEGA
 0.3 ; [P] INTERINDIVIDUAL VARIABILITY IN CL
```

```
$SIGMA
 0.2  ; [P] PROPORTIONAL COMPONENT
 0.01 ; [A] ADDITIVE COMPONENT
$EST    PRINT=5  METHOD=1  INTERACTION  MAXEVAL=9999
        NOABORT  SIGDIG=3
$COVARIANCE PRINT=E
$TABLE  ID  TIME  IPRED  IWRES  NOPRINT  ONEHEADER
        FILE=704.TAB
```

Appendix B

NONMEM control stream for the final model of the population pharmacokinetics of carbamazepine in community-dwelling elderly patients (relevant to Chapter 3)

```
$PROB RUN# 405
$INPUT  C  ID  CT  WEEK=DROP  DATE=DROP  TIME  AMT  DV
        MDV  EVID  II  SS  AGE  AGE2  WT  IBW=DROP  PHT
        BSA=DROP  LBW=DROP  BMI=DROP  RACE  ALC=DROP  AST
        SMK=DROP  ALB  BUN=DROP  CR=DROP  PROT  CRCL  ALT
$DATA   CBZ_VA.CSV   IGNORE=C
$SUBROUTINES   ADVAN2
$PK
   IF (PHT.EQ.0) THEN
   TVCL = THETA(1)
   ELSE
   TVCL = THETA(1)*THETA(2)
   ENDIF
   CL = TVCL*EXP(ETA(1))
   IF (CL.LE.0) EXIT 1 100
   TVV = THETA(3)
   V=TVV*EXP(ETA(2))
   IF (V.LE.0) EXIT 1 200
   TVKA = THETA(4)
   KA = TVKA
   K = CL/V
   S2=V
$ERROR
   DEL = 0
   IF (F.EQ.0) DEL=0.1
   W = F
   IPRED = F
   IRES = DV-IPRED
   IWRES = IRES/(W+DEL)
   Y= F+F * ERR(1)
$THETA
 (0,3)    ;  THETA(1)
 (0.5)    ;  THETA(2)
 (0,100)  ;  THETA(3)
 (0,0.3)  ;  THETA(4)
$OMEGA
 0.3 ;  [P] INTERINDIVIDUAL VARIABILITY IN CL
 0.3 ;  [P] INTERINDIVIDUAL VARIABILITY IN V
```

```
$SIGMA
 0.2 ;  [P] PROPORTIONAL COMPONENT
$EST    PRINT=5  METHOD=1  INTERACTION  MAXEVAL=9999
        NOABORT   SIGDIG=3
$COVARIANCE PRINT=E
$TABLE  ID  TIME  IPRED  IWRES  NOPRINT  ONEHEADER
        FILE=405.TAB
```

Appendix C

NONMEM control stream for the final model of the population pharmacokinetics of carbamazepine deinduction (relevant to Chapter 4)

```
$PROB RUN# 005
$INPUT  C  ID  OCC  SUBJ=DROP  DATE=DROP  TIME  AMT  MDV
        EVID  DV  CMT  RATE  WT
$DATA   001.CSV IGNORE=C
$SUBROUTINES   ADVAN6   TOL=5
$MODEL NCOMPARTMENT = 2
   COMP = (CENTRAL)
   COMP = (ENZ)
$PK
   TVCL = THETA(1)
   CL = TVCL*EXP(ETA(1))
   TVV = THETA(2)+(THETA(3)*(WT-80))
   V = TVV*EXP(ETA(2))
   K = CL/V
   KENZ = THETA(4)
   FACTOR = THETA(5)
   S1 = V
$DES
   CP = A(1)/V
   ENZ = A(2)
   DADT(1) = -(CL/V)*A(1)*A(2)
   DADT(2) = KENZ*(1-FACTOR)-KENZ*(A(2))
$ERROR
   DEL = 0
   IF (F.EQ.0) DEL=0.1
   W = F
   IPRED = F
   IRES = DV-IPRED
   IWRES = IRES/(W+DEL)
   Y= F+F*ERR(1)
$THETA
 (0, 3)     ; [THETA(1), CL]
 (0, 60)    ; [THETA(2), INTERCEPT]
 (0, 1)     ; [THETA(3), SL-V]
 (0, 0.008) ; [THETA(4), KENZ]
 (0, 0.5)   ; [THETA(5), FACTOR]
$OMEGA
 0.02   ; [P] INTERINDIVIDUAL VARIABILITY IN CL
 0.02   ; [P] INTERINDIVIDUAL VARIABILITY IN V
```

```
$SIGMA
 0.07   ; [P] PROPORTIONAL COMPONENT
$EST    PRINT=5  METHOD=1  INTERACTION  MAXEVAL=9999
        NOABORT   SIGDIG=3
$COVARIANCE PRINT=E
$TABLE  ID  OCC  CL  V  WT  ETA(1)  ETA(2)  ENZ  TIME
        IPRED  NOPRINT  ONEHEADER FILE=005.TAB
```

Appendix D

Example of NONMEM control stream for the simulation of plasma concentrations for N=20. The TVCL was modeled using covariates X_1 and $X_{2(1)}$ (relevant to Chapter 5)

```
$PROB RUN# 1
$INPUT  C ID TIME AMT MDV DV X1 X2(1) X2(2) X2(3) X2(4)
$DATA SIM201.csv  IGNORE=C
$SUBROUTINES ADVAN1 TRANS2
$PK
   TVCL=THETA(1)+THETA(2)*X1+THETA(3)*X2(1)
   CL = TVCL*EXP(ETA(1))
   TVV=THETA(4)
   V=TVV*EXP(ETA(2))
   S1=V
$ERROR
   DEL=0
   IF (F.EQ.0) DEL=0.1
   W=F
   IPRED=F
   IRES=DV-IPRED
   IWRES=IRES/(W+DEL)
   Y=F + F*ERR(1)
$THETA 10 FIX
$THETA 0.3 FIX
$THETA 0.3 FIX
$THETA 100 FIX
$OMEGA 0.09 FIX    ;[P] INTERINDIVIDUAL VARIABILITY IN CL
$OMEGA 0.09 FIX    ;[P] INTERINDIVIDUAL VARIABILITY IN V
$SIGMA 0.1 FIX
$SIMUL ( 65248743 ) ONLYSIM SUBPROBLEMS=1
$TABLE C ID TIME AMT MDV DV X1 X2(1) NOPRINT ONEHEADER
       FILE=SIM201.tab
```

Appendix E

Example of NONMEM control stream for analyzing simulated data for N=20. Covariate X_1 and $X_{2(1)}$ was added into the base model (relevant to Chapter 5)

```
$PROB RUN# 201_204
$INPUT  C ID TIME AMT MDV DV X1 X2(1) X2(2) X2(3) X2(4)
$DATA SIM_FIT201.csv  IGNORE=C
$SUBROUTINES ADVAN1 TRANS2
$PK
   TVCL=THETA(1)+THETA(2)*X1+THETA(3)*X2(1)
   CL = TVCL*EXP(ETA(1))
   TVV=THETA(4)
   V=TVV*EXP(ETA(2))
   S1=V
$ERROR
   DEL=0
   IF (F.EQ.0) DEL=0.1
   W=F
   IPRED=F
   IRES=DV-IPRED
   IWRES=IRES/(W+DEL)
   Y=F + F*ERR(1)
$THETA
(5)      ; [THETA(1)]
(0,0.5)  ; [THETA(2)]
(0,0.5)  ; [THETA(3)]
(0,150)  ; [THETA(4)]
$OMEGA
 0.05    ; [P] INTERINDIVIDUAL VARIABILITY IN CL
 0.04    ; [P] INTERINDIVIDUAL VARIABILITY IN V
$SIGMA
 0.3     ; [P] PROPORTIONAL COMPONENT

$EST PRINT=5 METHOD=1 INTERACTION MAXEVAL=9999 NOABORT
     SIGDIG=3
$COVARIANCE PRINT=E
$TABLE C ID TIME AMT MDV DV X1 X2(1) NOPRINT ONEHEADER
       FILE=201_204.tab
```